



College of Engineering

In-situ Regeneration of Spent Activated Carbon used for the Removal of Geosmin and Methyl-isoborneol (G-MIB) in Dwr Cymru Water Supplies.

A thesis submitted to Swansea University, College of Engineering in fulfilment of the requirements for the degree of Master of Science by Research in Chemical Engineering

Written by: George Onyekwere, BEng

Name of Supervisor: Dr Chedly Tizaoui

Date of submission: 04/07/2021


Abstract

After repeated use, activated carbon becomes spent because of the adsorption of contaminants like trans-1,10-dimethyl-trans-9-decalol (geosmin) and methyl-isoborneol (MIB), pesticides, and natural organic matter, etc.. The adsorption capacity of the activated carbon needs to be replenished for activated carbon to be re-used as an adsorbent, thus regeneration is required. The common regeneration methods imply moving the activated carbon to dedicated facilities where it is regenerated using thermal and steam processes. These processes are energy-intensive, costly, and have a high carbon-footprint. Due to its strong oxidation power, ozone can potentially be used to regenerate activated carbon *in-situ* by removing the contaminants. This project evaluated the effectiveness of ozone in the regeneration of granular activated carbon (GAC), focusing on the effect of ozone on the GAC physical and chemical characteristics. GAC was characterised through the iodine number, methylene blue number, Brunner-Emmett-Teller (BET), Fourier transform infrared spectroscopy measurement (FTIR), and the pH point of zero charge to determine the change in chemical and physical properties of the GAC following ozonation. The results show that the pH_{pzc} slightly decreased as GAC is treated with ozone (90 minute) from 9.92 pH to 9.52. However, the iodine and the methylene blue numbers decreased from 3.60 (virgin GAC) to 2.33 mmole/g (decrease of 35.18 %) and from 0.399 (virgin GAC) to 0.198 mmole/g (decrease of 32.27%) after 90 min ozone treatment, respectively. The effect of ozonation at lower exposure times was more beneficial since 30 minute ozonation yielded lower reductions in iodine and methylene blue numbers. The iodine and methylene blue numbers of the 30 minute ozonated samples yielded a decrease of 11.1% and 10.94%, respectively when compared with the virgin carbon adsorption capacity, which suggests exposure time goes

through an optimum value. Although this result shows a reduction of the virgin GAC adsorption capacity, 30 minute ozonation of the spent GAC showed increased adsorption capacity of the spent carbon from 1.53 to 1.91 mmole/g, and FTIR analysis proved that the functional groups imparted by the adsorbed species had been fully removed after ozonation. Ozonation of GAC removes the adsorbed contaminants, while it also increases the amount of highly oxidised species, as seen in the FTIR data. This study has also evaluated a new analysis method based on fluorescence, which was able to determine the concentration of G-MIB before and after adsorption on GAC. Overall, this study shows that increasing the concentration of ozone used to treat activated carbon decreases the activated carbon's adsorption capacity, thus optimisation of the ozone dose and contact time is required. Ozone regeneration of spent activated carbon removes most of the adsorbed contaminants present on the spent activated carbon surface, as evidenced by FTIR results. It can be concluded that ozone regeneration of spent GAC is an effective method for *in-situ* regeneration of GAC. However, further optimisation of the process is required.


Declarations

This work has not previously been accepted in substance for any degree and is not being concurrently submitted in candidature for any degree.

Signed: 


Date: 08/10/2021.....

This thesis is the result of my own investigations, except where otherwise stated. Other sources are acknowledged by footnotes giving explicit references. A bibliography is appended.

Signed: 


Date: 08/10/2021.....

I hereby give consent for my thesis, if accepted, to be available for photocopying and for inter-library loan, and for the title and summary to be made available to outside organisations.

Signed: 

Date: 08/10/2021.....

The University's ethical procedures have been followed and, where appropriate, that ethical approval has been granted.

Signed: 

Date: 08/10/2021.....

Table of contents

1.0	Introduction.....	13
1.1	Introduction	13
1.2	Aims of research.....	15
2.0	Literature review	16
2.1	The history of drinking water treatment	16
2.2	Taste and odour in drinking water	17
2.3	Geosmin	20
2.3.1	2-Methylisoborneol (MIB).....	21
2.3.2	Analysis of geosmin and MIB	22
2.4	Removal of geosmin and MIB from water	23
2.4.1	Advanced oxidation process (AOP).....	24
2.4.2	Biofiltration	26
2.4.3	Activated carbon	27
2.5	Analysis of geosmin & MIB.....	27
2.5.1	Solid-phase extraction	27
2.5.2	Gas chromatography/mass spectrometry	29
2.5.3	Fluorescence spectrometry	32
2.6	Activated carbon	34
2.6.1	History of activated carbon.....	34
2.6.2	Preparation of activated carbon	35
2.6.3	Carbonisation	35
2.6.4	Activation	36
2.6.5	Structure of activated carbon	39
2.6.6	Activated carbon applications.....	48
2.7	Classification of activated carbon	49
2.7.1	Granular activated carbon (GAC)	49
2.7.2	Powdered activated carbon (PAC)	52
2.8	Characterisation of activated carbons	53
2.9	Adsorption.....	54
2.9.1	Classification of adsorption Isotherms.....	59
2.9.2	Brunauer-Emmett-Teller (BET).....	61
2.9.3	Langmuir Isotherm.....	63
2.9.4	Freundlich Isotherm.....	66

2.9.5	Adsorption kinetics	67
2.10	Regeneration of activated carbon.....	68
2.10.1	Thermal regeneration.....	69
2.10.2	Steam regeneration	71
2.10.3	Bio-regeneration.....	72
2.10.4	Chemical regeneration.....	74
2.11	Use of ozone for the regeneration of activated carbon.....	76
2.11.1	Ozone generation	77
2.11.2	Ozone solubility	78
2.11.3	Ozone measurement by the indigo method.....	79
2.11.4	Ozone reaction mechanisms.....	80
2.11.5	Ozone regeneration of activated carbon.....	81
3.0	Materials and methods	85
3.1	Materials and reagents	85
3.2	Characterisation	85
3.2.1	Iodine number (IN).....	85
3.2.2	Methylene blue number (MBN).....	87
3.2.3	Brunauer-Emmett-Teller (BET) method.....	89
3.2.4	Fourier transform infrared spectroscopy measurement (FTIR).....	92
3.2.5	The pH of zero charge (pH _{pzc}).....	92
3.3	Ozonation of activated carbon.....	93
3.3.1	Ozone analysis in liquid phase	94
3.4	Adsorption of geosmin & MIB.....	95
3.4.1	Geosmin & MIB stock solutions	95
3.4.2	Geosmin and MIB adsorption experiment.....	95
3.5	G-MIB analysis.....	97
4.0	Results & discussion	98
4.1	Characterisation of virgin activated carbon.....	98
4.1.1	Iodine number.....	98
4.1.2	Methylene blue.....	103
4.1.3	The pH point of zero charge.....	107
4.1.4	Fourier transform infrared spectroscopy measurement (FTIR).....	109
4.2	Ozonation of virgin activated carbon.....	110
4.2.1	Ozone concentration in water	111
4.2.2	Iodine number.....	112
4.2.3	Methylene blue.....	113

4.2.4	The pH point of zero charge.....	116
4.2.5	Fourier transform infrared spectroscopy measurement (FTIR).....	117
4.3	Spent GAC characterisation	120
4.4	Geosmin and MIB adsorption	125
5.0	Conclusions and recommendations for future work.....	129
5.1	Summary	129
5.2	Conclusions	129
5.3	Recommendations for future work.....	131
6.0	References.....	133
7.0	Appendices.....	139
7.1	Iodine number experiment	139
7.2	Methylene blue	140
7.3	pH point of zero charge.....	143
7.4	Fourier transform infrared spectroscopy measurement (FTIR).....	144
7.5	Ozonation of activated carbon.....	146
7.6	Geosmin and MIB adsorption experiment.....	147

List of tables

Table 1: Henry's law constants for geosmin and MIB (Omur-Ozbek, Little, & Dietrich, 2007)	19
Table 2: Geosmin and MIB characteristics.....	21
Table 3: AOP's for removal of geosmin and MIB (Elias-Maxil, Rigas, de Velasquez, & Ramirez-Zamora, 2011)	25
Table 4: Advantages and disadvantages of HPLC and GC (Wu et al., 2014)	32
Table 5: Properties of a variety of PAC's (Crittenden, 2012)	39
Table 6: Proximate analysis of an activated carbon sample (Cuhadaroglu & Uygun, 2008)	41
Table 7: Classification of pores sizes (IUPAC) (Bubanale, 2017)	42
Table 8: Application of activated Carbon (Bansal & Goyal, 2005)	49
Table 9: Properties of different activated carbons (Crittenden 2012)	51
Table 10: Properties of GAC and PAC (Greenbank & Knepper, 2002)	52
Table 11: Summary of the forces of attraction for adsorption (Crittenden, 2012)	57
Table 12: Physical properties of ozone	76
Table 13: Standardisation results for sodium thiosulfate (left) iodine (right)	98
Table 14: Iodine number results for initial masses.....	100
Table 15: Comparison between the BET and iodine number results for virgin GAC.....	101
Table 16: Methylene blue isotherm results for virgin GAC.....	106
Table 17: Identification of the peaks observed in FTIR analysis of the virgin GAC.....	109
Table 18: Iodine number of activated carbons exposed to ozone/oxygen	112
Table 19: Adsorption of methylene blue on activated carbon exposed to ozone/oxygen	115
Table 20: pH_{pzc} results for activated carbon exposed to ozone/oxygen.....	116
Table 21: Identification of the peaks observed in FTIR analysis of activated carbon exposed to ozone/oxygen	118
Table 22: Iodine numbers and regeneration dates for the six spent GAC samples.....	121
Table 23: Identification of the peaks observed in FTIR analysis of spent activated carbon	122
Table 24: Iodine number of GAC-D with varying exposure to ozone	123
Table 25: G-MIB adsorption data.....	126
Table 26: Virgin iodine number replications.....	139
Table 27: Calibration curve values for methylene blue	141
Table 28: Methylene blue number experiment for virgin GAC raw data	141
Table 29: pH_{pzc} raw data for virgin GAC.....	144
Table 30: Indigo experimental results	146

List of figures

Figure 1: Procedure for Geosmin & MIB release	188
Figure 2: Vacuum manifold for SPE (Dean 2000).....	288
Figure 3: Gas Chromatography system (Evers, 2014).....	30
Figure 4: Gas chromatography/ Mass spectrometry diagram (Kolapkar, 2018)	311
Figure 5: Mass spectrum of geosmin (Watson, Brownlee, Satchwill, & Hargesheimer, 2000)	322
Figure 6: Fluorescence absorption and emission spectra (Coble, 2014)	333
Figure 7: Production of activated carbon (Leon, Silva, Carrasco, & Barrientos, 2020).....	355
Figure 8: Process of chemical activation for wood precursor (Johnson, Setsuda, & Williams, 1999)	388
Figure 9: Graphite planes structure (Marsh, 2006)	40
Figure 10: Activated carbons porous structure (Callewaert, 2014).....	422
Figure 11: Representation of the porous structure of activated carbon (Bubanale, 2017)	444
Figure 12: The hexagonal structure of activated carbon (Marsh, 2006)	455
Figure 13: Representation of the activated carbons: (a) Graphitized (b) Non-graphitized (Bubanale, 2017)	466
Figure 14: Basic representation of the adsorption process (Worch, 2012).....	544
Figure 15: Three steps of adsorption onto activated carbon (Ergenekon, 2010).....	555
Figure 16: Mechanisms for adsorption kinetics (Crittenden, 2012).	599
Figure 17: Types of physisorption isotherms according to the IUPAC classification (Alhamami, Doan, & Cheng, 2014).....	60
Figure 18: Representation of the some different adsorption models (Flores, 2014).....	644
Figure 19: The steps of thermal regeneration of activated carbon (Guo & Du, 2012).....	70
Figure 20: Mechanisms of bio-regeneration (Çeçen & Aktas, 2012)	722
Figure 21: Concentration profile of adsorbate during bio-regeneration (Çeçen & Aktas, 2012)	733
Figure 22: Chemical methods of regeneration of activated carbon (Salvador, Martin-Sanchez, Sanchez-Hernandez, & Sanchez-Montero, 2014)	754
Figure 23: Solubility of ozone and oxygen in water with respect to temperature (Sonntag & Gunten, 2012).	799
Figure 24: Model of indirect and direct ozonation (Gottschalk, 2010)	80
Figure 25: Ozonation of a double carbon bond (Gottschalk, 2010).....	81
Figure 26: Diagram that represents the ozonation setup (Rivas, Beltran, Gimeno, & Frades, 2004)	833
Figure 27: Ozone system rig.....	944
Figure 28: Least square regression graph for iodine number experiment for the virgin GAC.....	101
Figure 29: Calibration curve for methylene blue	1044
Figure 30: Q vs C graph for virgin GAC.....	1055
Figure 31: Langmuir isotherm of virgin GAC adsorption of methylene blue	1055
Figure 32: Freundlich isotherm of virgin GAC adsorption of methylene blue	1066
Figure 33: pH final vs pH initial for virgin GAC.....	1088
Figure 34: FTIR analysis of the virgin GAC.....	11010
Figure 35: Ozone concentration vs ozone exposure time graph	11111
Figure 36: Q vs C graph for activated carbon exposure to ozone/oxygen.....	1144
Figure 37: Freundlich isotherm for activated carbon exposed to ozone/oxygen.....	1144
Figure 38: FTIR analysis of activated carbon exposed to ozone/oxygen	1188
Figure 39: FTIR analysis of the spent activated carbons.....	12222
Figure 40: FTIR analysis of ozonated spent activated carbon.....	1244
Figure 41:G-MIB Fluorescence intensity vs concentration calibration curve	1266

Figure 42: GMIB uptake by GAC.....	1277
Figure 43: Iodine number X/M vs C graphs: 1) 30 min ozonated GAC 2) 60 min ozonated GAC 3) 90min ozonated GAC 4) 60 min oxygenated GAC.....	14040
Figure 44: Langmuir and Freundlich isotherms for ozonated activated carbon samples: 1) Freundlich isotherm for 30 minute ozonated GAC sample 2)) Langmuir isotherm for 30 minute ozonated GAC sample 3)) Freundlich isotherm for 60 minute ozonated GAC sample 4) Langmuir isotherm for 60 minute ozonated GAC sample 5) Freundlich isotherm for 90 minute ozonated GAC sample 6)) Langmuir isotherm for 90 minute ozonated GAC sample 7)) Freundlich isotherm for 30 minute oxygenated GAC sample 8) Langmuir isotherm for 30 minute oxygenated GAC sample.....	Error! Bookmark not defined. 3
Figure 45: FTIR data of virgin activated carbon measuring the adsorbance	1444
Figure 46: FTIR data of the virgin activated carbon measuring the transmission	1455
Figure 47: Image of the Perkin-Elmer Spectrum Two FTIR	1466
Figure 48: Image of the ozone reactor	1477
Figure 49: Image of Incu-Shake MAXI.....	148
Figure 50: Image of Fluorescence spectrometry	148

List of Acronyms

<i>Abbreviation</i>	<i>Meaning</i>
<i>Geosmin</i>	Trans-1,10-dimethyl-trans-9-decalol
<i>MIB</i>	Methyl-isoborneol
<i>OTC</i>	Odour threshold concentration
<i>BOM</i>	Biodegradable organic matter
<i>BET</i>	Brunauer-Emmett-Teller
<i>FTIR</i>	Fourier transform infrared
<i>IN</i>	Iodine number
<i>MBN</i>	Methylene blue number
<i>pH_{pzc}</i>	pH point of zero charge
<i>G-MIB</i>	Geosmin and MIB
<i>GC/MS</i>	Gas chromatography/ Mass spectroscopy
<i>SPE</i>	Solid phase extraction
<i>AC</i>	Activated carbon
<i>GAC</i>	Granular activated carbon
<i>PAC</i>	Powdered activated carbon
<i>AOP</i>	Advanced oxidation process

Acknowledgements

- *I would like to express my deep and sincere gratitude to Dr Chedly Tizaoui for his invaluable supervision and guidance. As my supervisor, his insight, observations, and suggestions helped me to establish the direction of my project and to achieve my objectives.*
- *I would like to sincerely thank the Knowledge Economy Skills Scholarships (KESS 2) for funding this work. KESS2 is a pan-Wales higher level skills initiative led by Bangor University on behalf of the HE sector in Wales. It is part-funded by the Welsh Government's European Social Fund (ESF) convergence programme for West Wales and the Valleys.*
- *I would also wish to acknowledge Dwr Cymru (Welsh Water) for their financial contribution to this programme and providing samples of activated carbon and geosmin & methyl-isoborneol used in this study.*
- *I would also like to thank Dwr Cymru (Welsh Water) staff, especially Dr Paul Gaskin, Katherine Martin, and Helen Cantwell, for all their support, resources, and guidance throughout my project.*
- *I would like to acknowledge all my research scholars, friends, and staff of the chemical engineering department for their invaluable support during my research project.*

1.0 Introduction

1.1 Introduction

Taste and odour compounds in water cause customer complaints. Therefore, to achieve the greatest customer satisfaction, taste and odour compounds must be removed (Andreadakis & Mamais, 2010). The causes of taste and odour in water are from methylisoborneol (MIB) and trans-1,10-dimethyl-trans-9-decalol (geosmin). Geosmin causes an earthy odour while MIB causes a musty odour, and together they cause earthy, musty odour and taste (Andreadakis & Mamais, 2010). MIB and geosmin are mainly produced from the metabolism and biodegradation of specific varieties of cyanobacteria and filamentous bacteria (Actinomycetes). The aqueous odour threshold concentration of geosmin ranges from 6 to 10 ng/L at 45 °C the intensity of the odour is temperature-dependent. Similar to geosmin, 2-MIB has an aqueous odour threshold concentration of 2 to 20 ng/L at 45 °C (Omur-Ozbek et al., 2007). One way to remove geosmin and MIB from the water source is through the use of activated carbon. Activated carbon is a porous *carbon compound* similar to a *char* that is exposed to reactions with gases. Typically, chemicals (e.g. $ZnCl_2$) before, during or after carbonisation are used to increase activated carbons adsorptive properties (Marsh, 2006). Activated carbon, in powder (PAC) or granular (GAC) forms, are used across the world to handle earthy or musty odours; PAC only demands small capital costs to feed and has the flexibility to be applied as and when needed. However, when the taste and odour (T&O) problem persists, it becomes more economical to employ a GAC adsorbent bed. If a GAC bed is maintained and correctly designed, a GAC adsorbent bed can easily operate effectively for several years at low to moderate T&O compound concentrations before carbon replacement/regeneration is necessary (Chen, Dussert, & Suffet, 1997). In contrast, PAC is

used for seasonal control of taste and odour compounds. It strongly adsorbs pesticides at low concentrations ($< 10\mu\text{g/L}$) and can easily be added to the water supply (Jung, Baek, & Yu, 2004). GAC is generally used as a barrier to spikes in concentration of toxic organic compounds and also to control disinfection by-product precursors. It is easy to reactivate, and it has a lower carbon usage rate per volume of water treated when compared with PAC (Jung et al. 2004).

Adsorption is a mass transfer operation where an adsorbate in liquid (or gas) phase is adsorbed onto a solid phase (adsorbent). In this project, geosmin and MIB are the adsorbate, and carbon is the adsorbent. During adsorption, geosmin and MIB are transported into the activated carbon by means of diffusion; then, they undergo adsorption onto the inner pores of activated carbon, which have a considerable surface area. This leads to geosmin and MIB being concentrated on the solid surface through physical adsorption (Crittenden, 2012).

Regeneration of activated carbons is when adsorbed solute molecules are removed from the adsorbent surface through desorption. This can be achieved using a variety of different methods. Complete regeneration of activated carbon can never be achieved but activated carbon can be almost fully regenerated. The point of exhaustion is when the influent and effluent are equal; therefore, the adsorbate can no longer be removed. Chemical regeneration, ozone (and AOPs) can be used to oxidise and thus terminating geosmin and MIB (Nerenberg, Rittmann, & Soucie, 2000). Each of the oxidants power to remove G-MIB varies with each odour compound. It is stated that ozone effectively removes G-MIB, primarily when used with hydrogen peroxide or UV irradiation to produce the hydroxyl radical, which is a very powerful oxidant. The pH has a significant effect on the removal of G-MIB. Geosmin is more rapidly destroyed by ozonation than MIB; this is because MIB contains more tertiary carbons

in its molecular structure than geosmin, therefore, the removal of MIB is more complicated (Liang, Wang, Chen, Zhu, & Yang, 2007). However, prolonged exposure of activated carbon to ozone gas can affect the chemical composition of the carbon surface. Basic sites are transformed into acid sites because of oxidation. The modification of the oxygenated groups influences the adsorptive properties of activated carbon; thus, the surface area decreases (Valdes, Sanchez-Polo, Rivera-Utrilla, & Zaror, 2002). This indicates that regenerated carbon may not be able to remove as much G-MIB as virgin AC.

1.2 Aims of research

The aim of the research is to examine the effect of ozone regeneration on the characteristics of GAC and evaluate how this regeneration affects the properties of a spent GAC. Specifically this project had the following objectives:

- Characterise GAC using common methods including iodine number, methylene blue number, pH point of zero charge, Fourier transform infrared spectroscopy measurement, and BET surface area measurement
- Evaluate the effect of ozonation at three different exposure times (30, 60 and 90 minutes) on the GAC characteristics
- Evaluate the effect of ozonation on a spent GAC sampled from one of the Dwr Cymru sites
- Evaluate the adsorption of G-MIB on GAC.

This chapter gave a brief introduction to the project and the use of activated carbon for the removal of geosmin and MIB, it also summarised the aim and objectives of this project.

2.0 Literature review

2.1 The history of drinking water treatment

The first drinking water treatment was documented to remove taste and odour compounds in approximately 4000 BC in Greece (EPA, 2001). The process they used included charcoal, sunlight, boiling and straining (EPA, 2001). Over time the water treatment processes became more advanced. By the 1800s, water treatment systems were using slow sand filtration. Throughout the 1800s, scientists started making advancements in the understanding of water contaminants, mainly concerning non-visible contaminants. Dr John Snow proved cholera was a waterborne disease; he managed to link an outbreak of general illness within London to a water well that became contaminated by sewage (Hall & Dietrich, 2000). In 1806, Paris unveiled a large water treatment plant; it used the river Seine as its water supply. The water was then settled for 12 hours prior to its filtration; the primary filters were coarse river sand, clean sand and charcoal (Hall & Dietrich, 2000). During the 1900s, water treatment was driven towards reducing microbial contaminants which were causing typhoid and cholera epidemics. In 1908, chlorine was first introduced as a primary disinfectant of drinking water in New Jersey (Hall & Dietrich, 2000). The disinfectant ozone began to be used in Europe in the early 1900s. In the late 1900s, there was a considerable problem with chemical contamination of the water supply because of factory discharge and farm field runoff; these artificial chemicals were a substantial environmental and health concern (EPA, 2001). Presently, chlorination and filtration are still used to protect the water supply against harmful contaminants effectively.

There has been significant improvement in membrane development for reverse osmosis filtration and ozonation treatment systems.

2.2 Taste and odour in drinking water

Problems with taste and odour in drinking water are frequent in water treatment plants across the entire world. However, standard water treatment methods inefficiently remove taste and odour compounds, which is urging drinking water businesses to look for alternative cost-effective solutions for water purification. Taste and odour in drinking water is recognised by day-to-day people as an obvious sign that the potential safety of the drinking water is not to the requested standard, therefore incurs complaints and dissatisfaction. For most members of the public, the taste and odour of water is the only way to evaluate the safety of drinking water (Srinivasan & Sorial, 2011). The leading causes of taste and odour are the presence of 2-methylisoborneol (MIB) and trans-1,10-dimethyl-trans-9-decalol (geosmin); they are both semi-volatile compounds. MIB and geosmin are mainly caused by the metabolism and biodegradation of specific varieties of cyanobacteria. These bacteria most commonly bloom with the aid of nutrients at warmer temperatures. Cyanobacteria contain a sizable and morphologically heterogeneous group of phototrophic bacteria (Komárek, 2009). Cyanobacteria live in fresh and or marine water all over the world. Usually, small quantities of cyanobacteria do not result in any harm to a consumer. Cyanobacteria experience rapid growth and these algal cells release odorants (geosmin and MIB), causing the taste and odour problem within drinking water (Giglio, Chou, Ikeda, Cane, & Monis, 2011).

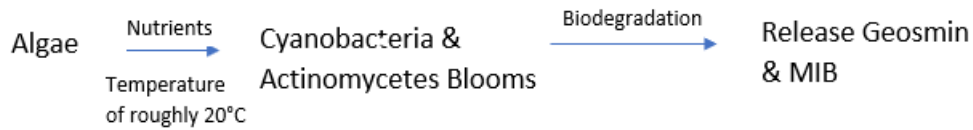


Figure 1: Procedure for geosmin & MIB release

No regulations for either MIB or geosmin exists, and they have not been recognised to cause any damage to health. However, the major problem with the presence of MIB and geosmin in water is their exceedingly low odour threshold concentrations (OTC) and, as stated, their perseverance to removal in standard water treatment operations like flocculation, coagulation, sedimentation, filtration and disinfection. The OTC's for MIB and geosmin ranges from around 4 to 20 ng/L (Srinivasan & Sorial, 2011). The odour's strength depends on the temperature, while, on average, customer complaints start at 7 and 12 ng/L for geosmin and MIB, respectively. The detection of geosmin and MIB varies with specific individuals being hypersensitive and can detect at low concentrations whilst others are hyposensitive, thus struggle to detect the earthy taste/odour. Geosmin and MIB in water are volatile and must exceed OTC to allow them to be detected by the human nose. Henry's law can be used to find the amount of geosmin and MIB volatilising. Henry's law shows that each volatile compound owns its individual Henry's law constant, m (dimensionless) and K_H (L-atm/mol). The equations for the relationship between the constants are stated below (Omur-Ozbek et al., 2007):

$$m = C_{gas}/C_{liq} \quad (2.1)$$

$$K_H = P_v/C_{liq} \quad (2.2)$$

where C_{gas} is the concentration in the headspace (mol/L), C_{liq} is the concentration in the aqueous phase (mol/L), P_v is the partial pressure in the vapour phase (atm). Many variables affect Henry's law constants, such as pH, temperature, concentration, suspended solids, dissolved organic materials, salts, and surfactants. The constants for geosmin and MIB are stated in Table 1. Henry's law is temperature dependant as shown in equation (2.3).

$$\ln\left(\frac{m_1}{m_2}\right) = -\left(\frac{\Delta H^\circ}{R}\right) \times \left(\left(\frac{1}{T_2}\right) - \left(\frac{1}{T_1}\right)\right) \quad (2.3)$$

where m_1 is the dimensionless Henry's law constant at T_1 (K), m_2 is the dimensionless Henry's law constant at T_2 (K), ΔH° is the enthalpy of the aqueous vaporisation reaction (J/mol) and R is the universal gas constant (8.314J/molK) (Omur-Ozbek et al., 2007).

Table 1: Henry's law constants for geosmin and MIB (Omur-Ozbek, Little, & Dietrich, 2007)

Compound	m at 20°C	ΔH° (kJ/mol)
Geosmin	0.0023	80
2-MIB	0.0027	89

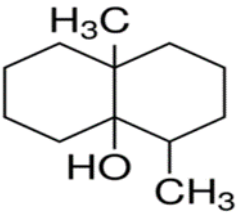
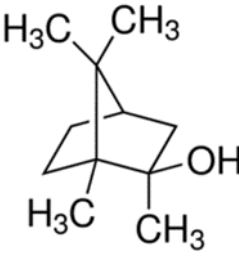
If drinking water contaminated with geosmin and MIB is used at home, the odour concentration in the air increases, therefore, becomes apparent. The use of hot water makes

the odour more distinct because the amount of odorant that is volatilising into the air inside the building increases, as shown by Henry's law (Omur-Ozbek et al., 2007).

2.3 Geosmin

Geosmin (trans-1,10-dimethyl-trans-9-decalol) is a metabolite of numerous fungi and actinomycetes (Jung et al., 2004). It's an organic compound with a distinct earthy odour and taste. Geosmin is a bicyclic tertiary alcohol that is a derivative of decalin. Geosmin was initially isolated by Gerber and Lechevailier (1965) using actinomycetes bacteria. It has now been realised that it can be produced by various micro-organisms like: streptomyces bacteria myxobacteria, and fungi. As stated, geosmin gives an earthy or musty taste in water that customers assume is an indication of the water quality. Water providers must constantly monitor the amount of geosmin, enabling them to optimise the removal of geosmin. Humans can detect geosmin at low odour threshold concentrations these vary depending on the person, hypersensitive people can detect geosmin at lower 7 ng/L. Many countries have responded to the drinking water taste and odour complaints by imposing a maximum OTC. For example, in 2006, the Ministry of Health of the People's Republic of China released the standards for drinking water quality, which set a maximum of 10 ng/L for geosmin and MIB(G-MIB) (Bristow, Young, Pemberton, Williams, & Maher, 2019).

Table 2: Geosmin and MIB characteristics

Compound	Geosmin	MIB
Molecular structure	C ₁₂ H ₂₂ O	C ₁₁ H ₂₀ O
Structure		
Molecular weight (g/mol)	182.31	186.28
pKa	-0.0047	-0.42
Water solubility (mg/L)	150.2	450
Odour	Earthy smell	Musty smell
Odour threshold concentration (OTC)	7 ng/L	12 ng/L

The natural degradation of geosmin is relatively slow and can take around three days (Lawton, Robertson, Bruce, & Robertson, 2003). Geosmin's terpenoid structure was initially defined in the late 20th century (Bentley & Meganathan, 1981).

2.3.1 2-Methylisoborneol (MIB)

2-Methylisoborneol (MIB) is an organic chemical that causes a powerful musty/ earthy odour, although it does not have a known biological function. MIB is derived from borneol. MIB, like geosmin, has a very low OTC, but MIB is generally detected at a slightly higher concentration

than geosmin. Lots of different algae can produce MIB, the foremost is blue-green algae (cyanobacteria) like *Anabaena*. MIB is much more resilient to biodegradation than geosmin as it takes around 5 to 14 days to degrade (Lawton et al., 2003).

Table 2 has details on geosmin and MIB. It shows that geosmin's OTC is lower than MIB, distinguishing the difference in the molecular structures. Geosmin and MIB have a very similar size and molecular mass, but their structure differs. MIB contains more tertiary carbons in its molecular structure than geosmin (Liang et al., 2007). The structure of geosmin allows the adsorptive capacity of activated carbon to be about five times greater than MIB (Andreadakis & Mamais, 2010). Geosmin and 2-MIB are tertiary alcohols, each of which exists as positive and negative enantiomers. Odour outbreaks are caused by the biological production of the naturally occurring negative enantiomers (Juttner & Watson, 2007).

2.3.2 Analysis of geosmin and MIB

Geosmin and MIB are analysed to determine their concentrations in water. In the late '80s and '90s, conventional analytical methods like purge and trap (P & T) were used for the analysis of G-MIB. Although they were effective, they had drawbacks related to the accuracy, speed of analysis, and cost (Srinivasan & Sorial, 2011). This prompted the development of membrane-based methods to increase the accuracy of the measurements. Methods were introduced like Hollow fibre stripping analysis (HFSA), the apparatus setup was very complex. Solid-phase extraction (SPE) was developed, although it was more expensive to set up. SPE could extract even very low concentrations and can then be followed by an injection into a gas chromatograph-mass spectrophotometry (GC-MS) for analysis (Srinivasan & Sorial, 2011).

In 1996, solid-phase micro-extraction (SPME) was introduced. This technique uses silica fibre for extraction of the taste and odour compounds and then, just like SPE, can be followed by (GC-MS) for analysis (Srinivasan & Sorial, 2011). High-performance liquid chromatography (HPLC) can also be used with atmospheric pressure chemical ionisation (APCI)/MS detection (Bedner & Saito, 2020). Although HPLC is a prevalent analysis method, it may not obtain accurate concentration values at such low concentrations for geosmin and MIB.

2.4 Removal of geosmin and MIB from water

As stated, removing geosmin and MIB is a significant problem in the drinking water industry since they are immensely resistant to removal, especially by conventional drinking water treatment operations. The conventional water treatment operations are flocculation, coagulation, sedimentation, filtration and disinfection. The conventional treatment processes ineffectively remove MIB and geosmin dissolved in water. In the water treatment industry, there are three main methods used to remove geosmin and MIB effectively, advanced oxidation processes (AOP's), biological treatment and GAC/PAC adsorption. The removal rates for geosmin and MIB can vary drastically from as low as 30% up to 100% removal using various removal methods like activated carbon or ozone (Collivignarelli & S.Sorlini, 2004). The removal rates are dependent on raw water characteristics, the concentration of geosmin and MIB, the dosage of activated carbon. Initially, coagulation was considered for the removal of geosmin and MIB, but it was found that aluminium coagulation could not be optimised for MIB and geosmin removal. Many different variables were changed in order to try to optimise the removal, but there was no increase in removal within a range of pH and coagulation

conditions. Exclusively using oxidants were found not to be very effective; for example, Cl_2 , ClO_2 and KMnO_4 are ineffective at removing geosmin and MIB whereas O_3 has good removal of geosmin and MIB (Kim & Park, 2021). In a study conducted by Srinivasan & Sorial (2011), who used O_3 to destroy geosmin and MIB, it was reported that 85% of GMIB were removed at 3.8mg/L ozone. In a study conducted by Ndongue et al. (2006), it was found that a GAC column operating at an Empty Bed Contact Time (EBCT) removed 59% of the geosmin and 46% of the MIB in the influent stream with a concentration of 13.8 ng/L and 65 ng/L respectively. However, when the EBCT increased to 15 min, the removal efficiencies increased to 70 % and 60% for geosmin and MIB respectively. In another study conducted by Andreadakis & Mamais (2010), who used PAC to remove geosmin and MIB in a Jar test experiment (15 mg/L of PAC (WP-7) and 100 ng/L of geosmin and MIB, the removal percentages were 87.4% and 30.8% for geosmin and MIB respectively. In the following sections, the performance of advanced oxidation processes, biological treatment, and GAC/PAC adsorption, which are commonly used in the water industry to remove GMIB, will be discussed.

2.4.1 Advanced oxidation process (AOP)

Oxidation processes using either ozone or other oxidants combined with UV light are proven effective in removing geosmin and MIB (Kutschera, Bornick, & Worch, 2009). Most oxidation processes use ozone as the primary oxidant to remove G-MIB. However, the use of ozone in bromide-containing waters can produce bromate and aldehydes, which are toxic disinfection by-products (Kim & Park, 2021). Using ozone with UV or H_2O_2 increases the removal drastically

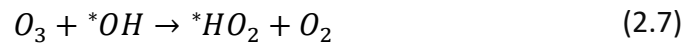
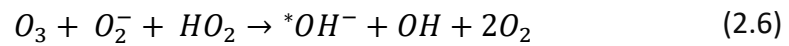
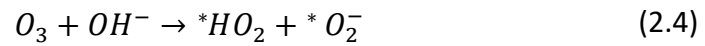
because it promotes the production of hydroxyl radicals (OH) which react with geosmin and MIB, causing the destruction of such compounds (Srinivasan & Sorial, 2011). There are various AOP's used to remove geosmin and MIB, as summarized in Table 3. It is shown that O₃ with UV light, UV/Visible light and TiO₂/UV light can completely destroy geosmin and MIB. The problem with AOP's is that many factors need to be controlled, for example, pH and organic matter concentration (Elias-Maxil et al., 2011). AOP's are less feasible than other removal methods because the energy and capital costs for these technologies are high.

Table 3: AOP's for removal of geosmin and MIB (Elias-Maxil, Rigas, de Velasquez, & Ramirez-Zamora, 2011)

Process	Efficiencies	Water matrix	Experimental conditions	References
O₃/Catalyst	75% MIB	Synthetic	MIB: 100 ng/L; pH 5.7; Retention time 10 min	(Qi, Chen, Xu, & Xu, 2008)
O₃/H₂O₂	80% MIB & 90% geosmin	Surface water	O ₃ : 2 mg/L; H ₂ O ₂ /O ₃ :0.2	(Koch, Gramith, Dale, & Ferguson, 1992)
UV/Visible light	100% MIB and geosmin	Ultra-pure water	MIB and geosmin 100mg/L ; UV/VUV: 245/185 nm; UV radiation 4 kJ/m ² Reaction time: 30 s	(Kutschera et al., 2009)
O₃/UV light	100% MIB and geosmin	Surface water	O ₃ : 1.5 – 3 mg/L; UV radiation: 5-6 kJ/m ² ; Retention time: 2-3 min	(Collivignarelli & S.Sorlini, 2004)
TiO₂/UV light	100% MIB and geosmin	Synthetic	MIB and geosmin: 200 ng/L; TiO ₂ 1%; radiation: 6.2 x 10 ⁻³ Jmin ⁻¹ , complete degradation: MIB in 30 min, geosmin in 60 min	(Lawton et al., 2003)
UV/H₂O₂	70% MIB and geosmin	WTP influent	MIB:25 ng/L; geosmin: 10 ng/L ; UV radiation: 10 kJm ⁻² ; H ₂ O ₂ : 7.2 mg/L; Medium pressure UV light	(Rosenfeldt, Melcher, & Linden, 2005)

The main advantage of using AOP's for removing geosmin and MIB is the ease of oxidant access and simple operation. On the other hand, AOP's can have high capital costs and energy costs and they can produce by-products (DBP's).

OH⁻ radicals are crucial for the oxidation of geosmin and MIB. An Increase in the OH⁻ radicals increases the removal of geosmin and MIB. O₃ and H₂O₂ are involved in the production of OH⁻ radicals, this can be seen in the oxidation process in the Equations below:



The * represents an electron, thus shows that the compound is a radical.

2.4.2 Biofiltration

The main biofiltration systems used for the removal of geosmin and MIB are slow sand filters and ultra/nano filtrations. Several factors can have an influence on the removal of geosmin and MIB by biofiltration: these include biodegradable organic matter (BOM) concentrations, water temperature variations, biofilter media, biomass and empty bed contact time (EBCT) (Elhadi, Huck, & Slawson, 2006). Biofilters are used, but they are not particularly effective at

removing geosmin and MIB by themselves, higher removal rates are obtained when integrated with O₃ or GAC/PAC to produce decent removal rates.

2.4.3 Activated carbon

Activated carbon is the most commonly used treatment method for the removal of geosmin and MIB. As a technique, it is widely used across the whole of the drinking water industry. Activated carbon is categorised into two different variations depending on the particle size: granular activated carbon (GAC) and Powdered activated carbon (PAC). GAC is used as granular media above a sand filter, while PAC is generally mixed with water. Activated carbon can be used to remove geosmin and MIB to below the odour threshold concentration (OTC) (Crittenden, 2012). The activated carbon removal efficiency is dependent on the:

- Surface area of AC
- Contact time
- Type of AC
- Filter age for GAC
- Concentration of dissolved organic carbon (DOC)
- Mass of activated carbon

2.5 Analysis of geosmin & MIB

2.5.1 Solid-phase extraction

One of the main methods used to extract geosmin and MIB from the sample drinking water for analysis is solid-phase extraction (SPE). The SPE works essentially by the water sample

being forced by a vacuum through a solid phase adsorbent packed into a cartridge. The drinking water sample is exposed to the solid phase to adsorb geosmin and MIB onto the surface of the solid phase, thus extracting the desired compounds from the water sample (Dean, 2000). The geosmin and MIB cannot pass through the adsorbent; they are adsorbed onto the surface of the adsorbent. The solid phase is separated from the solution and washed using distilled water (Dean, 2000). An eluting solvent is then contacted with the solid phase to desorb the geosmin and MIB. The solvent obtained from this elution can be finally analysed. SPE process should allow for more effective detection and identification of geosmin and MIB than other extraction methods as long as the adsorbent material, and eluent solvent are chosen correctly (Dean, 2000).

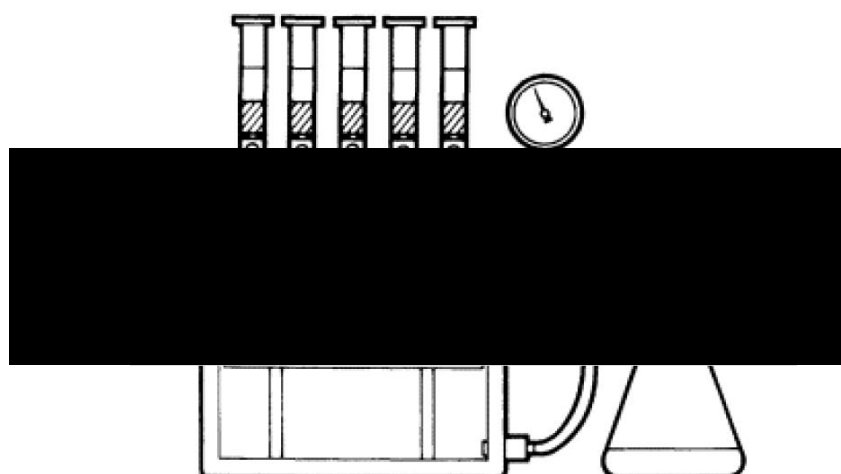


Figure 2: Vacuum manifold for SPE (Dean 2000)

The apparatus needed for SPE is shown in Figure 2. The cartridges are put on top of the manifold, the sample is then fed through the solid phase. The general operation of SPE has five steps including: initially, the adsorbent is wetted, the adsorbent is conditioned, the sample is loaded onto the adsorbent, and the adsorbent is washed and finally, elution of the adsorbates (Dean, 2000). Wetting of the adsorbent is required to allow the bonded alkyl

chains to be solvated, which allows them to spread open, forming bristle. This then induces good contact between the adsorbent and the adsorbate in the initial adsorption of geosmin and MIB from the water sample. It is imperative that the adsorbent is constantly wet to ensure a good recovery. The subsequent step is applying a solvent, normally methanol, to condition the adsorbent (Dean, 2000). The cartridge is then filled with the sample, which is forced through the adsorbent, and the adsorbates are adsorbed onto the adsorbent. The adsorbent is then washed with distilled water, this does not affect the elution. Finally, a small amount of solvent is added to the cartridge to elute the adsorbates.

2.5.2 Gas chromatography/mass spectrometry

Once the SPE is used to extract the organic compounds from the water sample, the compounds need to be determined and quantified. Gas chromatography/mass spectrometry (GC/MS) is the common method to analyse these compounds. The gas chromatography (GC) step is used to separate the organic compounds present in the eluted sample. GC has been used broadly for volatile and thermally unstable compounds like geosmin and MIB for more than 50 years and therefore is a very established separation technique in the water industry (Bristow et al., 2019). GC produces highly accurate, sensitive and reproducible results. The compounds are separated out in the carrier gas stream, thus presenting different retention times. The times are based upon their own physical and chemical properties and their interactions with the film in the column (Bristow et al., 2019). These properties then affect how the compounds interact with the stationary phase within the column. The retention time

is used to define the individual compounds. The greater the affinity the compounds have with the stationary phase, the greater the retention time (Bristow et al., 2019).

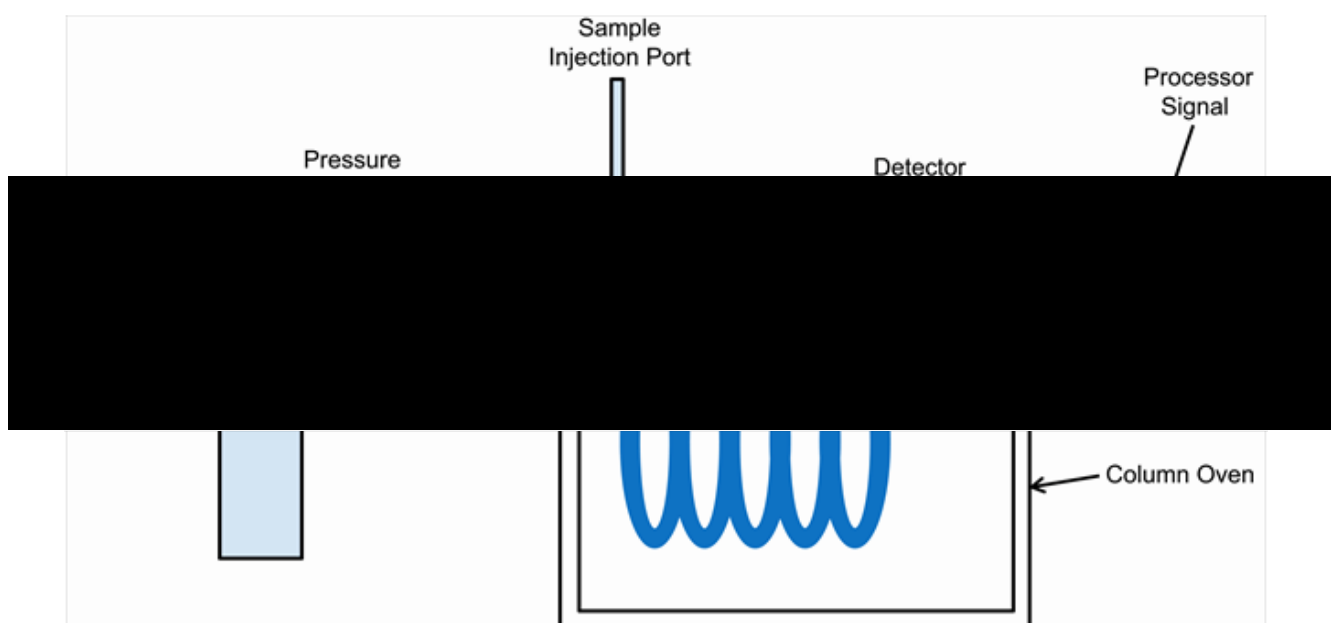


Figure 3: Gas Chromatography system (Evers, 2014)

The extracted compounds, by SPE (or headspace), are injected into the injection port, the compounds are then vaporised. The vaporised compounds are sent down the capillary column forced along by the mobile phase, as shown in Figure 3. The mobile phase is an inert gas, commonly helium, but hydrogen can also be used; hydrogen can improve separation (Li & Liu, 2019). The stationary phase is a layer of liquid and or polymer on an inert solid used as a support. The gaseous compounds interact with the walls of the column, the stationary phase (Li & Liu, 2019). The compounds will elute at different times; the retention time is then obtained for each compound. Each compound has its own specific retention time, allowing the identity of the compounds to be obtained (Li & Liu, 2019).

After the GC column, there is a detection unit; this is usually mass spectrometry (MS) this is shown in Figure 4. In mass spectrometry, the compounds are fed from the GC to the MS, where they are ionised. Ionisation produces fragment ions that produce m/z peaks used to

quantify the compounds (Milman, 2015). When the compounds are ionised, each compound's molecular weight determines their detection within the mass analyser; therefore, a heavier compound produces a different peak with respect to a lighter compound (Milman, 2015).

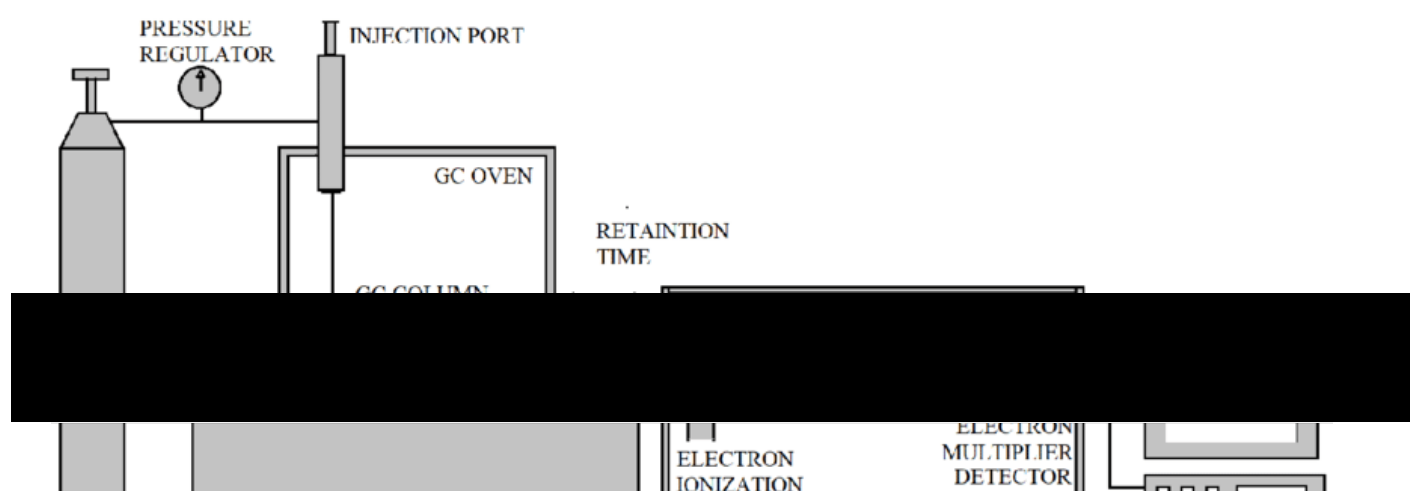


Figure 4: Gas chromatography/ Mass spectrometry diagram (Kolapkar, 2018)

MS essentially has three main components, the ionisation chamber, which is a metal heated coil; this coil emits electrons that strike the compounds, the electrons repeatedly strike the compounds, thus creating positive ions. The next component is the mass analyser, the positive ions are pushed along by the repulsive forces of the positive plates. The ions are then exposed to magnetic fields forcing them to move about in various directions, this can be quantified by their individual mass to charge ratio (m/z). The lighter ions will be deflected much more than the heavier ions. The final component of the system is the detector, which records the movement of the ions and thus creates a mass spectrum. The relative abundance of each ion is plotted against the m/z as shown in Figure 5. Table 4 compares the advantages and disadvantages of GC- and HPLC- based techniques.

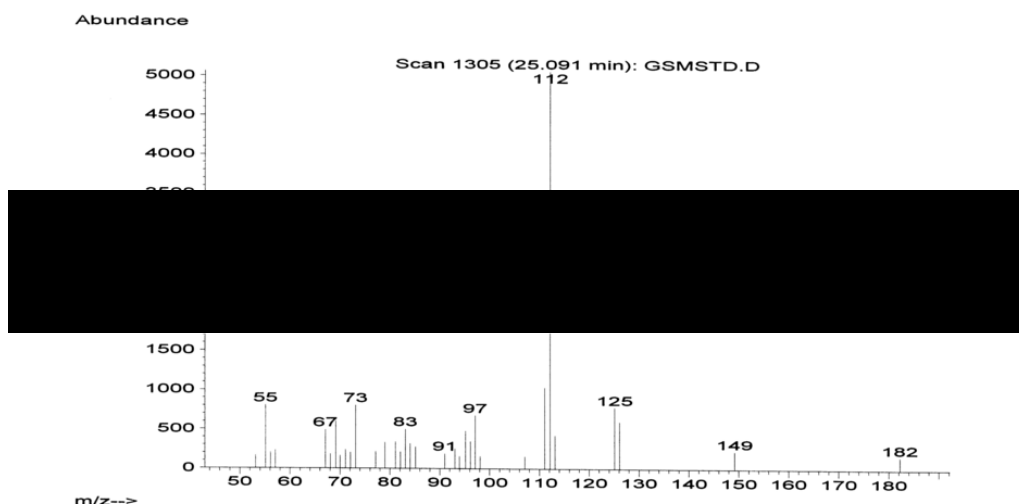


Figure 5: Mass spectrum of geosmin (Watson, Brownlee, Satchwill, & Hargeshimer, 2000)

Table 4: Advantages and disadvantages of HPLC and GC (Wu et al., 2014)

Chromatography		Advantages	Disadvantages
HPLC	UV	Low cost, simplicity, rapidity, can simultaneously detect nitrite and nitrate for sample with little interference.	Relatively low sensitivity, interference with chloride at 210-220 nm.
	CL	High sensitivity, can detect small samples.	Inability to directly detect nitrite, complicated reactions, interference with NOS inhibitor and some compounds.
	Fluorescence	High sensitivity, rapidity and simplicity, there is no interference.	It needs reaction for the determination of G-MIB
	MS	High sensitivity rapidity and simplicity, there is no interference.	It needs reaction for the determination of G-MIB
GC	NPD, ECD, FID	High sensitivity, rapidity, wide linear range and low cost.	Complicated sample pre-treatment
	MS	High sensitivity rapidity and simplicity, there is no interference, ability to simultaneously detect nitrite and nitrate by the reaction with PFB-Br, can evaluate the actions of other NO products.	Complicated sample pre-treatment.

2.5.3 Fluorescence spectrometry

Fluorescence spectrometry can be used to detect and potentially quantify geosmin and MIB within sample solutions (Sharma, 1998). Fluorescence is an optical process during which molecules emit light. The specific absorbance and emission wavelengths of a molecule that absorbs and emits light are unique to that molecule. Most molecules occupy the lowest vibrational level at room temperature, ground state. Once the light is absorbed, the molecule

is elevated to an excited state. Once the molecules have reached the higher vibrational levels, the molecules rapidly lose the vibrational energy due to colliding with other molecules and thus falls down to lower vibrational levels in the excited state (Valeur, 2002).

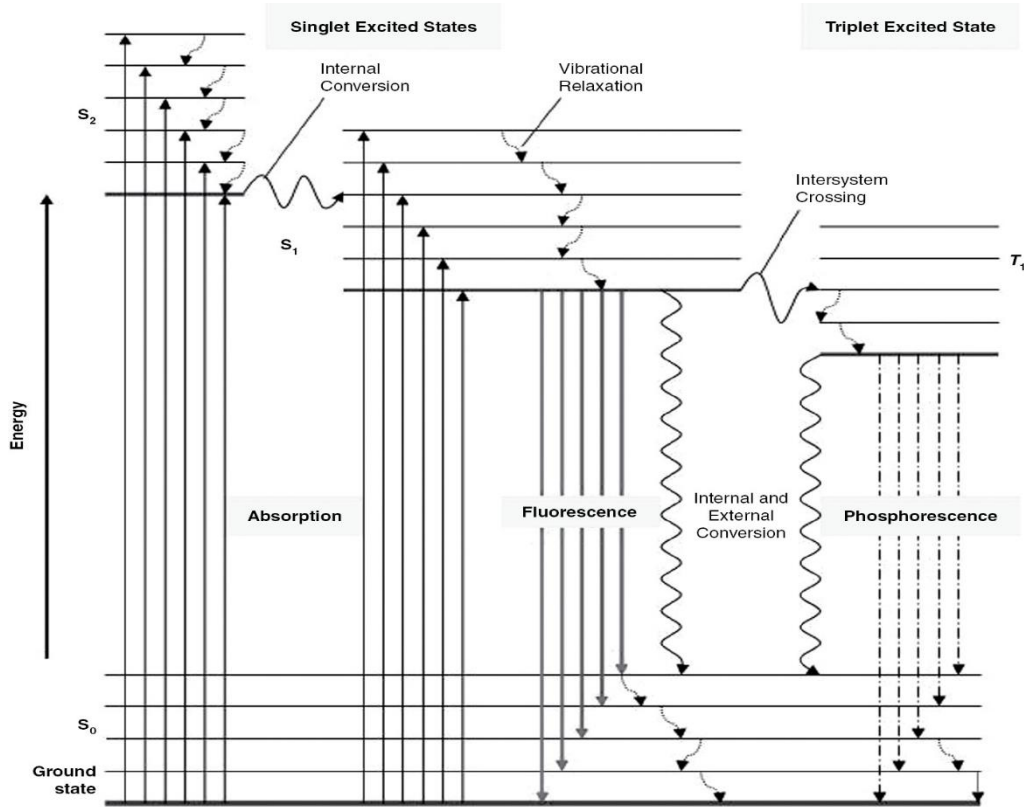


Figure 6: Fluorescence absorption and emission spectra (Coble, 2014) λ_1

Figure 6 shows the absorption of light produces molecules that elevated to the first S_1 or second S_2 excited state (Kasha, 1950). Molecules slowly fall to lower vibrational excitation levels. Once the molecules are at the lowest vibrational level of the first excited state (S_1), they then can return to the ground state excitation levels, during which energy is emitted; this is fluorescence.

The intensity of the incident beam is independent of the fraction of a parallel beam of light absorbed by a sample and is related to the concentration of the absorbing species by the Beer-Lambert Law as seen in Equation (2.8).

$$\log_{10} \frac{I_0}{I} = EcL \quad (2.8)$$

where I is the intensity of transmitted light, I_0 is the intensity of incident light, E is the molecular extinction coefficient, C is the concentration, L is the pathlength of the sample.

$\log_{10} \frac{I_0}{I}$ is known as the optical density of the sample.

2.6 Activated carbon

Activated carbon is the most widely used absorbent in the drinking water industry. Activated carbon has a great microporous structure which gives it a huge internal surface area and porosity making it an excellent adsorbent for removing organic and inorganic contaminants. Being non-polar, activated carbons adsorb non-polar substances in preference to polar substances while its porous structure defines the extent of adsorption (Rodriguez-Reinoso & Silvestre-Albero, 2016).

2.6.1 History of activated carbon

Activated carbon has been used for over two centuries because of its versatile and unique properties. The powerful adsorptive strength of activated carbon was first discovered in 1773 by Scheele who conducted experiments with gases (Allen & Whitten, 1998). The industrial production of activated carbon started in the 19th century due to Ostrejko setting the basis for developing the commercial activated carbon (Allen & Whitten, 1998).

2.6.2 Preparation of activated carbon

Many carbonaceous materials can be used in the production of activated carbon including wood, petroleum coke, and bituminous coals because of their high carbon content. Other substances like agricultural wastes and by-products, hazelnuts and coconuts are also used to produce AC (Cuhadaroglu & Uygun, 2008).

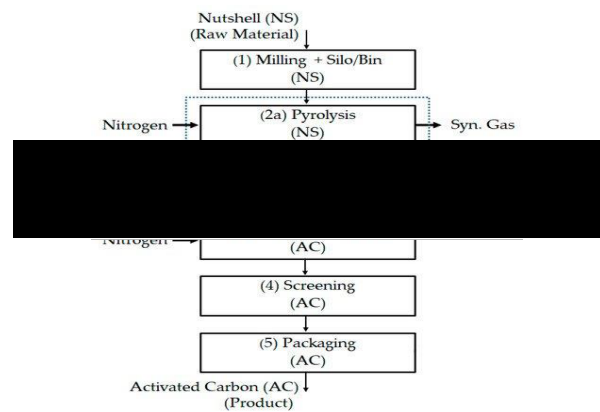


Figure 7: Production of activated carbon (Leon, Silva, Carrasco, & Barrientos, 2020)

The structure of activated carbon is like graphite; there are only minor differences; the structure is more random and unorganised than graphite. When the carbon is in the process of activation, the regular array of carbon bonds at the surface becomes disturbed, which produces highly reactive free radicals (Safe Drinking Water Committee, 1980).

2.6.3 Carbonisation

Carbonisation is a process where material rich in carbon are converted into a carbon char using high temperatures (max of 800°C) in the absence of oxygen. Carbonisation is a form of

slow pyrolysis, which aims to produce char as a product, whereas pyrolysis applies higher heating rates to produce pyrolytic liquids and gases instead of char. During carbonisation, syngas and bio-liquids are formed as by-products, they have been suggested as a means of maintaining the thermal process (Strezov et al., 2007). Carbonisation removes almost all non-carbon elements, including hydrogen, oxygen, sulphur, and nitrogen. The conversion into char varies depending on the amount of carbon being removed with oxygen and hydrogen in the form of carbon oxides and hydrocarbons (Antal & Gronli, 2003). Carbonisation can be simplified into three steps. The first step is the loss of some light volatiles and moisture. The primary formation of the char takes place in the second step, during this step, liquid fractions evolve, and carbon oxides form at a high rate. The third step is secondary carbonisation at higher temperatures (Glassman, Yetter, & Glumac, 2014). Complex hydrocarbons are typically detected below 600°C, they are the main product of the secondary cracking of the liquid compounds and the dominant reaction is the condensation of carbon char at over 600°C (Strezov et al., 2007; Wigmans, 1989). A structure of randomly cross-linked flat aromatic sheets (forming the porous structure) is the final carbonisation product. The pore structure during this point is not fully developed due to it being filled with tarlike materials. These tarlike materials are a by-product of secondary reactions. The char produced during this stage has a low adsorptive capacity and thus needs a further activation stage to improve the activated carbon's porosity (Wigmans, 1989).

2.6.4 Activation

The activation process is used to enhance the porous structure of the char. The final properties of the activated carbon are high due to the activation step. The initial part of the

activation step is to remove the disorganised carbon produced after carbonisation and open the blocked-up pores. The porous structure is then further developed, resulting in micropores' formation, widening existing pores, and creating larger size pores by burning away the walls between pores (Bansal & Goyal, 2005). The extent of the carbon burn-off indicates the degree of activation at this stage. The two most common processes for preparing activated carbon are chemical and physical activation. Physical activation involves carbonisation of the raw materials and then thermal activation whereas, chemical activation involves the addition of a chemical agent and carbonisation simultaneously.

Physical activation is a two-step process: firstly, the raw material is carbonised at around 800°C in completely oxygen-depleted conditions. This step is essentially changing the raw material into charcoal, the charcoal has a low surface area and is not active (Cuhadaroglu & Uygun, 2008; Manocha, 2003). The next step is to change the non-active charcoal to activated carbon, this is performed by activation utilising high temperatures of around 900°C in a highly oxidised environment (such as CO₂), this also converts the low surface area of the charcoal to a high surface area. Chemical activation is a single-step process where carbonisation and activation of the raw material are conducted simultaneously (Buczek, 2016). Firstly; raw material is mixed with a specific activating agent, acting as a dehydrating agent and oxidant in order to destroy the structure (Cuhadaroglu & Uygun, 2008; Manocha, 2003). The treated material is concurrently carbonised in an airless environment at around 400 - 800°C, this allows pyrolytic disintegration to be reached (Cuhadaroglu & Uygun, 2008; Manocha, 2003). Chemical activation is a well-established activation method, it is more practical than physical activation and has many advantages compared to physical activation. One of the main advantages of chemical activation is that the obtained activated carbon has a very high surface area, therefore, is much more efficient than a physically activated (Cuhadaroglu &

Uygun, 2008; Manocha, 2003). There are many other advantages of chemical activation over physical: activation temperature is much lower, thus less energy needed (El-Hendawy, Alexander, Andrews, & Forrest, 2008), higher yields, single-step activation, creates a better porous network and has a shorter activation time (Nowicki, Pletrzak, & Wachowska, 2008).

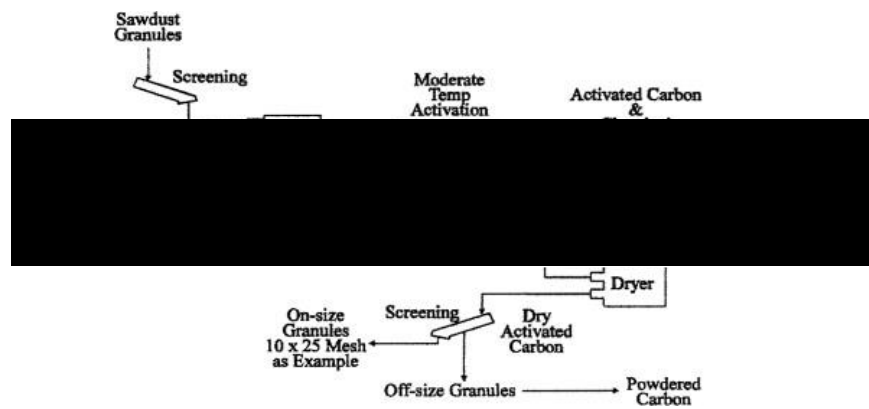


Figure 8: Process of chemical activation for wood precursor (Johnson, Setsuda, & Williams, 1999)

There are many different raw materials used to produce activated carbon. The activation method has a considerable effect on the properties of the final product as shown in Table 5.

Table 5: Properties of a variety of PAC's (Crittenden, 2012)

Pac Type	PAC-20B Atochem, A	Nuchar SA-20 Westvaco, B	HydroDarco B American Norit, C	WaterCarb Acticarb, D	WPL Calgon, E
Carbon source	Bituminous coal	wood	Lignite	Wood	Bituminous coal
Activation method	Steam	Phosphoric acid and steam	Steam (1000°C) rotary kiln	Steam (1600°C)	Steam (800 - 1050°C)
Iodine number (mg/g)	848	1040	547	604	897
Tannin value	750	30	281	1115	952
Molasses number	204	1076	286	113	179
Molasses decolour index	4.72	25.17	16.15	0.70	4.32
Phenol value	2.4	5.1	3.5	2.0	2.4
Percent ash %	11.2	4.5	28.7	5.6	6.6
Pore volume (mL/g)	0.494	1.258	0.555	0.280	0.214
Mean particle size (µm)	28.9	46.27	23.44	48.54	21.36
Median particle size (µm)	23.47	38.72	19.63	30.8	16.77
Modal particle size (µm)	35.52	56.00	32.43	32.43	32.43

2.6.5 Structure of activated carbon

Activated carbon can be distinguished from elemental carbon by removing all non-carbon impurities and the oxidation of the carbon surface. Activated carbon is defined as being made up of a graphite structure and as primarily an amorphous solid with a large internal surface area and pore volume (Callewaert, 2014). Activated carbon can be defined as a porous material predominantly formed with carbon and characterised by a well-developed porosity. The commonly known feature of activated carbon is its graphite-like planes (which shows a varying degree of disorientation, the space between these planes results in porosity) this is shown in Figure 9.

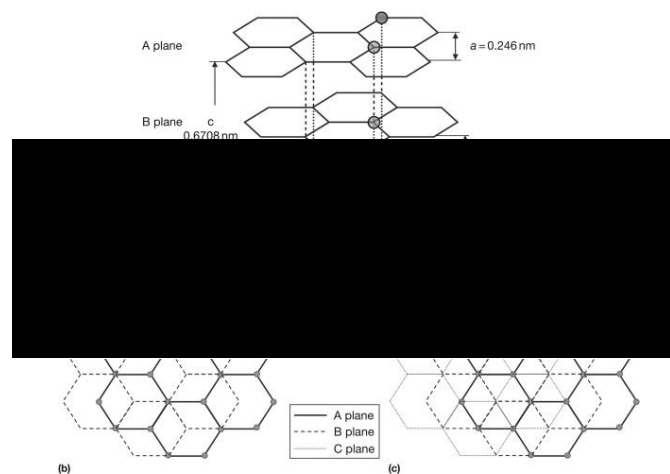


Figure 9: Graphite planes structure (Marsh, 2006)

2.5.5.1 Porous structure

The adsorptive capacity of activated carbon is due to the porous characteristics (surface area, pore-volume, pore size distributions). During the carbonisation process, the porous structure of activated carbon was formed. During the activation step, the spaces between the elementary crystallites are removed of tar and other carbonaceous material built up, this tar is disorganised carbon, once removed, the crystallites are exposed to the activating agent, leading to the activation development of the porous structure. The raw material and the activation method employed determines the pore structure and pore distribution of the activated carbon. The porous system within activated carbon has a wide variety of different kinds of pores, and the individual pores vary significantly concerning the size and shape (Bansal & Goyal, 2005).

Generally, the structure of standard types of active carbons are layers of hexagons. They contain micropores (18-20 Å), transitional pores (40-200 Å) and macropores (500-20000 Å)

(Suffet, 1980). Within the activated carbon, there is a variety of structural consistency in the carbon structure. Table 6 shows an example of activated carbons content. All activated carbons have a porous structure containing up to 15% of mineral matter in the form of ash content (Bubanale, 2017). Activated carbon's proximate analysis separates activated carbon into ash, volatile matter, and fixed carbon.

Table 6: Proximate analysis of an activated carbon sample (Cuhadaroglu & Uygun, 2008)

Ash (%)	Volatile matter (%)	Fixed carbon (%)
10.10	35.60	54.30

Activated carbon is essentially a crude form of graphite, it has an entirely random and amorphous structure. This random structure is highly porous, with various pore sizes. There are some visible cracks and or crevices, these cracks and crevices are as small as molecular dimensions. The size of the activated carbon pore and the pores specific function can be used to classify the individual pore type. When classifying the pores concerning the function of the pores, there are two main pore classifications adsorption and transport pores (Callewaert, 2014). Adsorption pores are the pores within the activated carbon with enough adsorption forces to adsorb geosmin and MIB. Adsorption pores are smaller than transport pores. The other classification is transport pores, they are large pores inside the particles, they can be as vast as visible cracks and cervices. Their structures consist of a variety of different sizes and shapes (Callewaert, 2014).

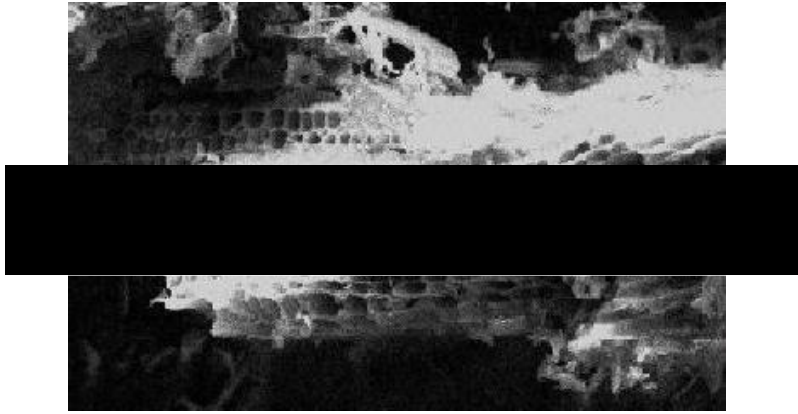


Figure 10: Activated carbons porous structure (Callewaert, 2014)

Activated carbon pores can be recognised by their size, as stated by IUPAC (International Union of Pure and Applied Chemistry). They distinguish different pores purely by their size, three types of pores: macropores, mesopores and micropores (Callewaert, 2014).

Table 7: Classification of pores sizes (IUPAC) (Bubanale, 2017)

Pores	Size
Micropores	< 2nm (20° A)
Mesopores	2 - 50 nm (20 – 500 ° A)
Macropores	> 50 nm (500° A)

In micropores, as the radii are less than 2 nm, the adsorption in the micropores occurs through volume filling in the form of adsorption taking place in micropores with no capillary condensation. The pore volume of micropores ranges from around 0.15 – 0.70 cm³/g and contribute up to 95% of the total surface area (Manocha, 2003). The micropores can be further classified into two microporous regions, which are supermicropores (0.7-2.0 nm diameter) and ultramicropores (<0.7nm diameter) (Manocha, 2003). The most common characterisation methods of the microporous region are through gas and vapour adsorption.

Mesopores only contribute to around 5% of the total surface area and have a volume of 0.1 – 0.2 cm³/g. Mesopores have capillary condensation and adsorption/desorption hysteresis, which are the characteristic features of mesopores (Aworn, Thiravetyan, & Nakbanpote, 2008; Hao et al., 2011; Lei, Miyamoto, Kanoh, Nakahigashi, & Kaneko, 2006). Mesopores are also referred to as transitional pores. The volume and surface area of the mesopore can be enhanced using unique methods; the enhanced mesopores attain a volume of 0.2 to 0.65 cm³/g and a surface area of 200 m²/g. The primary role of mesopores is to act as channels that lead to the adsorbate molecules to the microporous network. Mesopores are commonly characterised by adsorption-desorption isotherms, mercury porosimetry, and electron microscopy (Liou, 2010; Zhu, Li, Yan, Liu, & Zhang, 2007).

Macropores have a minimal contribution to the total surface area and pore volume, their pore volumes do not exceed 0.2 to 0.4 cm³/g and the surface area does not exceed 0.5m²/g. Macropores do not aid the adsorption process but act as transport tunnels for the adsorbates from the surface of the activated carbon to the mesopores and micropores. Macropores can be characterised by mercury porosimetry and electron microscopy (Duran-Valle, Gomez-Corzo, Pastor-Villegas, & Gomez-Serrano, 2005).

Few of the micropores lead to the outer surface of the carbon particle. So, as a guide, typically, macropores reach the surface and form cracks or cervices on the particle's outer surface, transitional pores branch from the macropores and micropores, as shown in Figure 11. The micropores make up, on average, about 73% of the total adsorption pore volume, up to 95% of total surface area; therefore, the micropores are the most crucial part of the porous network in aid of adsorption (Manocha, 2003).

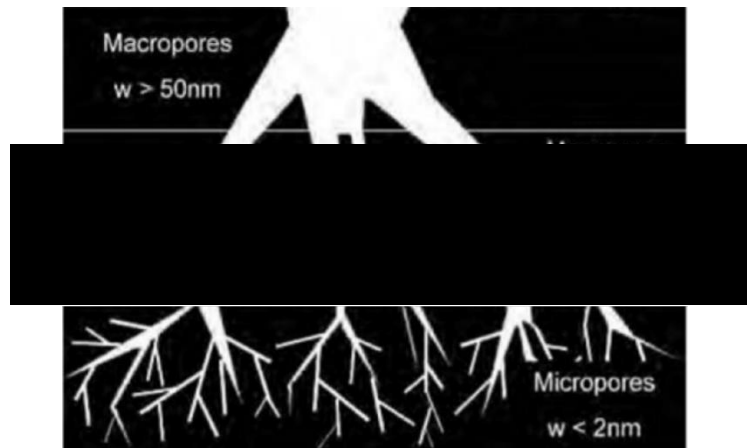


Figure 11: Representation of the porous structure of activated carbon (Bubanale, 2017)

2.5.5.2 Crystalline structure

As carbonisation and activation occur in the preparation of activated carbons, the microcrystalline structure of activated carbons is created. The structure is like disordered graphite layers with fragile interlayer connections. The interlayers are the main component that causes graphite and activated carbons to differ structurally (Bubanale, 2017). The interlayer spacing for activated carbon is 0.34 to 0.35 nm, whereas, for graphite, it is 0.335 nm (Bubanale, 2017). The graphite structure is very similar to that of the structural unit of activated carbon. The graphite crystal comprises a layer of fused hexagons held together by weak Van der Waals forces this is seen in Figure 12 (Marsh, 2006).

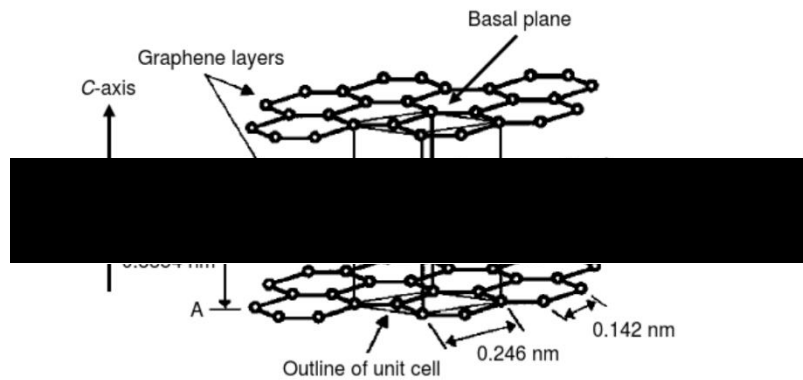


Figure 12: The hexagonal structure of activated carbon (Marsh, 2006)

Literature suggests that activated carbon has a modified graphite layer structure. Throughout the carbonisation process, free valences are created this is due to the bonding disruption of the micro-crystallites being regular. The pores in the microcrystalline structure are affected by the process conditions and the existence of impurities (Skubiszewska-Zieba, 2010; Yang & Lua, 2006).

There are two types that activated carbons are classified into, the two types are based on their graphitising ability, they are classified as graphitising and non-graphitising carbons. The graphitising carbons contain several graphene layers parallel to each other (Bubanale, 2017); the graphene layers are aromatic carbon sheets in groups of 3 to 30 layers. The graphitising carbon is delicate, it has weak cross-linking between the individual microcrystal layers, also the porous network is poorly developed. Non-graphitising carbons have strong cross-linking between the individual microcrystal layers and a well-developed porous network (Bubanale, 2017). To promote the formation of substantial cross-linking of non-graphitising structures, the presence of oxygen or low hydrogen in the raw material is introduced to produce the activated carbon (Bubanale, 2017). Figure 13 shows a schematic representation of the graphitising and non-graphitising structures of carbon.

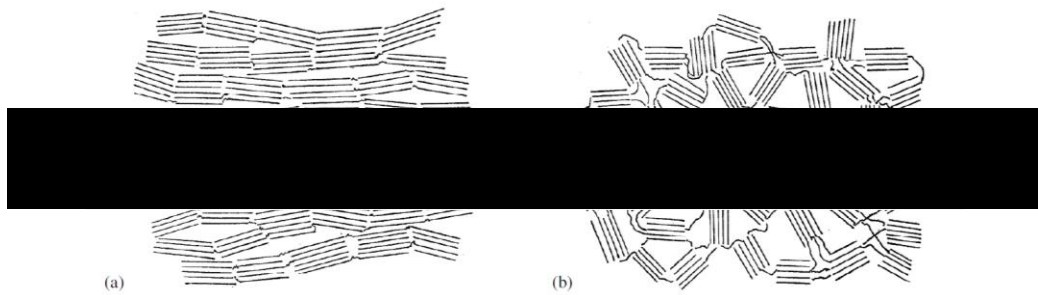


Figure 13: Representation of the activated carbons: (a) Graphitized (b) Non-graphitized (Bubanale, 2017)

The porous and crystalline structures explain why activated carbon is an excellent absorbent, but the chemical structure is also imperative. The porous structure evaluates the adsorption capacity, but the small amounts of chemically bonded oxygen and hydrogen atoms strongly influences the adsorption capacity (Bubanale, 2017). The electron clouds' arrangement varies the chance that unpaired electrons and incompletely saturated valences are created. The electrons and valences influence the adsorption properties of active carbons, mainly for polar compounds (Bubanale, 2017).

2.5.5.3 Chemical structure

The adsorption capacity is dependent on the surface chemistry within the activated carbon. Heterogeneity on the surface of activated carbon significantly results from the surface oxygen groups even in small quantities. The change in the surface oxygen groups affects the surface properties such as acidity on the surface, polarity or hydrophobicity and the charge on the surface (Çeçen & Aktas, 2012). The adsorption capacity of the activate carbon is reduced with an increase in the amount of heterogenous oxygen groups on the surface, the reduction is

because of the hydrogen bonds from the oxygen groups adsorbing water molecules. Activated carbon is a non-polar compound as the oxygen groups are increased the polarity of the surface increases. The increase in polarity adversely induces an increase in adsorption of water molecules which may block carbon pores when clustered (Çeçen & Aktas, 2012). The water clusters reduce the adsorbate interaction with the activated carbon surface, thus block the adsorbates entry to the micropores. The van der Waals forces of interaction are reduced due to oxygen groups forming on the surface because they are involved in the depletion of π -band of graphite layers (Çeçen & Aktas, 2012).

Activated carbon is associated with high amounts of oxygen, hydrogen and other heteroatoms, e.g. sulphur, nitrogen and halogens (Rodriguez-Reinoso, Molinasabio, & Munecas, 1992; Valix, Cheung, & Zhang, 2006). The heteroatoms are formed from the raw material and thus become part of the structure during the carbonisation process, or they could become chemically bonded to the surface during activation (Rodriguez-Reinoso, 1998). The heteroatoms are bonded to carbon atoms, generally on the edges and corners of the aromatic ring, or they are bonded to carbons at flawed positions to form carbon-oxygen, carbon-hydrogen, carbon-sulphur, carbon-nitrogen and carbon-halogen compounds, these are known as surface compounds, and they can be measured (Valix et al., 2006). The oxygen heteroatom is the most influential heteroatom as it affects the surface behaviour, wettability and the electrical and catalytic properties of the carbon (Boehm, 1994). The oxygen-containing functional group can be obtained through oxidation treatments like ozonation of activated carbon.

2.6.6 Activated carbon applications

Activated carbon has unique and versatile adsorptive properties, thus, it is used in various industries for processes ranging from purification to separation. Its main applications include removal of colour, taste and odour, undesirable organic and inorganic impurities from drinking water, treatment of industrial waste, purification of many chemicals, food and pharmaceutical products, in a variety of gas-phase applications (Çeçen & Aktas, 2012). Moreover, activated carbon has been applied in solvent recovery, gold and silver recovery and in applications as a catalyst and catalyst support (Bansal & Goyal, 2005). Generally, the main applications for activated carbon are liquid and gas phase adsorption. Roughly 80% of the total activated carbon is used for liquid phase applications, including GAC and PAC (Moreno-Castilla & Rivera-Utrilla, 2001). In gas-phase applications, GAC is usually used instead of PAC.

Table 8: Application of activated Carbon (Bansal & Goyal, 2005)

Types of applications	Activated carbon applications
Liquid Phase	<ul style="list-style-type: none"> – Municipal water treatment: Taste and odour removal - micropollutant removal (e.g. pesticides, THMs). – Domestic water treatment: Jug filters, in-line filters, cartridge filters, coffee makers. – Process water treatment: hydrocarbon removal from condensate, trace organics removal – Wastewater and ground water treatment: Trace organics removal. – Food industry: Oil removal from beverages, removal of undesirable flavours and improve colour, decaffeination of coffee beans. – Sugar, oil and fat refining: To improve colour, higher rates of crystallisation (sugar industry). – Medicine: removal of infectious toxins, treating gastritis and poisoning caused by mushrooms, food, phenols and phosphorus. – Gold and silver recovery.
Gas Phase	<ul style="list-style-type: none"> – Gas purification: Hydrogen, natural gas, carbon dioxide, landfill gas. – Air treatment: Decolourisation, vapour removal (e.g. vent filters, anaesthetics, compressed air) – solvent recovery - ductless fume cupboards, war gas protection filters, industrial and military respirators, incinerator flue gas, cooker hoods, deep fryers.
Miscellaneous	<ul style="list-style-type: none"> – Nonwoven fabric (e.g. NBC suiting), impregnated fibre, foam and paper, cigarette filters, catalysts and catalyst support, radioactive vapour containment and delay beds, land remediation.

2.7 Classification of activated carbon

It is challenging to classify activated carbons on their preparation methods, surface characteristics and physical properties. The standard classification of activated carbon is solely based on particle size. Using this classification method, activated carbon can be split into powdered activated carbon (PAC), granular activated carbon (GAC), and activated carbon fibres (ACF) (Babel & Kurniawan, 2004).

2.7.1 Granular activated carbon (GAC)

Granular activated carbon (GAC) has large particle sizes (0.6 to 0.4 mm) compared to powdered activated carbon (15 – 25 µm). Therefore, GAC has a smaller external surface area compared to that of PAC. GAC is typically used for a continuous process, for both liquid and gas phase treatment. GAC is more desirable than PAC for specific applications because it has a well-established micropore size distribution, high density, high hardness and a low abrasion index (Hijnen, Suylen, Bahlman, Brouwer-Hanzens, & Medema, 2010; Scharf, Johnston, Semmens, & Hozalski, 2010). GAC also offers a lower pressure drop, and it can be regenerated after becoming spent more than once.

In water treatment, GAC is commonly used in filtration beds to remove, amongst other organic contaminants, geosmin and MIB to concentrations below or equal to the OTC until it is completely saturated. As the contact time of water with GAC increases, the higher the removal of geosmin and MIB when virgin GAC is used. In a study conducted by Srinivasan & Sorial (2011), increasing the contact time from 3 min to 14 mins drastically increased the removal of geosmin from 43% to about 78% and for MIB from 43% to about 66% . Therefore the increased contact time can increase the removal rates. The problem with GAC is that it is effective at removing geosmin and MIB for a period of time of around 2-5 years when used in industry, dependent on the flowrate and contaminants present. However, after this period of time, the removal rates can start to drop leading to the concentration of geosmin and MIB eventually rising above the OTC. The main reason for GAC being spent quickly is due to competitive adsorption of organic matter in the water, this adsorption can reduce the performance of GAC significantly (Srinivasan & Sorial, 2011).

Wood-based GAC's have a better breakthrough behaviour than coal-based GAC's, but their adsorption of MIB is significantly lower than coal-based GAC's (Srinivasan & Sorial, 2011).

Table 9: Properties of different activated carbons (Crittenden 2012)

Adsorbent	Manufacturer	Type	Surface area (m ² /g)	Packed Bed Density (g/cm)	Pore Volume (cm ³ /g)
Filtrisorb 300 (8 x30)	Calgon	GAC	950-1050	0.48	0.851
Filtrisorb 400	Calgon	GAC	1075	0.40	1.071
CC-602	US Filter/Wastates	Coconut-shell based GAC	1150-1250	0.47-0.52	0.564
Aqua Nuchar	MWV	PAC	1400-1800	0.21-0.37	1.3-1.5

Different types of GAC's and PAC's are used in industry (Table 9). The properties for each GAC shown in Table 9 are relatively similar, except for the overall pore volume which varies with the activation method used for GAC. GAC can readily control the toxic organic compounds that reside in the water by adsorption of the toxic compounds onto the surface area of the GAC, thus removing them from the water stream. GAC is an exceptional barrier to spikes of geosmin and MIB, even when the concentrations of geosmin and MIB drastically increased, GAC still removes the vast majority of geosmin and MIB (Crittenden, 2012). Some advantages of GAC are: GAC is very easily reactivated, the reactivated GAC can have an efficiency close to that of virgin GAC, GAC also has a lower carbon usage rate per volume of water treated when in comparison with PAC (Crittenden, 2012). On the other hand, the disadvantages of GAC are: GAC is challenging to distribute the flow and replace the exhausted carbon, GAC adsorbed compounds can sometimes desorb and thus appear in the treated water stream (Crittenden, 2012).

2.7.2 Powdered activated carbon (PAC)

PAC usually is in the form of powders or very fine granules. The average diameter of PAC is roughly 15 – 25 μm . Due to its small particle size, PAC has an enormous surface area and small diffusion distances (Manocha, 2003). Typical applications for PAC are industrial and municipal wastewater treatment, food industry, sugar decolourisation, pharmaceutical and dioxin and mercury removal (Cook, Newcombe, & Sztajn bok, 2001; Ormad, Miguel, Claver, Matesanz, & Ovelleiro, 2008).

Every water treatment plant is different, but most commonly, PAC is added at the intake or at the flocculation or sedimentation basins. PAC is the most common technology used for geosmin and MIB removal. PAC allows the water industry to adjust the dosage depending on the severity of the seasonal outbreak of taste and odour (Srinivasan & Sorial, 2011). PAC can be used when necessary, therefore, it excels in seasonal odour spikes.

Table 10: Properties of GAC and PAC (Greenbank & Knepper, 2002)

Activated carbon type	Granular	Powdered
Normal starting material	Coal-based	Coal- based
Mesh size	12X40	95 percent pass through 325 mesh
Mean particle Diameter (mm)	1	0.043
Particle per gram	2,200	24,000,000
Rate if adsorption CHCl_3	1/40 of PAC	40 times GAC
Particle shape	Spheroid – 0.72 sphericity	Spheroid – 0.72 sphericity
Bulk density (g/cc)	0.48	0.48 (tamp density)
Transport pore size	<10 microns	Same as GAC
Adsorption pore size	Same as PAC	Same as GAC
Cost	Two times more than PAC	Half of GAC

PAC is much cheaper than GAC and is made of much smaller particles. Industries usually do not reactivate PAC as it is a lot easier and more economical to replace the spent PAC. PAC has

faster reaction kinetics due to its small particle size (10-100 times smaller than GAC), which drastically increases the rate of adsorption of geosmin and MIB onto the surface of the PAC. GAC is often pulverised to form PAC sludge (Crittenden, 2012). The number of particles in PAC is more significant than in GAC, which leads to an increase in the PAC contact with the water. The tiny particles keep the PAC suspended with agitation and makes PAC more readily dispersed sludge (Crittenden, 2012). The main disadvantage of PAC is that it must be used in a batch process, whereas GAC can be used in a continuous process. PAC has to be used in a batch process because of the time it takes for geosmin and MIB to diffuse and contact the particle's exterior. Contact time takes around a few hours for most of the taste and odour chemicals to be removed using PAC, while for GAC bed filters, the contact time varies. Ndiongue et al. (2006) conducted an experiment where the contact time was as low as 5 minutes and achieved a geosmin removal rate of 83%. PAC is complicated to reactivate and impractical to recover from the coagulation sludge (Crittenden, 2012).

2.8 Characterisation of activated carbons

Activated carbons have various pores sizes (macropores, mesopores and micropores), which makes activated carbon to be prominently heterogenous. There are many functional groups on the surface of activated carbon such as oxygen and hydroxyl groups.

Characterisation of activated carbon can be obtained by applying various techniques including Brunauer-Emmett-Teller (BET), pH point of zero charge experiments, iodine number experiments, methylene blue number experiments and Fourier transform infrared spectroscopy measurement experiments. Activated carbon can also be analysed using gas and dye adsorption. The data obtained from these analyses can be used to determine porosity

and surface area. This data can then be used to determine the adsorption capacity of activated carbon.

The chemical structure of activated carbon can be determined using Fourier transform infrared spectroscopy measurement (FTIR) spectroscopy, which is a common spectroscopic method of analysis of activated carbons' chemical structure (Islam, Aug, Gharehkhani, & Affi, 2015).

2.9 Adsorption

Adsorption is essentially a mass transfer process where compounds in the liquid phase are adsorbed on a solid phase. Thus, this process physically removes contaminants from the liquid phase (Piccin, Pinto, & Cadaval, 2017). Geosmin and MIB are adsorbed onto the surface of activated carbon, removing them from the liquid phase. The compound that is adsorbed is known as the adsorbate, and the solid that the adsorbate adsorbed onto is the adsorbent (Everett & Koopal, 1971). When the adsorption operation occurs, dissolved compounds are transported into the porous solid by diffusion. Once the compounds have diffused, they are then adsorbed onto the inner surface.

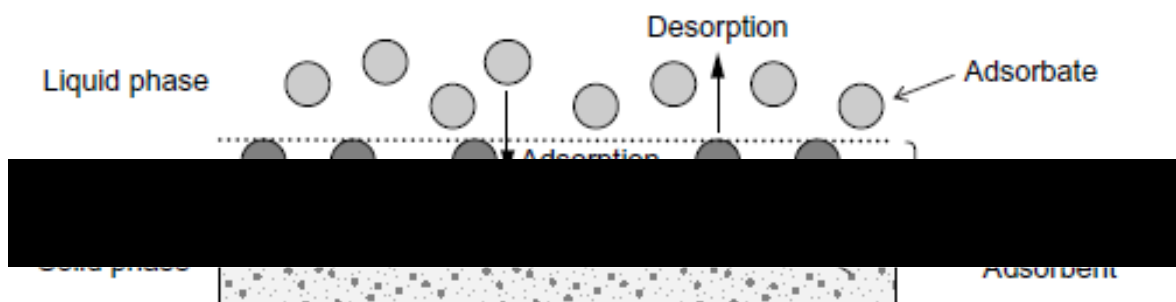


Figure 14: Basic representation of the adsorption process (Worch, 2012)

There are two main adsorption mechanisms chemical (chemisorption) and physical adsorption (physisorption). Chemisorption is based on a chemical reaction that transfers electrons between the adsorbent and adsorbate, causing a chemical bond with the surface (Everett & Koopal, 1971). Chemisorption causes the adsorbate to chemically bond to the surface, resulting in chemisorption being irreversible. Chemisorption is not the adsorption mechanism that takes place between activated carbon and taste and odour compounds, but it is physical adsorption instead. Physical adsorption caused by the binding mechanisms like van der Waals forces, which cause the adsorption to be a rapid process. Unlike chemisorption, physical adsorption is reversible as the adsorbate can desorb off the adsorbent (Everett & Koopal, 1971). Adsorption takes place in three main steps; these are shown in Figure 15. The initial step is the diffusion of the geosmin and MIB onto the activated carbons outer surface; then, the adsorbates travel down the porous structure through the mesopores, the macropores and the micropores; finally, there is a build-up of an adsorbate monolayer.

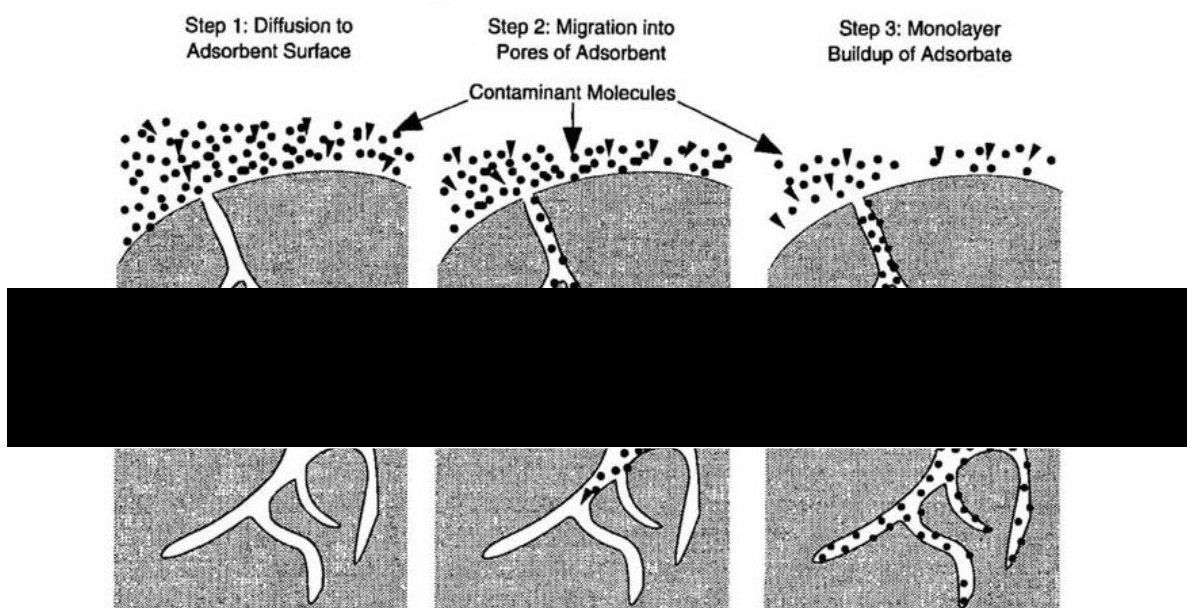


Figure 15: Three steps of adsorption onto activated carbon (Ergenekon, 2010)

During physical adsorption, the interactions that take place are water to the surface interactions, adsorbate to water interactions and adsorbate to the surface interactions (Snoeyink & Weber, 1967). If the strength of the adsorbate to surface interactions are strong compared to the adsorbate to water and water to the surface interactions, then the adsorption of the adsorbate onto the adsorbent is strong. The surface chemistry on the adsorbent is directly used to determine the strength of adsorbate to the surface of the adsorbent interactions; therefore, the surface chemistry of activated carbon determines the amount of geosmin and MIB adsorbed (Snoeyink & Weber, 1967). The solubility of geosmin and MIB determines the strength of the adsorbate and water interactions. The surface chemistry also determines the water and surface of the adsorbent interactions. Given that activated carbon is hydrophobic, the water to surface interactions are weak. However, activated carbons that have oxygen functional groups become hydrophilic, which favours interaction with water (Ania, Cabal, Parra, & Pis, 2007). Pore size and surface area are essential variables that drastically affect adsorption onto activated carbon. These variables determine how easily the adsorbates adsorb onto the surface and determine the number of potential adsorption sites. Activated carbons that possess a large surface area for adsorption result in having small pores per volume (Crittenden, 2012). There are many forces involved in adsorption and these are summarised in Table 11.

Table 11: Summary of the forces of attraction for adsorption (Crittenden, 2012)

Force	Energy of interaction KJ/mol	Interface		
		Adsorbate/ Adsorbent	Adsorbate/water	Water/adsorbent
Coulombic repulsion	>42	Yes	No	No
Coulombic attraction	>42	Yes	No	No
Ionic species-neutral species attraction		Yes	No	No
Covalent bonding	>42	Yes	No	No
Ionic species-dipole attraction	<8	Yes	Yes	Yes
Dipole-dipole attraction	<8	Yes	Yes	Yes
Dipole-Induced dipole attraction	<8	Yes	Yes	Yes
Hydrogen bonding	8-42	Yes	Yes	Yes
Van der Waal's attraction	8-42	Yes	Yes	Yes

The main force causing adsorption onto activated carbon is the London dispersion force, which is a form of Van der Waals force. The London dispersion force is an intermolecular interaction that is only within a small range between molecules (Greenbank & spotts, 1995).

There are four characterisations that distinguish London dispersion forces:

- Short ranged: The magnitude of the force is extremely sensitive to the separation of the adsorbate from the carbon plate. The force is negligible if the separation is greater than two molecular layers. The adsorptive forces can only have any effect if the gaps

in the active carbon structure are less than around five molecular layers (Greenbank & spotts, 1995).

- Additive: The sum of all the individual interactions of the adsorbate and the opposite graphite plates equal to the London forces. The significance of the adsorptive force is linked to the number of carbon plates within the adsorbate (Greenbank & spotts, 1995).
- Nonspecific: London forces are in between all molecules; thus, all molecules adsorb on activated carbon to some degree and this depends on a few variables like solubility and their vapour pressure (Greenbank & spotts, 1995).
- Temperature-independent: The adsorptive force remains constant with temperature as the temperature does not affect the London forces. The adsorptive capacities will remain sensitive to changes in temperature (Greenbank & spotts, 1995).

The pore surface diffusion model (PSDM) can be used to represent the adsorption kinetics. It explains how the adsorbate molecules diffuse from the bulk mass onto the outer surface of the activated carbon; this is called film diffusion (Crittenden, 2012). The adsorbate then diffuses into the activated carbon particle, this is called pore diffusion. Once adsorbed onto the surface, the adsorbate can then diffuse along the surface, this is called surface diffusion (Crittenden, 2012). Equation (2.9) is used to determine the flux (intraparticle),

$$J = -D_s \rho_a \frac{\delta q}{\delta r} - \frac{D_l \varepsilon_p}{\tau_p} \frac{\delta C_p}{\delta r} \quad (2.9)$$

where J is the intraparticle flux ($\text{mg}/\text{m}^2\text{s}$), D_s is the surface diffusion coefficient (m^2/s), D_p is the pore diffusion coefficient, which is equal to $\frac{D_l \varepsilon_p}{\tau_p}$ (m^2/s), ρ_a is the adsorbent particle density (kg/m^3), D_l is the liquid phase diffusion coefficient (m^2/s). ε_p is the porosity of the particle (dimensionless), τ_p is the tortuosity of the path adsorbate takes compared to the radius (dimensionless), C_p is the liquid phase concentration of the adsorbate in the pores (mg/L), q is the adsorbent phase concentration ($\text{mg adsorbate}/\text{g}$), r is the radial coordinate (m).

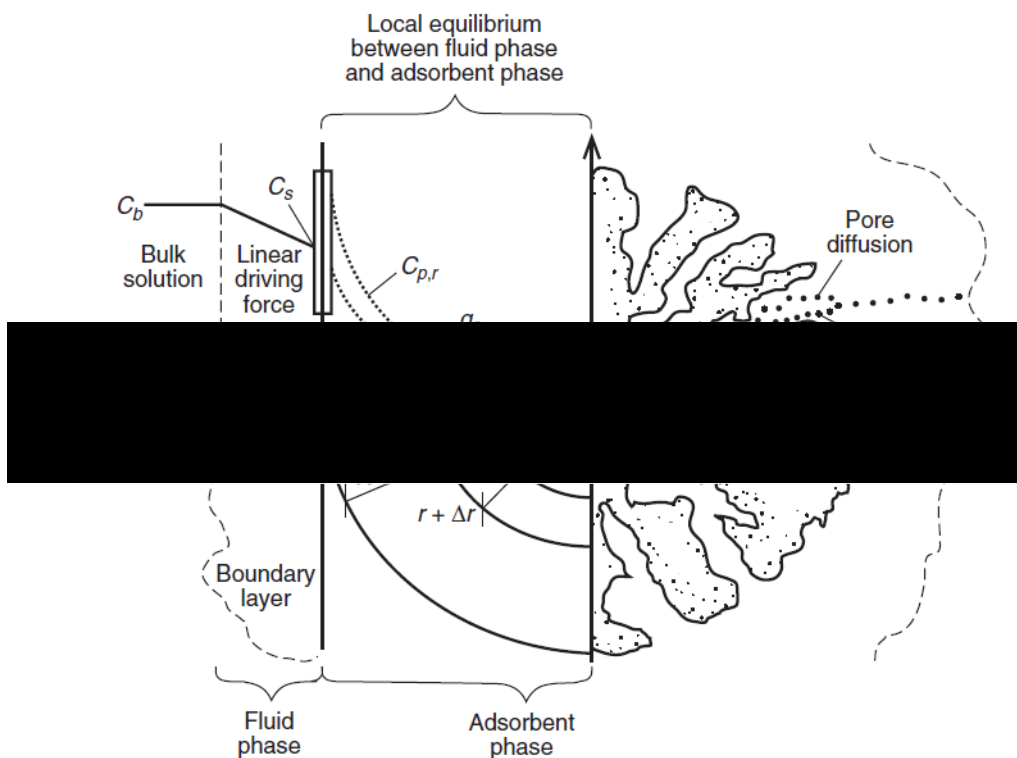


Figure 16: Mechanisms for adsorption kinetics (Crittenden, 2012).

2.9.1 Classification of adsorption Isotherms

The shape represented by the adsorption isotherm provides considerable information regarding the extent of the adsorption and, more significantly, the porous network within the

adsorbent. A variety of isotherms have been discovered through gas adsorption experiments; the majority of these isotherms can be categorised into the six classes of isotherms as shown in Figure 17. The initial five isotherms type - I to type - V were initially proposed by Brunauer et al., (1940) they were determined as the BDDT classification. The BDDT is the core of the more modern classification introduced by the IUPAC in 1985, they added a type - VI isotherm for surfaces with extremely homogeneous structures (Marsh, 2006; Sing et al., 1985).

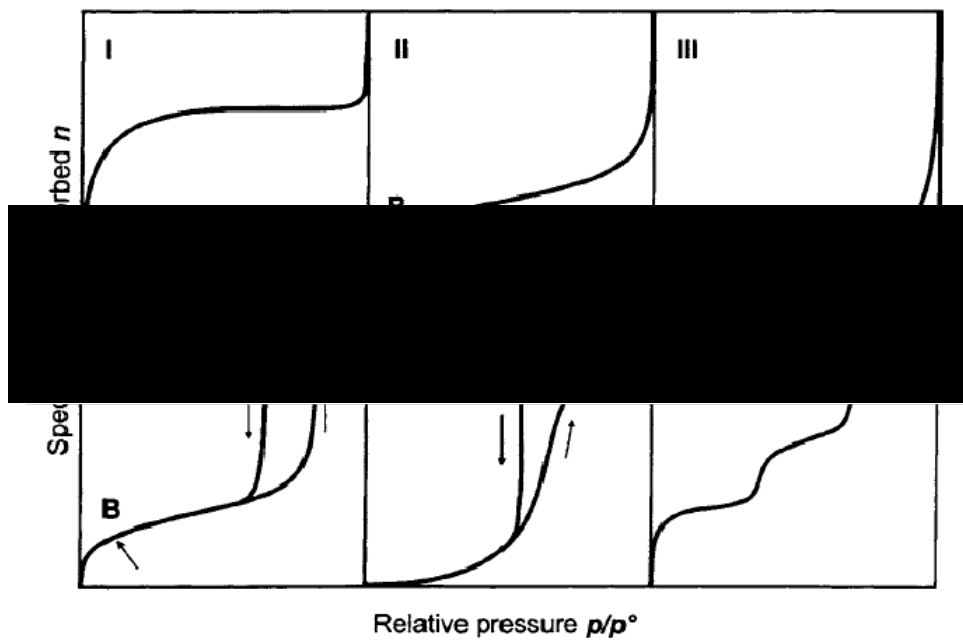


Figure 17: Types of physisorption isotherms according to the IUPAC classification (Alhamami, Doan, & Cheng, 2014)

Isotherm type I is most commonly recorded during chemisorption or physisorption in a highly microporous material like activated carbon. The plateau during this isotherm is significant as it represents the maximum monolayer capacity of the microporous structure is reached (Manocha, 2003). The gradient of the first part of the isotherm is increased with smaller micropores. The porous structure can be filled with reasonably low relative pressure due to the high interaction energy between narrow micropores (Marsh, 2006).

Type I isotherms cannot hold more than a single layer of adsorbate molecules, whereas Type II isotherms accommodate multilayer physical adsorption on non-porous solids or open surfaces, thus not having a limiting value like monolayer adsorption (Manocha, 2003). Point B, as shown in the figure, isotherm II represents the point where monolayer adsorption is finished and thus is used to calculate the monolayer capacity this was discovered by Emmett and Brunauer (1937).

Type III and V isotherms are both characterised as being concave to the pressure axis, as shown in Figure 17. The concave shape of the isotherm represents cooperative adsorption; strong adsorbate-adsorbate interactions impact the adsorption of other molecules (Bansal & Goyal, 2005). The Type V isotherms are obtained from mesoporous or microporous; on the other hand, Type III is from nonporous or highly microporous materials during the adsorption of vapours (Bansal & Goyal, 2005).

Type IV isotherm is obtained from mesoporous materials with monolayer-multilayer adsorption with capillary condensation, forming a hysteresis loop (Bansal & Goyal, 2005). The type VI isotherm is very rare. Its formation is related to layer-layer adsorption on a highly uniform surface. Examples of Type VI isotherms are the isotherms obtained from argon or krypton on graphitised carbon black whilst the temperature is constantly with liquid nitrogen at (-196°C) (Manocha, 2003).

2.9.2 Brunauer-Emmett-Teller (BET)

The surface area (S_T) value of activated carbon is then calculated using the adsorption isotherm. This isotherm is calculated over a pressure range of 0.01 to 0.3, which is done using

the standard BET (Brunauer, Emmett and Teller) method. Below is the BET equation (Ambroz & Macdonald, 2018),

$$\frac{P/P_0}{V(1 - P/P_0)} = \frac{1}{V_m C} + \frac{C - 1}{n_m C} (P/P_0) \quad (2.10)$$

where V is the volume of N_2 adsorbed (cm^3/g), V_m is the max monolayer layer capacity (cm^3/g), C is the BET constant it is related to the energy of desorption and the energy of vaporisation, the value given indicates the degree of activated carbon-nitrogen interactions (Ambroz & Macdonald, 2018). The total pore volume (V_T) of the samples is calculated using the total volume of N_2 gas adsorbed on the surface of activated carbon at high relative pressure.

Isotherms are used to characterise activated carbons. They are a graphical representation of equilibrium relationship at a constant temperature (Allen & Whitten, 1998). Isotherms are essentially used to determine the amount of adsorbate that can be adsorbed onto the surface of the adsorbent at equilibrium and constant temperature. The best two isotherms for representing the adsorptive properties of activated carbons are Langmuir (Eq. 2.11) and Freundlich (Eq. 2.12) isotherm equations given by:

$$\frac{1}{q} = \frac{1}{q_{max} K} \times \frac{1}{c} + \frac{1}{q_{max}} \quad (2.11)$$

where q is the amount of adsorbate absorbed per mass of activated carbon (mg/g), q_{max} is the limiting amount of adsorbate that can be adsorbed per mass of activated carbon (mg/g), K is

a constant, c is the concentration of the solute (mg/L) (Piccin et al., 2017). The Freundlich adsorption isotherm equation can be defined as,

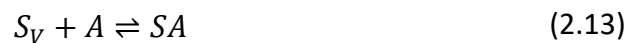
$$\ln q = \ln K + \frac{1}{n} \ln c \quad (2.12)$$

where n is a constant and K, q, c are the same as in the Langmuir isotherm (Potgieter, 1991).

2.9.3 Langmuir Isotherm

Equilibrium isotherms are used to quantify the amount of adsorbate needed for an adsorbent, evaluating the amount of the adsorbate that can be adsorbed onto the surface of the adsorbent at equilibrium and a constant temperature.

The Langmuir isotherm describes the equilibrium between a surface and adsorbate compounds, which can be described as a reversible chemical equilibrium (Crittenden, 2012). The surface of activated carbon has a variety of specific sites where adsorbates can be chemically bound with Equation (2.13) shows the relationship between the free surface of activated carbon, adsorbate compounds and the adsorbate compounds bound to the surface sites (Crittenden, 2012).



where S_v is the uninhabited surface sites (mmol/m²), A is the adsorbate compounds in solution (mmol), SA is the adsorbate compounds bound to the surface sites (Crittenden, 2012).

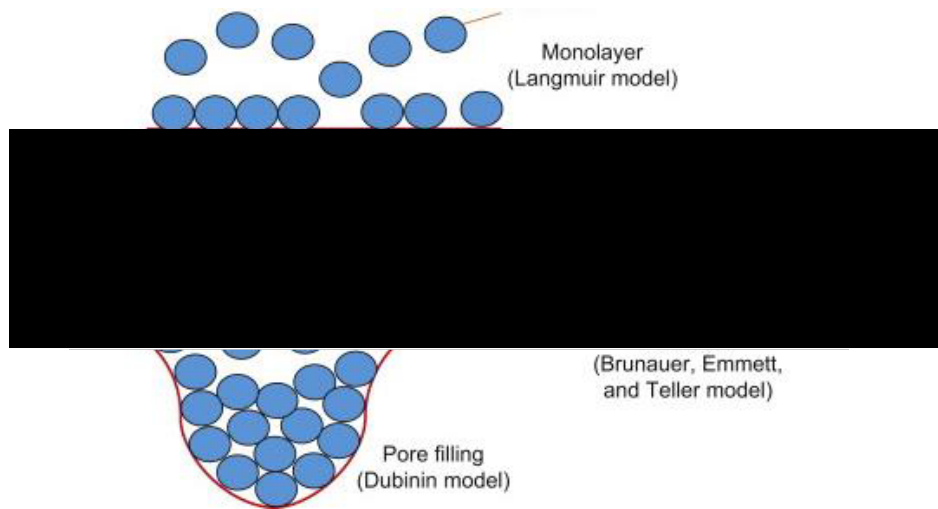


Figure 18: Representation of the some different adsorption models (Flores, 2014)

Langmuir model is based on the concept that only a monolayer of adsorbate compounds can accumulate on the activated carbon surface. Different models allow a different form of accumulation of the adsorbate compounds, as seen in Figure 18. It is assumed that the free energy change (ΔG°) for each individual site remains constant; therefore, the equilibrium equation is written as:

$$K = \frac{SA}{S_V C} = e^{-\Delta G^\circ / RT} \quad (2.14)$$

where K is the Langmuir adsorption equilibrium constant (L/mg), C is the equilibrium concentration of the adsorbate in solution (mg/L), ΔG° is the free energy change for adsorption, R is the universal gas constant 8.314 (J/mol K), T is the absolute temperature (K) (Crittenden, 2012).

Equation (2.14) is not the most appropriate way of representing the amount of adsorbate adsorbed as a function of concentration as S_V is unknown and C_A is also not known. Equation (2.15) can be used to fix this problem as it has a fixed number of sites v . Where S_T is the total number of sites available, this equation can then be rearranged and solved for S_A to get,

$$S_A = \frac{S_T}{1 + 1/(KC)} = \frac{K C S_T}{1 + KC} \quad (2.15)$$

The concentration is currently expressed as mmol/m² this is changed to a mass of adsorbent per mass of adsorbent, by multiplying through by the surface area per gram and the molecular weight, the equation is then arranged into the linear form as seen in equation (2.16) (Crittenden, 2012).

$$qA = (SA)(A_{ad})(MW) = \frac{q_{max} \times K \times C}{1 + K \times C} \quad (2.16)$$

where q is the equilibrium adsorbent phase concentration of the adsorbate (mg of adsorbate/g of adsorbent), q_{max} is the maximum adsorbent phase concentration when the surface sites are saturated with the adsorbate (mg of adsorbate/g of adsorbent).

$$\frac{1}{q} = \frac{1}{Kq_{max}} \times \frac{1}{C} + \frac{1}{q_{max}} \quad (2.17)$$

The equation (2.17) can be used to plot a straight of $1/q$ vs $1/C$; this is a straight line, the gradient is $1/q_{\max}$, and the intercept is $1/kq_{\max}$ (Crittenden, 2012).

2.9.4 Freundlich Isotherm

Freundlich adsorption isotherm is used to evaluate heterogeneous adsorbents; thus, activated carbon can be modelled effectively with the Freundlich model. The Freundlich equation is expressed as an empirical equation representing the isothermal variation of adsorption of a liquid or gas on a solid surface (Crittenden, 2012). The equation below is the Freundlich equation.

$$q = KC^{\frac{1}{n}} \quad (2.18)$$

where K is the Freundlich adsorption capacity parameter $(\text{mg/g})(\text{L/mg})^{1/n}$, n is the Freundlich adsorption intensity parameter (unitless). Equation (2.23) is natural logged (Ln) to produce a straight line (Crittenden, 2012).

$$\text{Ln}(q) = \text{Ln}(K) + \left(\frac{1}{n}\right) \text{Ln}(C) \quad (2.19)$$

2.9.5 Adsorption kinetics

Adsorption kinetics are used to determine the overall efficiency of adsorption. The kinetics of adsorption are determined from experimental data. The experimental results serve to determine the characteristic parameters of the kinetic equations that are useful for process design and scale-up (Sarici-Ozdemir, 2014). The adsorption kinetics also determines the potential rate-controlling step (the mass transfer) and the type of adsorption (i.e. physical adsorption or chemisorption). The common models used for the adsorption kinetics are the pseudo-first and second-order models.

Lagergren proposed the pseudo-first-order kinetic model (Shahwan, 2015). Lagergren's kinetics equation has widely been used for the adsorption of adsorbates and the adsorbent is most commonly activated carbon. The most popular form of the equation is the integral form of the model, as shown in equation (2.20) (Ho, 2004)

$$\ln(q_e - q_t) = \ln(q_e) - k_2 t \quad (2.20)$$

where q_e is the amount of adsorbate adsorbed at equilibrium (mg/g), q_t is the amount of adsorbate adsorbed with respect to time (mg/g), k_2 is the rate constant (1/min), t is the time (min). The values for k_2 and q_e were calculated from the slopes and intercepts of $\ln(q_e - q_t)$ against the time graphs (Ho, 2004).

The pseudo-second-order rate is based on the solid capacity used for sorption kinetics. The linearized integral model is shown in the equation.

$$\frac{t}{q_t} = \frac{1}{k_2 q_e^2} + \frac{1}{q_e} t \quad (2.21)$$

where k_2 is the pseudo-second-rate constant of adsorption (g/mg-min). The model assumes that the rate of inhabitants of the adsorption sites is proportional to the number of uninhabited sites squared. The pseudo-second-order values were calculated using the gradient and intercepts obtained from plotting t/q_t against t (Karthikeyan, Balasubramanian, & Yer, 2007).

Having discussed adsorption kinetics, adsorption isotherms, geosmin and MIB and activated carbon the following sections discusses regeneration of activated carbon.

2.10 Regeneration of activated carbon

The adsorption process onto GAC occurs for years to remove contaminants from water until the adsorption capacity of the activated carbon becomes exhausted. Regeneration is then required to reinstate the adsorbent capacity. The adsorption process entails the adsorption of adsorbate compounds, accumulating within the porous structure of the activated carbon. Micropores become much more congested than mesopores and macropores because the micropores contain the main adsorption sites (Vanvliet, 1991). The mesopores and macropores still adsorb some adsorbates, just not as much as the micropores (Vanvliet, 1991). Once the activated carbon is spent and inefficient, regeneration is needed, or a virgin GAC replacement is used. However, it is more cost-effective to reactivate than purchase fresh activated carbon. Although regeneration may be more economically viable than acquiring

fresh activated carbon, it is still an expensive process and has drawbacks when compared to fresh activated carbon. Regenerated activated carbon cannot be completely restored to its original adsorption capacity. After each regeneration, the adsorption capacity decreases, therefore, after multiple regenerations, the activated carbon must be replaced. Regeneration removes the adsorbates that have accumulated onto the adsorption sites on the activated carbon. There are various regeneration methods, thermal, chemical, and biological processes can be used to obtain the required result (Gamal, mousa, & El-Naas, 2018). The goal of regeneration is to restore the original adsorption capacity, porous structure and activity of the activated carbon with minimal damage to the original structure of the activated carbon.

2.10.1 Thermal regeneration

Thermal regeneration is conducted using either a rotary kiln, multiple-hearth furnace or a fluidizing-bed furnace (Cheremisinoff & Ellerbusch, 1978). Firstly, exhausted activated carbon is dried at about 105°C to remove any water molecules, and moisture present in the activated carbon next is the pyrolytic stage whereby the exhausted carbon is exposed to a temperature of around 400 - 800°C in inert conditions. All the volatile compounds are adsorbed onto the activated carbon, and any residual moisture is destroyed (Guo & Du, 2012). During this step, a residue of carbonised char becomes part of the structure of the carbon. The last stage is gasification of the residual organics to reactivate the carbon at a temperature of about 800°C and an oxidizing atmosphere, carbon dioxide or steam are commonly used for the gasification (Guo & Du, 2012). This stage is used to erase the carbonised char residue and essentially

reactivate the original porous structure. The high temperature induces weak oxidation to the water vapour, allowing it to oxidise the residual carbonated char (Guo & Du, 2012).

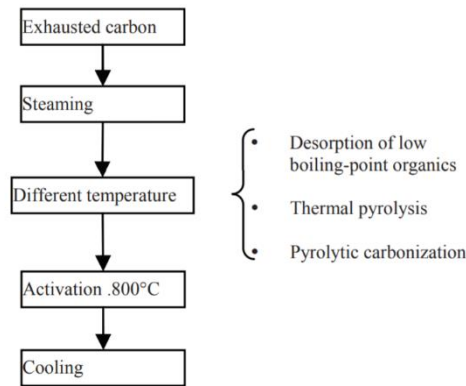


Figure 19: The steps of thermal regeneration of activated carbon (Guo & Du, 2012)

In thermal regeneration, the conditions are fundamental. If they are too harsh, the adsorption properties and porous structures may be damaged, whereas if the conditions are too weak, then the adsorption capacity may not be regenerated to maximum adsorption capacity (Guo & Du, 2012). Three main properties are used to evaluate the success of a thermal regeneration: granular regeneration strength, adsorption capacity, and the mass of activated carbon lost (burnt-off). These three properties have an antagonistic relationship with each other (Guo & Du, 2012). Fully restoring the adsorption capacity of activated carbon would mean harsher conditions that increase the mass loss. Thus, the carbon volume decreases, which lowers the adsorption capacity as fewer sites will be available for the adsorption of contaminants. The aim of regeneration for water treatment is to control the recovery rate of adsorption. Generally, the structure of the activated carbon is partly gasified or over-burned as well as the pyrolyzed adsorbate residue (Guo & Du, 2012). The potential of the activated carbon over-burning depends on the physical structure of activated carbon, the functional groups on the surface of the activated carbon, the concentration of steam/CO₂, the

temperature and the inorganic compounds on the surface of the activated carbon (Guo & Du, 2012).

2.10.2 Steam regeneration

Steam regeneration can be conducted at both high and low-temperatures dependant on the heat capacity of the adsorbent, the boiling point of the organic adsorbate and the solvency of the inorganic adsorbate (Shah, Pre, & Alappat, 2013). High-temperature steam regeneration is performed in inert conditions. This prevents oxidative reactions between steam, the adsorbent and the adsorbate. If not prevented, oxidative reactions would result in char formation and contribute to the deterioration of the porous network of the carbon (Shah et al., 2013). Steam regeneration is an economical and effective regeneration method. During steam regeneration, steam quickly heats up the bed, thus permitting more rapid desorption of the contaminants (Gamal et al., 2018). The adsorbate is only removed if the steam is still in gaseous form, thus contains adequate heat in order to remove the adsorbate (Gamal et al., 2018). During steam regeneration, there are five stages: thermal decomposition of AC (desorption of volatile matter, 100-260 °C), oxidation of AC, vaporization of the adsorbates, pyrolysis and carbonization of contaminants (pyrolysis and carbonization non-volatile compounds, 200-650 °C) and the oxidation decomposition of carbonization residue (650-850 °C) (Gamal et al., 2018; Shah et al., 2013)

2.10.3 Bio-regeneration

Bio-regeneration uses microbial colonies to regenerate the surface chemistry, porous structure and adsorption capacity. If organic adsorbates can be easily desorbed, bio-regeneration can occur (Gamal et al., 2018). Bio-regeneration is driven by the concentration gradient of adsorbates between the activated carbon and the bulk liquid (Gamal et al., 2018). The microorganisms degrade the substances, shifting the adsorption equilibrium leading to further desorption and partial replenishment of the solution concentration (Çeçen & Aktas, 2012). The regeneration will continue until all the adsorbate compounds are adsorbed by the microbes.

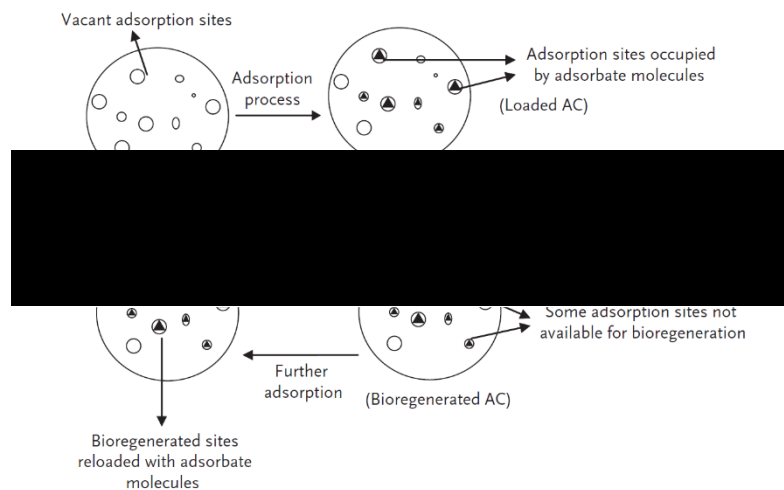


Figure 20: Mechanisms of bio-regeneration (Çeçen & Aktas, 2012)

Figure 20 represents the mechanisms of bio-regeneration due to the change in the adsorbate concentration. When the substrate concentration reaches a minimum value at the point of

zero gradient (PZG), the concentration gradient (DSf/dr) is also zero (Çeçen & Aktas, 2012). As the concentration of the adsorbates in the bulk liquid decreases, the PZG moves to the liquid film. This induces a change in the direction of the substrate, it travels from the carbon surface to the solvent. This subsequently results in the bio-regeneration of the activated carbon. The PZG moves towards the solid activated carbon surface and limits the bio regeneration when the adsorbate concentration in the bulk solution increases (Çeçen & Aktas, 2012).

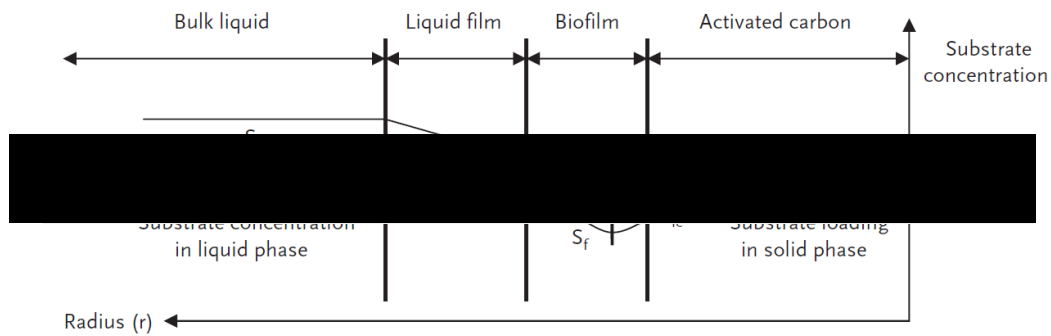


Figure 21: Concentration profile of adsorbate during bio-regeneration (Çeçen & Aktas, 2012)

Several factors can be used to evaluate the efficiency of bio-regeneration: the strength of contaminant to carbon interaction, biodegradability and the physical and chemical characteristics of the activated carbon (Gamal et al., 2018). Another factor that can control the efficiency of bio-regeneration is the Gibbs free energy difference between the adsorbed phase and bulk liquid phase (Gamal et al., 2018).

2.10.4 Chemical regeneration

Chemical regeneration of activated carbon is a widely used regeneration method, it is used to remove adsorbates without using a high amount of energy or expensive equipment. The chemical regeneration general method consists of the desorption of the adsorbates using a solvent or solution which contains a compound that will modify the adsorption equilibrium between the adsorbate and surface of the adsorbent (Berenguer, Marco-Lozar, Quijada, Cazorla-Amoros, & Morallon, 2010). The process does not result in any carbon attrition but recovers the adsorption capacity of the activated carbon (Berenguer et al., 2010). Chemical regeneration is usually conducted at 110°C by desorbing the adsorbates, during this process there is no change in the structure of the activated carbon. There are many different chemical regeneration processes, as shown in Figure 22. One of them is acidic and alkaline reagents. The adsorbates are firstly dissolved, the greater their affinity for the reagents, the more strongly dissolved the adsorbate will be (Gamal et al., 2018). The efficiency of this type of chemical regeneration depends on the adsorbate compounds' solubility and the adsorbent reactivity with the chemical reagents as well as the type of contaminants present in the activated carbon (Gamal et al., 2018). After the chemical regeneration of the activated carbon, the reagents are then extracted so that the activated carbon can be recovered (Gamal et al., 2018).

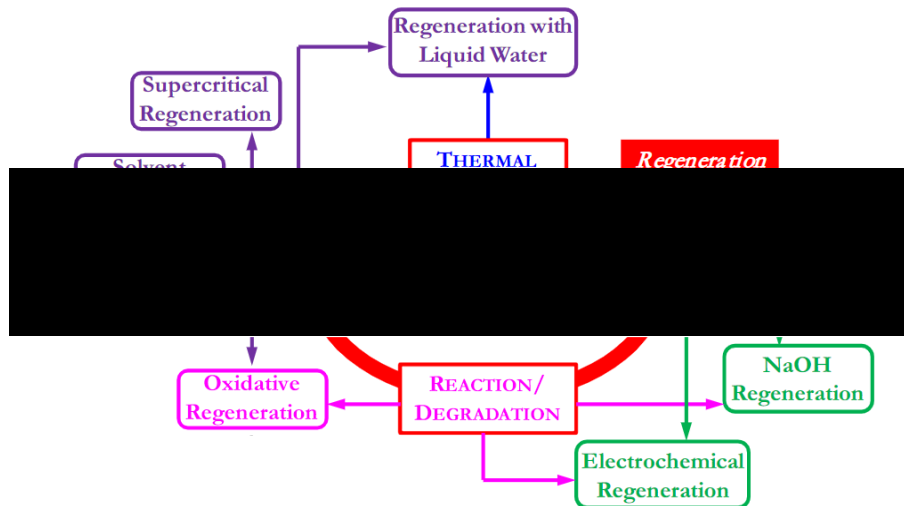


Figure 22: Chemical methods of regeneration of activated carbon (Salvador, Martin-Sanchez, Sanchez-Hernandez, & Sanchez-Montero, 2015)

The foremost step of solvent regeneration is the extraction of the adsorbate from the activated carbon by displacing an adsorbate molecule that is adsorbed on the surface of the activated carbon (Salvador et al., 2015). Extraction of the contaminants is heavily dependent on three main interactions (between solvent, adsorbate and adsorbent): solvent to adsorbent interaction because the solvent has to adsorb onto the activated carbon surface to bond with active sites located in the microporous network, solvent to adsorbate interactions because the greater the solubility of the adsorbate in the solvent the greater the removal of MIB and geosmin, adsorbent to adsorbate interactions as it is difficult to remove the adsorbates especially when the interaction is strong, the extraction becomes less effective when this interaction is strong (Salvador et al., 2015). The final step is removing the solvent, for example, by the circulation of hot N₂. Once this step is complete, the adsorption capacity is recovered (Salvador et al., 2015). Another way to perform chemical regeneration is using oxidising agents to induce decomposition of the adsorbate (Salvador et al., 2015).

2.11 Use of ozone for the regeneration of activated carbon

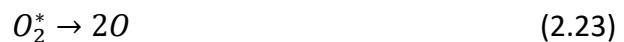
Ozone (O₃) was discovered by Christian Friedrich Schonbein (1839). He electrolysed dilute sulfuric acid to form ozone and determined that the autoxidation of white phosphorus also formed ozone (this was the standard for obtaining ozone in the first years of ozone chemistry) (Sonntag & Gunten, 2012). Schonbein determined the oxidising power of ozone but found it a lot more challenging to determine the structure of ozone. Ozone was given its name by Schönbein (1854) because of its strong smell and determined that ozone can be detected by smell at low concentrations. It was later calculated that the nose could indicate that ozone is in the air at a concentration of roughly 15 µg/m³ and can strongly detect ozone at around 30-40 µg/m³ (Sonntag & Gunten, 2012). Ozone (O₃) is a toxic, corrosive and unstable gas. Because of its instability, ozone is difficult to store, thus it is generated onsite when it is needed (Gottschalk, 2010). Ozone has great oxidising power, thus it can be used to oxidise organic matter and disinfect water. In water, ozone can react with substances either directly through molecular ozone or indirectly through free radical reactions (Gottschalk, 2010).

Table 12: Physical properties of ozone

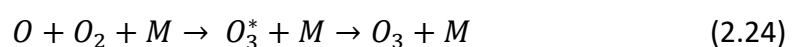
Property	Value
Molecular weight	48 Da
Dipole moment	0.537 Debye
Bond length	1.28 Å
Bond angle	117°
Melting point	-192.7 °C
Boiling point	-110.5 °C
Solubility in water at 0°C	2.2 x 10 ⁻² M
Solubility in water at 25°C	1.19 x 10 ⁻² M
Henry constant at 0°C	35 atm M ⁻¹
Henry constant at 25°C	100 atm M ⁻¹
Explosion threshold	10% Ozone

2.11.1 Ozone generation

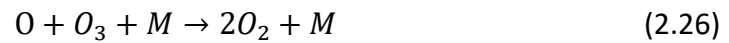
The most common method for ozone generation at a commercial scale is the use of ozone generators based on silent discharge; this was first developed by Siemens (1857). Either air or oxygen or a mixture can be used as the feed stream. When using air, an ozone concentration of around 1-5% (by weight) is produced while with oxygen feed gas, ozone at concentrations of 8-16% can be produced (Sonntag and Gunten 2012). Depending on the pressure and energy of ignition used, ozone concentration >10% can potentially be explosive, therefore, systems that yield high ozone concentrations must be operated in accordance with the suppliers' guidance (Sonntag & Gunten, 2012). To produce ozone, around 12-15 kWh/kg is needed, this includes oxygen production, transport and destruction. The energy gained by the electric field from the electrons produces excited molecular states of oxygen, the excited states of oxygen (O_2^*) (Sonntag & Gunten, 2012). The below equations show the dissociation of O_2 .



Ozone is formed through the three-body reaction as shown in the equation below:



where M can be (O_2 , O_3 , O , or when using air N_2), the formation of ozone reaction is in direct competition with the following reactions, they also consume O atoms.



2.11.2 Ozone solubility

Ozone's solubility in water is around ten times more than oxygen (Figure 23). Therefore, the water can be saturated with an ozone/oxygen mixture from an ozone generator and the final concentration is dependent on the gas concentration. As seen in Figure 23, the solubility of ozone is heavily dependent on the temperature. The concentration of ozone at 0°C is about double that at room temperature. When a highly rich stock solution of ozone is necessary, ice can be used for cooling to increase the ozone concentration, but this is not required in industrial water treatment.

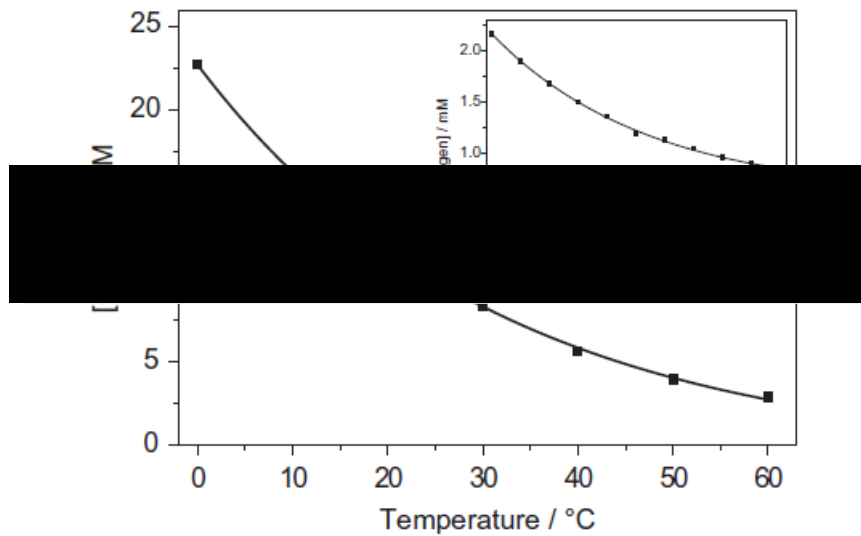


Figure 23: Solubility of ozone and oxygen in water with respect to temperature (Sonntag & Gunten, 2012).

2.11.3 Ozone measurement by the indigo method

The indigo method is commonly used to determine the concentration of ozone in water and gas phase. Schonbein (1854) developed the indigo method as he observed that the determination of the mass of ozonised oxygen in a given volume of air could be used to determine the amount of ozone up to a milligram within minutes (Sonntag & Gunten, 2012). This method works by measuring the bleaching of the indigo trisulfonate by ozone. Indigo trisulfonate reacts at a stoichiometry 1:1 and at a very high rate with a rate constant, $k = 9.4 \times 10^7 \text{ M}^{-1} \text{ s}^{-1}$ (Sonntag & Gunten, 2012).

2.11.4 Ozone reaction mechanisms

The indirect reactions of ozone utilise hydroxyl radicals. These radicals are highly unstable and instantaneously react with a compound to receive a missing electron. The mechanism for the production of radicals from ozone has three steps, initiation, chain progression and termination. The radical pathway is very complex and various compounds can easily alter it (Gottschalk, 2010).

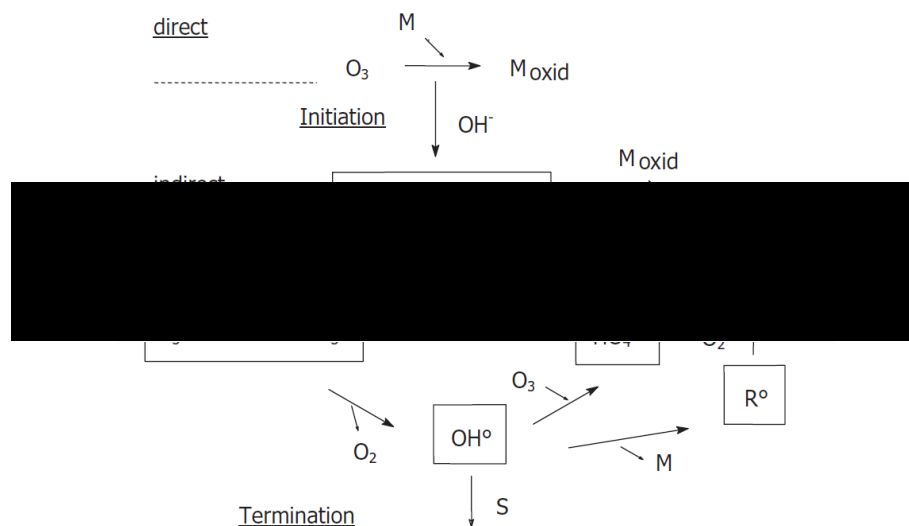
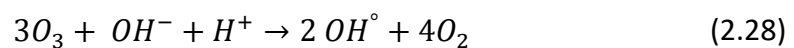


Figure 24: Model of indirect and direct ozonation (Gottschalk, 2010)

The overall ozone reaction for ozone to produce the hydroxyl radical is shown in equation (2.28); this overall reaction is the combination of the three steps.



where, OH° is the hydroxyl radical. The hydroxyl ion initiates the decay of ozone, thus causes many more reactions which react off each other, producing the unstable and very reactive OH radical. The hydroxyl radical reacts with the intended compound at the point with the greatest electron density (Gottschalk, 2010).

Direct reaction differs from indirect reactions as the ozone molecule reacts selectively with compounds. The ozone molecule reacts with the unsaturated bonds because ozone has a dipolar structure. This reaction will split the bond following the Criegee mechanism, as shown in Figure 25 (Gottschalk, 2010). Ozone reacts at its fastest with organic water compounds; therefore, geosmin and MIB can be ozonated quickly.

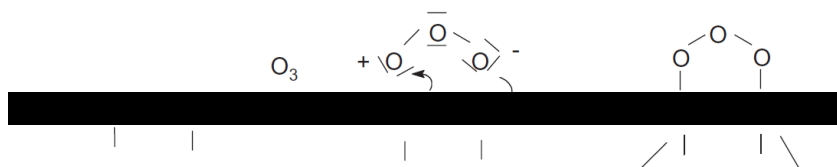


Figure 25: Ozonation of a double carbon bond (Gottschalk, 2010)

2.11.5 Ozone regeneration of activated carbon

Ozone regeneration of activated carbon is a regeneration method where a stream of O_2/O_3 is circulated through the spent activated carbon bed to remove the retained adsorbates at room temperature. Thus, resulting in ozone regeneration being more energy-efficient than using thermal-oxidative regeneration since O_3 does not need an additional energy source. Ozone requires less than two hours to regenerate spent activated carbon, and since the regeneration is *in-situ*, the cost of transport and the cost of disposal of the adsorbate for ozone regeneration are low (Salvador et al., 2015). Ozone can regenerate activated carbon once exhausted up to around 90% of its adsorption capacity. It works because of its great oxidation

power to degrade adsorbed species on the surface of the activated carbon, therefore removing such species. However, ozone can modify the carbon surface chemical properties and adsorptive textual characteristics (Valdes et al., 2002). Prolonged exposure of activated carbon to ozone gas transforms the chemical composition of the carbon surface. Basic sites are transformed into acid sites because of oxidation. The modification of the oxygenated groups influences the adsorptive properties. The surface area could also decrease, which may reduce the adsorption capacity (Valdes et al., 2002). However, through optimisation and control of the ozone dosage and exposure time, the degree to which the surface properties on the activated carbon are modified can be controlled. The optimal ozone dosage must be found, the optimal dose could restore a high adsorptive capacity whilst minimising the damage to the surface properties of the activated carbon (Valdes et al., 2002). Compared to thermal regeneration, which leads to 5-15% carbon burn-off, ozone regeneration does not lose any of the activated carbon mass. Therefore, if effectively optimised, ozone regeneration of activated carbon could be a more effective regeneration method than other conventional thermal regeneration techniques (Alvarez, Beltran, Gomez-Serrano, Jaramillo, & Rodriguez, 2004).

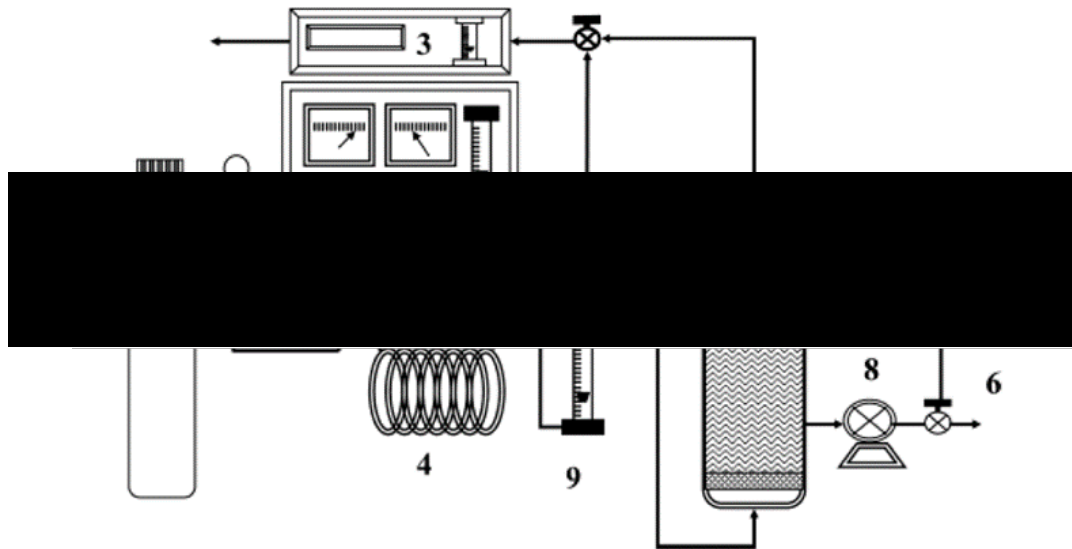


Figure 26: Diagram that represents the ozonation setup (Rivas, Beltran, Gimeno, & Frades, 2004)

An ozone regeneration system is as shown in Figure 26, ozonation setup: 1, oxygen cylinder; 2, ozone generator; 3, ozone gas analyser; 4, cooling water; 5, reactor; 6, sampling port; 7, AC bed; 8, peristaltic pump; 9, rotameter (Rivas et al., 2004). The oxygen is fed from the cylinder immediately to an ozone generator, converting the O_2 into O_3 .

A high voltage is required to produce O_3 , a lot of energy is needed to break apart the oxygen molecules in the atmosphere, the energy from the sun is used to break apart the oxygen molecule; therefore, high energy has to be applied to the oxygen in the generator. After the ozone is generated, it is passed through an ozone analyser which accurately quantifies the ozone levels. The reactor is used to ozonate a specific substance that could be exhausted GAC; this system is a pilot-scale system that could be adapted to accommodate *in-situ* regeneration, theoretically the pilot-scale system could be scaled up and thus, have industrial applications.

This chapter explained the chemical and physical structure of activated carbon and how this structure interacts with adsorbate molecules. Also, in this chapter the regeneration of

activated carbon using various methods are discussed, including the ozone regeneration of spent activated carbon, the oxidising effect of ozone on activated carbon is developed. Also the analytical methods used to determine the concentration of G-MIB are examined.

3.0 Materials and methods

3.1 Materials and reagents

All reagents were analytical grade and supplied by either Sigma-Aldrich (UK) or Fisher Scientific (UK). Distilled water was used for all solution preparations. Granular activated carbon (CARBSORB 208EA 12 x 40) was used throughout, it is a bituminous coal-based carbon provided by Welsh Water. In addition, six different spent activated carbon samples were received from Dwr Cymru (Welsh Water) that had varying bed ages and different regeneration dates varying between 2013 and 2020.

3.2 Characterisation

3.2.1 Iodine number (IN)

The iodine number is calculated using the ASTM D4607-94 method. The definition of the iodine number is the mass of iodine adsorbed by 1.0g of activated carbon while the iodine concentration of the filtrate is 0.02mol/L. The method uses a three-point isotherm, to do this, an iodine solution is treated with three varying weights of activated carbon. The initial masses of activated carbon were determined using Equation (3.1)

$$M = ((N_I \times 12693) - (DF \times C \times 126.93 \times 50))/E \quad (3.1)$$

where M is the mass of activated carbon, N_I is the iodine solution normality (mol/L), DF is the dilution factor, C is the residual iodine, E is an estimated iodine number of the carbon (mg/g).

The activated carbon was ground in order to meet the required particle size of 60wt% passing through a 325-mesh screen or 95wt% passing through a 100-mesh screen. Then the activated carbon was dried and cooled in a desiccator. After the iodine adsorption reaction, the solutions are then filtered to remove the activated carbon, to isolate the treated iodine solution. The remaining iodine can be measured using titration. Therefore, the amount of iodine removed per gram of activated carbon is determined for all three masses. The experiment subsists using 10.0 mL of 5% HCl to treat the activated carbon samples. The mixture is boiled for 30 s and then left to cool. After 100 mL of 0.1mol/L of iodine solution is added and then the mixture is stirred for 30 s. The solution is then filtered, and 50mL of the filtrate is used to titrate 0.1mol/L of sodium thiosulfate. A starch solution is used as an indicator. Then the amount of adsorbed iodine per gram of activated carbon (x/m) is plotted against the concentration of the iodine filtrate (C), logarithmic axes are used. If at this point, the filtrate iodine concentration (C) is not within the range of around 0.08 to 0.04mol/L, the initial carbon masses were incorrect, and the procedure needs to be repeated. The least-squares fitting regression is applied for the three points to calculate the least-squares fit. The iodine number is the value of X/M at the iodine filtrate concentration (C) of 0.02 mol/L. All experiments were carried out in triplicate, and the mean values were determined. The values were calculated using the equations below,

$$X/M = ((N_I \times 12693) - ((V_I + V_{Hcl})/F) \times (N_{Na_2S_2O_3} \times 126.93) \times S)/M_c \quad (3.2)$$

$$N_{Na_2S_2O_3} = (P \times R)/S \quad (3.3)$$

$$C_I = (N_{Na_2S_2O_3} \times S)/F \quad (3.4)$$

where N_I is the iodine solution normality (mol/L), V_I is the added volume of iodine solution (mL), V_{HCl} is the added volume of 5% HCl (mL), F is the filtrate volume used in titration (mL). P is potassium iodate volume (mL), R is potassium iodate concentration (mol/L), S is the volume of sodium thiosulfate (mL), $N_{Na_2S_2O_3}$ is the sodium thiosulfate solution normality (mol/L), C_I is the iodine residual filtrate concentration (mol/L) and M_c is the mass of activated carbon (g) (Nunes & Guerreiro, 2011).

3.2.2 Methylene blue number (MBN)

Methylene blue number is another method of characterising the adsorption capacity of activated carbon. It measures the maximum amount of methylene blue dye adsorbed onto 1 g of activated carbon. It can be represented as q_{eq} in literature. Masses of between 0.01 – 0.05g of activated carbon were used, five separate masses were placed into 40 mL tubes. The methylene blue solution was made up in a 250 mL conical flask with a concentration of 20 mg/L. The methylene blue solution is then analysed using UV/VIS at 625nm wavelength. The tubes were mixed for 12 hrs at 25°C until equilibrium was met (Valdes et al., 2002). The activated carbon is filtered out, and the treated methylene blue solutions are analysed with

the UV/VIS. The amount of methylene blue that has been absorbed can be calculated using the equation,

$$q = \frac{(C_o - C_e) \times V}{m} \quad (3.5)$$

where C_o is the concentration of the methylene blue solution at starting time $t=0$ (mg/L), C_e is the concentration of the methylene blue solution at equilibrium time (mg/L), V is the volume of the solution treated (L), and m is the mass of the adsorbent (g) (Nunes & Guerreiro, 2011).

Two adsorption isotherms Langmuir and Freundlich, can be used for the adsorption of methylene blue. The Langmuir adsorption equation can be defined as,

$$\frac{1}{q} = \frac{1}{q_{max}K} \times \frac{1}{c} + \frac{1}{q_{max}} \quad (3.6)$$

where q is the amount of methylene blue absorbed per mass of activated carbon (mg/g), q_{max} is the limiting amount of methylene blue that can be adsorbed per mass of activated carbon (mg/g), K is a constant, C is the concentration of the solute (mg/L). The Freundlich adsorption isotherm equation can be defined as,

$$\ln q = \ln K + \frac{1}{n} \ln c \quad (3.7)$$

Where n is a constant and K, q, C are the same as in the Langmuir isotherm (Potgieter, 1991). The methylene blue number is determined using the least-squares fitting regression on Langmuir and Freundlich isotherms, all experiments were carried out in triplicate, and the mean values were determined.

3.2.3 Brunauer-Emmett-Teller (BET) method

The BET is used to analyse the pore and surface characteristics of the GAC. These characteristics are used to calculate the amount of geosmin and MIB that can be adsorbed onto the surface of activated carbon. Cryogenic nitrogen is used to produce the adsorption-desorption isotherms on the surface of activated carbon. Activated carbon is cooled to -195.8°C . An e200 Quantachrome BET analyser was used to measure the BET surface area of the GAC. The BET was initially calibrated, then the samples were placed in the degassing chamber, which was done at 150°C for around 6hrs. Degassing is done to evacuate any adsorbed moisture and impurities or gases that are adsorbed onto the surface of the sample; this allows the analysis to be more accurate. Then the analytical stations are prepped, and then the analysis is run for around 12hrs. The surface area (S_T) value of activated carbon is then calculated using the adsorption isotherm that is calculated over a pressure range of 0.01 to

0.3, this is done using the standard BET (Brunauer, Emmett and Teller) method. Below is the BET equation (Ambroz & Macdonald, 2018),

$$\frac{P/P_0}{V(1-P/P_0)} = \frac{1}{V_m C} + \frac{C-1}{n_m C} (P/P_0). \quad (3.8)$$

where V is the volume of N_2 adsorbed (cm^3/g), V_m is the max monolayer layer capacity (cm^3/g), C is the BET constant related to the energy of desorption and the energy of vaporisation, the value given indicates the degree of activated carbon-nitrogen interactions. The total pore volume (V_T) of the samples is calculated by using the total volume of N_2 gas adsorbed on the surface of activated carbon at high relative pressure.

The Dubinin Radushevich (DR) equation is used to determine the micropore volume (V_m) and micropore surface area (S_m), the linear form is usually used for the analysis of activated carbons. The DR equation is adjusted to the N_2 isotherm data at 77K to calculate the micropore characteristics; this equation is written as (Marcilla, Gomez-Siurana, & Valdes, 2009),

$$\ln V = \ln V_0 - k \left(\ln \left(\frac{p^0}{p} \right) \right)^2 \quad (3.9)$$

where V is the volume of the absorbate in the micropores (cm^3/g), V_0 is micropore volume (cm^3/g), and k is,

$$k = 2.303K\left(\frac{RT}{\beta}\right)^2 \quad (3.10)$$

where β is the affinity coefficient, k is a constant, R is the universal gas constant (8.314 J/mol K), and T is the temperature (K). Then $\ln(V)$ can be plotted against $\ln(p^0/p)^n$; this is linear with the intercept $\ln(V_0)$, which is used to calculate the micropore volume (V_0). The DR equation sometimes cannot linearize data obtained for adsorbents that contain heterogeneous micropores or strongly activated carbon. This problem is resolved with the Dubinin and Astakhov equation (DA), the linearized and regular equation version of the DA equation (Afonso & Silveira, 2005),

$$\ln V = \ln V_0 - k\left(\ln\left(\frac{p^0}{p}\right)\right)^n \quad (3.11)$$

$$W = W_0 \exp\left(-\left(\frac{RT \ln(P/P_0)}{E}\right)^n\right) \quad (3.12)$$

where K is an empirical constant and n is the Dubinin-Astakhov parameter. The value of n can range from 2 to 5 depending on the microporous system.

3.2.4 Fourier transform infrared spectroscopy measurement (FTIR)

FTIR estimates the functional groups present on the surface of activated carbon. FTIR spectroscopy (Perkin-Elmer Spectrum 2) was used to analyse the samples. The spectral range was from 4000 to 750 cm^{-1} , thus recording the transmission spectra for multiple samples. The force gauge is increased to 100-120 range during the analysis, this creates a uniform disc of the sample. The transmission FTIR results are analysed to determine the functional groups present (Islam et al., 2015).

3.2.5 The pH of zero charge (pH_{pzc})

The pH_{pzc} is used to characterise the surface chemistry of the activated carbon, it evaluates the surface by the different functional group and sites on the solid surface. Six 0.15g samples of activated carbon are used, 50 mL of 0.01M NaCl are added to each of the activated carbon samples, the six NaCl and activated carbon mixtures are then shaken for 24 hrs at standard conditions. The six different samples of NaCl were differentiated by their pH values, which varied from 2-12 pH. The final pH for each sample was measured, the final pH is then plotted against the initial pH. The pH_{pzc} of the activated carbon is the point where the curve (pH_{final} vs $\text{pH}_{\text{initial}}$) crosses the straight-line $\text{pH}_{\text{final}} = \text{pH}_{\text{initial}}$. (Mahmoudi, Hamdi, & Srasra, 2015). All experiments were carried out in triplicate, and the mean values were determined.

3.3 Ozonation of activated carbon

Granular activated carbon with a particle size of around 500 -1000 μm . Initially, the carbon was washed with distilled water and then oven-dried at 120 °C for 12 hours. 5g of activated carbon was weighed and placed in a 500 mL sealable glass media bottle, 300 mL of distilled water was added. The activated carbon was continuously stirred to prompt uniform mixing and ozone exposure. Ozone is applied to the distilled water through a diffuser with a cap that secured itself onto the bottle. The ozone was produced using an ozone generator (BMT Messtechnik, Germany) which was supplied by oxygen gas. The ozone concentration in the gas phase was analysed using an ozone analyser (BMT Messtechnik, Germany). A constant ozone/oxygen mixture flowrate of 0.5 L/min was used. The ozone was transferred from the gas phase into the liquid phase. The GAC was treated for either 30, 60, or 90 minutes.



Figure 27: Ozone system rig

3.3.1 Ozone analysis in liquid phase

The indigo trisulphonate method was used to determine the concentration of ozone (Bader & Hoigne, 1981). The solution was prepared by dissolving 0.0770 g of indigo potassium trisulphonate, 11.5g of sodium phosphate and 8 ml of phosphoric acid in 1L of distilled water. Immediately after the ozonation experiment was complete, the indigo experiment was conducted due to the volatility of ozone. A syringe reactor was used, this was where the indigo trisulfonate solution and ozone bleaching reaction took place. Ozone in distilled water was reacted in a mass ratio of roughly 2:1-1.5. Then the absorbance of the bleached indigo solution was analysed using UV/VIS at 600 nm wavelength. The ozone concentration was then determined using the following equation,

$$C_{O_3} = 2.4 \times \left(\frac{m_I}{m_O}\right) \times (A_B - (A_S \times \left(1 + \left(\frac{m_O}{m_I}\right)\right))) \quad (3.13)$$

where, A_b , A_s are absorbance of the blank and sample respectively (AU), m_I , m_O , are the mass of the indigo trisulphonate solution and the ozone in water solution respectively (g) and C_{O_3} is the concentration of ozone (mg/L).

3.4 Adsorption of geosmin & MIB

3.4.1 Geosmin & MIB stock solutions

Preparation of stock solutions, geosmin and MIB, were dissolved in Milli-Q water. The volumetric flasks containing the geosmin and MIB solutions were sealed with parafilm and glass stoppers, wrapped in foil to prevent the potential degradation by light. The flasks were left to sit for 24 hours to dissolve the geosmin and MIB solids fully. Once dissolved, the stock solutions were stored in a dark fridge at 4°C. Stock solution concentration was 1 mg/L in a 100 mL volumetric flask.

3.4.2 Geosmin and MIB adsorption experiment

Batch adsorption experiments were for geosmin and MIB adsorption onto activated carbon were conducted. A geosmin and MIB stock solution was prepared at 100 ng/L by dissolving the geosmin and MIB with methanol into distilled water. Varying masses of activated carbon were used from 0-30 mg, the activated carbon is crushed until 95% can be passed through a

325 mesh screen. 1L samples of the G-MIB solution was used for each run with varying activated carbon masses in Erlenmeyer flasks. The adsorption experiments were carried out at a constant temperature using an incubator shaker SciQuip Incu-Shake MAXI benchtop, at a constant shaking speed of 120 rpm. The sample bottles were capped, sealed with Teflon tape and wrapped in aluminium foil (to prevent light penetration).

The varying masses of activated carbon allowed the production of the adsorption equilibrium isotherms. The amount of geosmin and MIB that was adsorbed onto the activated carbon can be determined using the equation below,

$$q = \frac{(C_o - C_e) \times V}{m} \quad (3.14)$$

where C_o is the concentration of the G-MIB solution at starting time $t=0$ (mg/L), C_e is the concentration of the G-MIB solution at equilibrium time (mg/L), V is the volume of the solution treated (L), and m is the mass of the adsorbent (g) (Nunes & Guerreiro, 2011).

The Freundlich adsorption isotherm equation can be defined as,

$$\ln(q) = \ln(K) + \frac{1}{n} \ln(C) \quad (3.15)$$

where n is a constant and where q is the amount of G-MIB absorbed per mass of activated carbon (mg/g), K is a constant, c is the concentration of the solute (mg/L). The G-MIB adsorbed

is determined using the least-squares fitting regression on Freundlich isotherms; all experiments were carried out in triplicate, and the mean values were determined.

3.5 G-MIB analysis

The initial part of the experiment is to produce a calibration curve for geosmin and MIB using known concentrations to determine the fluorescent intensity. A geosmin and MIB mixture (G-MIB) is used and is stored at -21°C. The Cary Eclipse Fluorescence Spectrophotometer is used to measure G-MIB across a range of 225 – 635 nm. The bandwidth used is 5 nm. The concentrations of the solutions were from 0 – 50 µg/L, the fluorescence intensity was plotted against the concentration to produce the calibration curve.

This chapter listed the methods used in this research study. Details of each method were provided following literature and established protocols in the water industry to analyse for iodine and methylene blue numbers of activated carbons. In addition, the techniques BET, FTIR, point of zero charge and ozone measurements were detailed and the conditions to use in this research were established.

4.0 Results & discussion

4.1 Characterisation of virgin activated carbon

4.1.1 Iodine number

Initially, the iodine and sodium thiosulphate solutions were prepared. A one-to-one colour change titration reaction would occur if the two solutions have the same molarity. This reaction is fundamental to the determination of the iodine number. The sodium thiosulphate and the iodine solution are both prepared to 0.1 N. The first part of the iodine number experiment is the standardisation of both these solutions to determine the exact molarity of both solutions due to the precise nature of the titration reaction.

Table 13: Standardisation results for sodium thiosulfate (left) iodine (right)

Run	Initial	Final	Titrate
1	0.0	24.9	24.9
2	0.0	25.0	25.0
3	0.0	24.9	24.9
Average	-	-	24.93±0.058

Run	Initial	Final	Titrate
1	0.0	24.7	24.7
2	24.7	49.4	24.7
3	20.0	44.5	24.5
Average	-	-	24.63±0.12

As shown in Table 13, the sodium thiosulphate titration was almost a one-to-one reaction. This is because the 25 mL of the iodine solution was titrated against 24.93 mL of sodium thiosulfate; thus, the concentration of sodium thiosulfate was 0.100267 N, which was close to desired 0.1 N concentration. The range of the three replications was less than 0.001 N, if this was exceeded, further replications would have been required. After the standardisation reaction has taken place, the iodine standardisation reaction was conducted. As seen in Table

13, 24.63 mL of the iodine solution was titrated against 25 mL of sodium thiosulfate solution. The iodine solution concentration was 0.09867; this is not within the desired concentration range of 0.001 N from 0.1 N concentration, but after multiple attempts to prepare the iodine solution to achieve the desired concentration without succeeding, any concentration within 0.002 N of 0.1 N concentration was accepted. Once the exact concentrations of the iodine and sodium thiosulphate solutions were determined, they were used in the calculation of iodine number, as seen in section 3.2.1.

The next step for the reaction was grinding the activated carbon so the particle sizes met the requirement of 60wt% passing through a 325-mesh screen or 95wt% passing through a 100-mesh screen. This is used to ensure the activated carbons have uniform particle sizes, which would ensure the reliability of the reaction and promote the adsorption of the iodine solution.

The BET surface area value was used to determine the initial iodine number estimate (860 m²/g). This BET surface area value was used to estimate the iodine number and determine the mass of activated carbon required for the iodine number analysis by Equation (3.1), as shown in Section 3.2.1. Initially, the equation estimated the GAC masses to be 1.11 g, 0.97 g and 0.83 g. These three masses were used to conduct the initial analysis.

$$M = ((N_I \times 12693) - (DF \times C \times 126.93 \times 50))/E \quad (4.1)$$

$$M = \frac{(0.0985 \times 12693) - (2.2 \times 0.1 \times 126.93 \times 50)}{1000} = 1.11g \quad (4.2)$$

Table 14: Iodine number results for initial masses

Mass (g)	Volume of sodium thiosulphate (mL)	Concentration of the filtrate (N)
1.11	4.1	0.0082
0.97	7.7	0.0154
0.83	11.3	0.0227

The required values of iodine filtrate concentration are only acceptable with the range 0.04 to 0.08 N (see Section 3.2.1.). As seen in Table 14, the results were outside this range. Thus, these results were not valid because the selected masses of GAC were too high. Therefore, lower masses were selected and the tests were repeated since the initial estimation did not produce results within the range of acceptability. After various experiments adjusting the masses of the carbon, the carbon masses were acceptable at 0.65 g, 0.34 g and 0.13 g for the virgin GAC. The iodine number experiment was conducted using these masses.

The iodine number was determined from a three-point adsorption isotherm (see Section 3.2.1). The three points are plotted on a graph of X/M vs C , which were fitted by a linear line using the least-squares regression method. The iodine number was then determined from this graph at the point corresponding to $C = 0.02$ N.

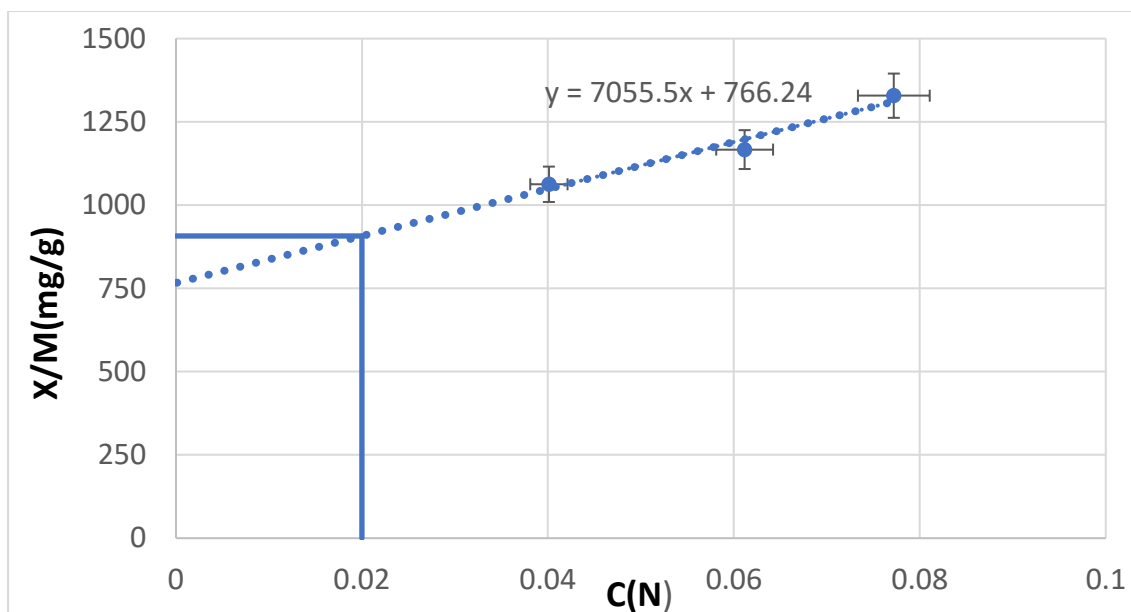


Figure 28: Least square regression graph for iodine number experiment for the virgin GAC

As shown in Figure 28, the iodine number was defined when $C=0.02$ from the least-squares fit. Thus, for this replicate of the iodine number experiment conducted on the virgin GAC, the iodine number was 3.57 mmole/g. An average is derived from the three replicates.

Although the iodine number is commonly used in industry for measuring the adsorption capacity of activated carbon, BET surface area is also used as a highly accurate method to determine the surface area within the activated carbon. The iodine number and BET surface area, both represent the adsorption capacity of activated carbon and their values obtained for the virgin GAC in this study are shown in Table 15.

Table 15: Comparison between the BET and iodine number results for virgin GAC

Activated Carbon	BET surface area (m^2/g)	Iodine number (mmole/g)	Ratio IN/BET area (mg/m^2)
GAC	860.99	3.60 ± 0.065	1.062

As seen in Table 15, the iodine number of the virgin GAC was determined to be 3.60 mmole/g this is similar to literature. For example Biniak et al. (2010) showed that virgin Filtrasorb -300 carbon has an iodine number of 3.65 mmole/g and virgin Carbsorb-38, (which is very similar to the carbon used CARBSORB 208EA) has an iodine number of 3.90 mmole/g. As seen in Table 15, the ratio of the iodine number (which is a good predictor of the surface area) for the virgin GAC and BET surface area is almost 1 (mg/m²) as shown in Equation (4.3), which agrees with the literature (Aygün, Yenisoý-Karakas, & Duman, 2003; Mianowski, Owczarek, & Marecka, 2007).

$$Iodine\ number\left(\frac{mg}{g}\right) = \alpha \times BET\ surface\ area\left(\frac{m^2}{g}\right) \quad (4.3)$$

The iodine number of the virgin GAC represents the adsorptive properties of the activated carbon, iodine adsorption capacity has a relationship with the micropores and mesopores present in the activated (Okibe, Gimba, Ajibola, & Ndukwe, 2013). Since the virgin GAC has no occupied active sites thus, the measured iodine number represents the action of the activated carbons maximum capacity. Even after regeneration, this capacity cannot be exceeded. In theory, the total adsorption capacity can be used to adsorb contaminants, as all active sites could be occupied. It is suggested that the ion exchange involving the hydroxyl groups bound to the positively charged carbon surface by electrostatic interactions is one of the main effects contributing to the adsorption of iodine, another effect that contributes is the specific interactions (Mianowski et al., 2007).

4.1.2 Methylene blue

4.1.2.1 Calibration

To carry out the methylene blue measurements, many variables needed to be determined. These include the initial concentration of the methylene blue solution, the masses of the activated carbon samples used, and the time required for the activated carbon to reach equilibrium. Literature was used to determine rough values for these variables. Concentrations ranged from 15-100 mg/L, the masses of carbon varied from 0.001 g to 0.1 g, and the equilibrium time varied from 12 to 24 hrs. After various initial experiments, the variables were decided, which were 12 hrs spinning time to reach equilibrium, initial concentration of 50 mg/L, masses of carbon varied for 0.01 -0.05 g at room temperature.

Initially, the maximum absorbance wavelength was determined, and its value was found 625 nm. The calibration curve was then determined at concentrations below 15 mg/L so the concentration-absorbance relationship is linear (absorbance at 625nm was less than approximately 1.3 AU). Higher absorbances than 1.3 resulted in non-linear relationship, thus the maximum concentration of methylene blue solution used for the calibration was 15 mg/L.

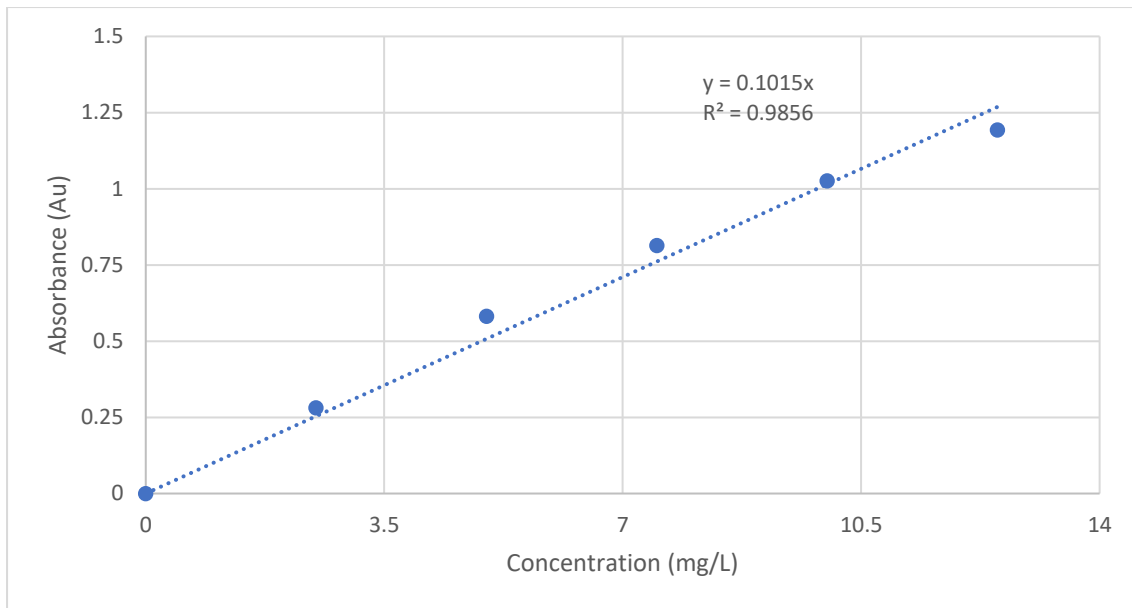


Figure 29: Calibration curve for methylene blue

As seen in Figure 29, the calibration curve displays a linear progression with the line equation of $Y=0.1015x$ and the regression coefficient $R^2= 0.9958$, which is acceptable as its above 0.995. Thus, the concentration curve can be used to determine the concentration of the methylene blue samples after the adsorption reaction using the absorbance values at 625nm.

4.1.2.2 Methylene blue adsorption on activated carbon

Methylene blue adsorption is a commonly used technique to determine the adsorptive properties of GAC similar to the iodine number. The apolar methylene blue molecule has a minimum diameter of roughly 0.9 nm; thus, it is only adsorbed onto the mesopores, macropores, and large micropores (Valdes et al., 2002). The methylene blue number (MBN) was determined from the Langmuir isotherm, the MBN is the maximum adsorption of the dye onto one gram of activated carbon thus, the MBN is equal to the Langmuir value q_{max} , which

is determined by the least squares regression fit. The Y-intercept of the Langmuir isotherm is equal to $1/q_{\max}$, thus q_{\max} is the reciprocal of the Y-intercept.

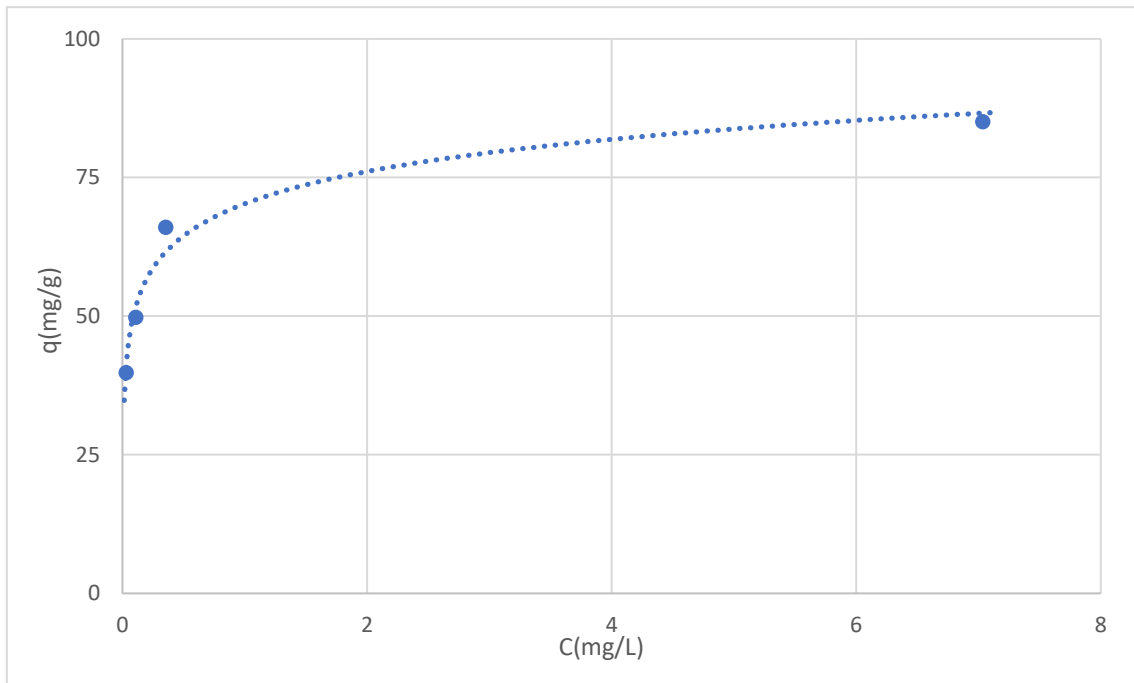


Figure 30: Q vs C graph for virgin GAC

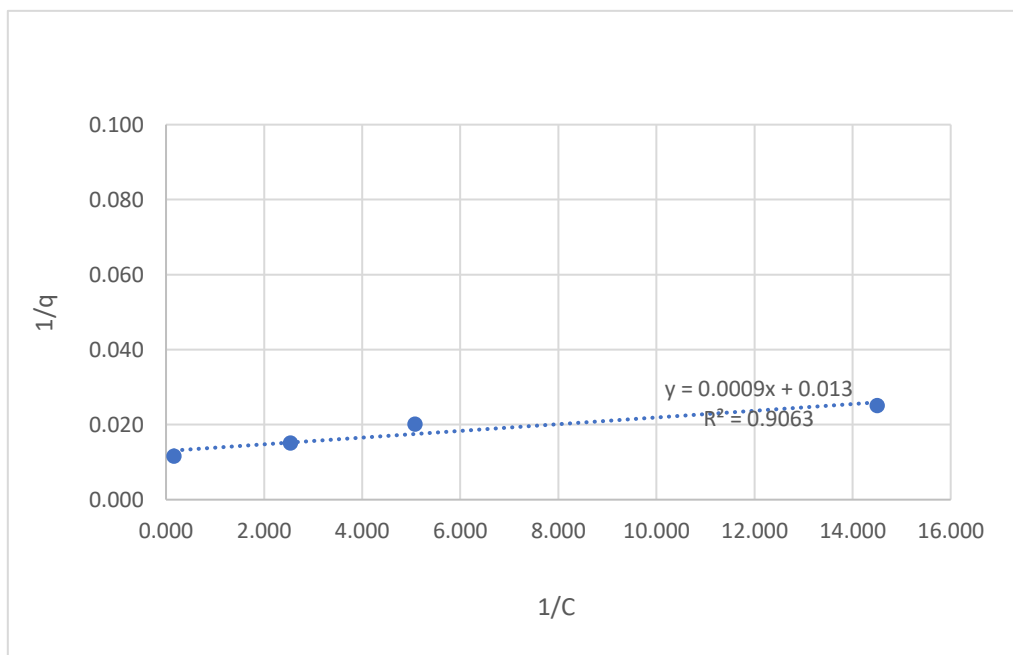


Figure 31: Langmuir isotherm of virgin GAC adsorption of methylene blue

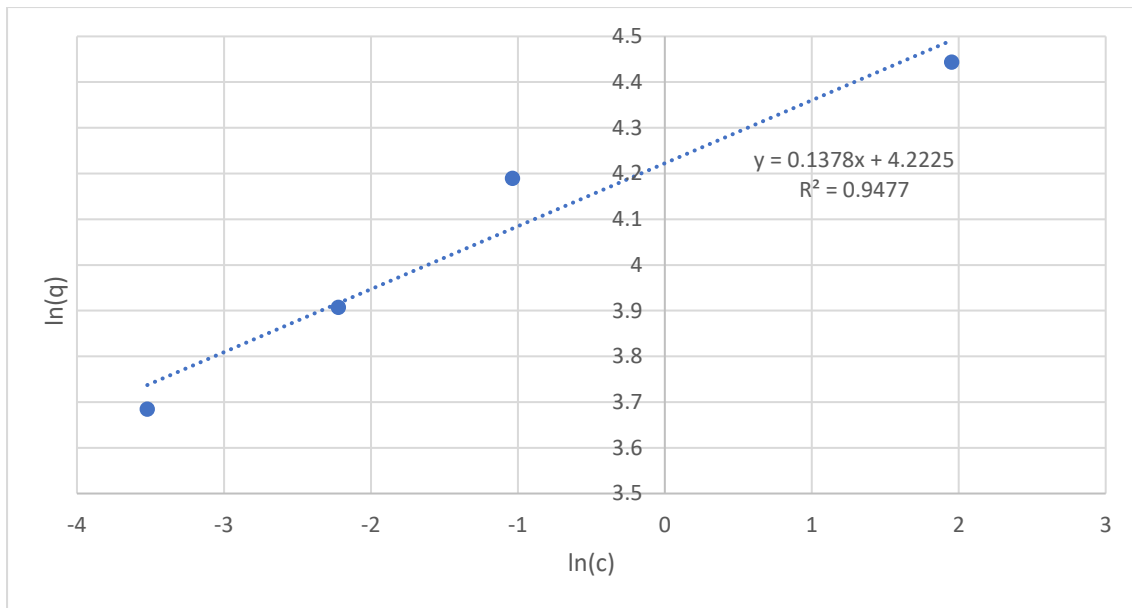


Figure 32: Freundlich isotherm of virgin GAC adsorption of methylene blue

Table 16: Methylene blue isotherm results for virgin GAC

Activated carbon	Freundlich Isotherm	Langmuir isotherm
Virgin GAC	Y=0.1378x +4.2225; R ² = 0.947 K = 68.2, 1/n = 0.1378, q= 116.93	Y=0.0009x + 0.013; R ² = 0.9063 q _{max} = 77.41, k = 14.3

The concentration curve was used to determine the concentration of the methylene blue solution after the batch experiments. Langmuir and Freundlich models were used to analyse the data; however, the Freundlich model produced a better fit for the data obtained than the Langmuir model. The Langmuir model produced a regression coefficient R² = around 0.75-0.91, whereas the Freundlich isotherm produced a regression coefficient R² of 0.91-0.99. This means that the Freundlich isotherm is more adequate and thus is more reliable and accurate in analysing the data.

The reason for the Freundlich isotherm producing a more linear fit could be because the Freundlich model typically has the most success in defining the adsorption capacity of highly

adsorptive compounds. The Langmuir model is based on monolayer, uniform and finite adsorption and also assumes no interaction between the molecules adsorbed on neighbouring sites (Bernal, Giraldo, & Moreno-Pirajan, 2018). However, the Freundlich equation, which assumes multilayer heterogeneous adsorption, is probably more realistic to represent real adsorption on the surface of the activated carbon. This is true when adsorbate interactions with varying active sites differ in energy. A good fit to this model suggests a heterogeneous surface (Bernal et al., 2018; Meriem Belhachemi, 2011).

Table 16 summaries the isotherm data, the methylene blue number for the virgin activated carbon was 0.228 mmole/g. Sources suggest higher methylene blue numbers (Okibe et al., 2013) of around 0.563 – 0.750 mmole/g, possibly due to variations in the type of carbon used. Overall, the methylene blue numbers found are within the range of methylene blue numbers for activated carbons as seen in the literature (Nunes & Guerreiro, 2011). The molar mass of methylene blue (319.85 g/mol) and iodine (126.90 g/mol) are used to convert the mass into molar concentrations (to compare the adsorption), when doing so the methylene blue numbers are much smaller than the iodine numbers obtained. This is due to iodine being able to penetrate the micropores because of their smaller dimensions in comparison to methylene blue. Thus, the methylene blue number can give a good indicator of the adsorption capacity of the mesopores in activated carbon.

4.1.3 The pH point of zero charge

The pH point of zero charge experiment is when the pH at which the surface charge of the material is zero. This is used to determine the total acidity and basicity of a specific compound.

pH_{pzc} is a vital experiment to conduct as the formation of acidic functional groups can reduce the adsorption capacity of activated carbon when adsorbing many organic compounds. This is due to the positive surface charge of the activated carbon opposing the adsorption because of the charge of the adsorbate being the same. If the pH of the solution is lower than the pH_{pzc} then the surface of the activated carbon has a net positive charge, and when the pH is higher than the pH_{pzc} the surface has a net negative charge (Adam, 2016). The pH point of zero charge experiment was determined by using the drift method.

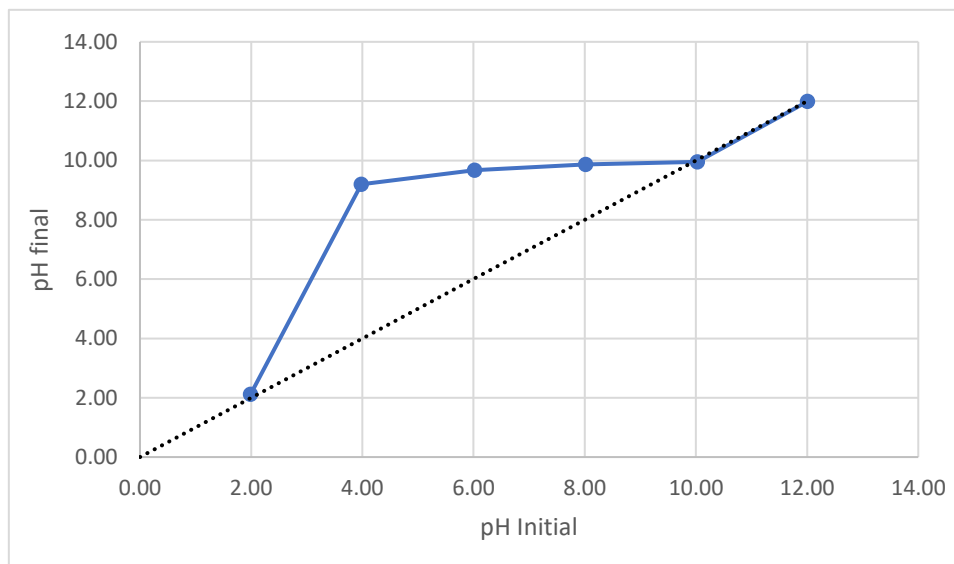


Figure 33: pH_{pzc} vs $\text{pH}_{\text{initial}}$ for virgin GAC

As shown in Figure 33, the pH_{pzc} was 9.92. In comparison in literature, the pH_{pzc} tends to be at around pH 8 (Adam, 2016), which indicates that the result obtained in this study is higher than literature. The difference in the pH_{pzc} could be due to the different methods used to activate the carbon or the type of carbon used.

The pH_{pzc} being 9.92 means that when the activated carbon is within a solution of a pH lower than 9.92, the surface charge of the activated carbon will be positive due to the protonation

of the functional groups such as amine groups (Bernal et al., 2018). Through the experiments, the distilled water used had a pH of 6.02; thus, the activated carbon samples had a positive surface charge.

4.1.4 Fourier transform infrared spectroscopy measurement (FTIR)

The Fourier transform infrared spectroscopy measurement is used to determine the surface chemistry characteristics of the virgin activated carbon. The spectra were measured from 750 – 4000 cm^{-1} . The band wavelength and their respective functional groups are stated in Table 17.

Table 17: Identification of the peaks observed in FTIR analysis of the virgin GAC

Wavelength (cm^{-1})	Indicated species
3044	C-H
2324	O=C=O
2162	C=C=O
2050 - 1980	C=C=C
1106	C-O

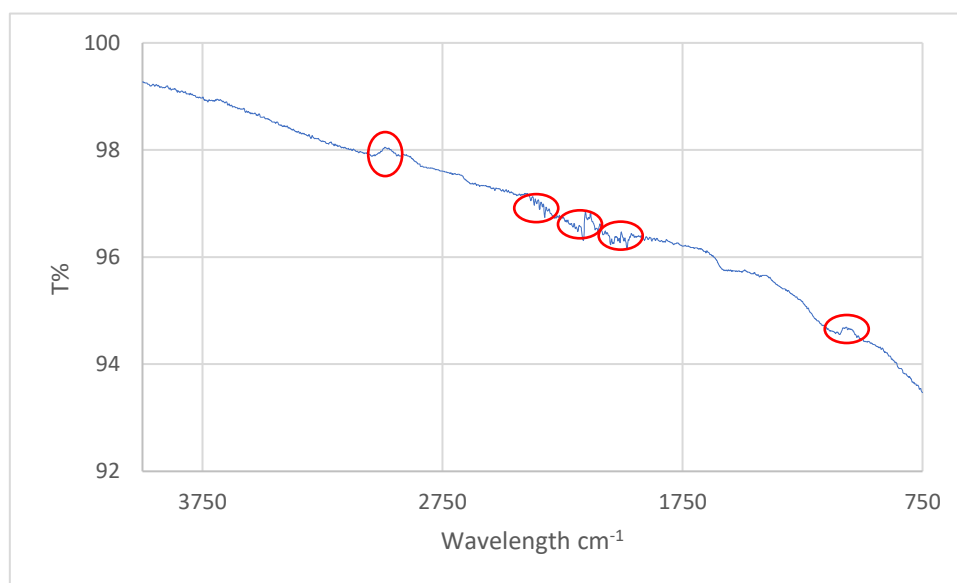


Figure 34: FTIR analysis of the virgin GAC

The peak observed at 3043.95 cm⁻¹ represents C-H stretching vibrations of the methyl group found in alkanes (Farinella, Matos, & Arruda, 2007). This bond is expected in the virgin activated carbon due to the carbon being untreated. The peak observed at 2324 cm⁻¹ represents the O=C=O stretching bond. The peak observed at 2162 cm⁻¹ represents stretching of C=C=O bond found in ketene groups. The peaks observed from 1980 cm⁻¹ to 2050 cm⁻¹ represent the C=C=C bond of an allene group. The peak observed at 1105.7 cm⁻¹ represents the C-O bond found in a primary alcohol.

4.2 Ozonation of virgin activated carbon

The GAC samples were ozonated for 30-90 mins to distinguish the change in characterisation of the carbon due to oxidation by ozone. Also, a 60 min oxygenated sample was used for comparison and to distinguish if oxygenation by pure oxygen affected the characteristics of the activated carbon.

4.2.1 Ozone concentration in water

The indigo colorimetric method used to measure ozone concentration in water is quantitative and straightforward. The method is based on the fact that in acidic solution, ozone rapidly decolourises indigo at a stoichiometry 1:1 (Bader & Hoigne, 1981). The decrease in indigo absorbance at 600 nm is linear with increasing ozone concentration. Thus, the indigo method is a powerful tool to determine the ozone concentration in water and was used in this study to quantify the change in ozone concentration in water across the 30 – 90 min ozone exposure times at an inlet ozone gas concentration of 50 -60 g/Nm³ NTP (normal temperature and pressure).

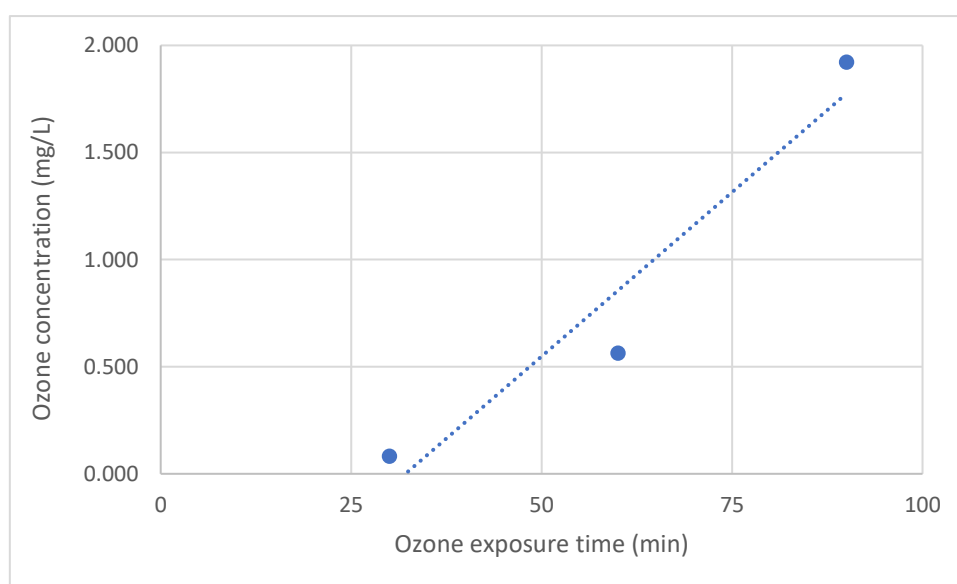


Figure 35: Ozone concentration vs ozone exposure time graph

Figure 35 shows that when the ozone exposure time increases, the ozone concentration dissolved in water also increases. The dissolved ozone concentration at 30 minutes was just above zero, indicating that the supplied ozone reacted quickly in solution due to the presence

of GAC. As the ozonation time increased to 60 then to 90 minutes, the dissolved ozone concentration also increased, indicating that the ozone demand by the solution was reducing.

4.2.2 Iodine number

The iodine number of the virgin GAC is stated in Table 18. The effect of ozone on iodine number was determined by ozonating the virgin activated carbon samples for varying lengths of time.

Table 18: Iodine number of activated carbons exposed to ozone/oxygen

Activated carbon	q(mmole/g)
Virgin GAC	3.60± 0.065
60 min oxygenated GAC	3.37±0.11
30 min ozonated GAC	3.20±0.11
60 min ozonated GAC	2.88±0.069
90 min ozonated GAC	2.33±0.16

As shown in Table 18, ozonation of GAC reduces the iodine number. The initial 30 min ozonation reduced the GAC iodine number from 3.60 to 3.20 mmole/g (11.1%), indicating that ozone reduced the adsorption capacity of virgin activated carbon. After 90 min of ozonation exposure, the original iodine number has reduced by more than a third. A reduction in the iodine number due to increased ozone exposure is also reported by other researchers (Biniak et al., 2010). The reduction in IN could be due to the ozonation of the activated carbon, producing oxygen functional group onto the surface of the carbon. These groups then block the iodine solution's adsorption, thus reducing the iodine number.

Literature suggests that after a 10-minute exposure length of ozone onto activated carbon, the adsorption capacity (surface area) has slightly increased (Valdes et al., 2002). The results

obtained in this study do not display this phenomenon, possibly to the extended ozonation time (i.e. 30 minutes versus 10 minutes). This is corroborated by when the ozonation time increased to 30-minute, the adsorption capacity was reduced (Valdes et al., 2002). As seen in the table, the iodine number was reduced from 3.60 to 3.37 mmole/g using oxygen. This could be due to the oxygenation of the activated carbon producing species that block the active sites similar to ozone but less effectively due to ozone being highly oxidative.

The adsorption capacity of the activated carbon after 90-minute ozonation time produced a 35.18 % decrease when compared to the virgin activated carbons capacity (914.16 ± 16.45 to 592.58 ± 40.57). These results indicate that as the ozone exposure time increases, the greater the oxidation effect is on the activated carbon, which modifies the activated carbon. Also, the bonding of the oxygen groups within the pore entrances could obstruct the iodine access to the micropores and obstruct the active sites. The oxygen molecules extract electrons from the π band on the activated carbon, thus reducing the interactions between iodine and activated carbon (Valdes et al., 2002).

4.2.3 Methylene blue

The effect of ozonation time on MBN of the treated virgin GAC was studied. Ozonation was carried out for 30, 60 and 90 minutes. In addition, oxygenation of virgin GAC for 60 minutes was carried out as a blank.

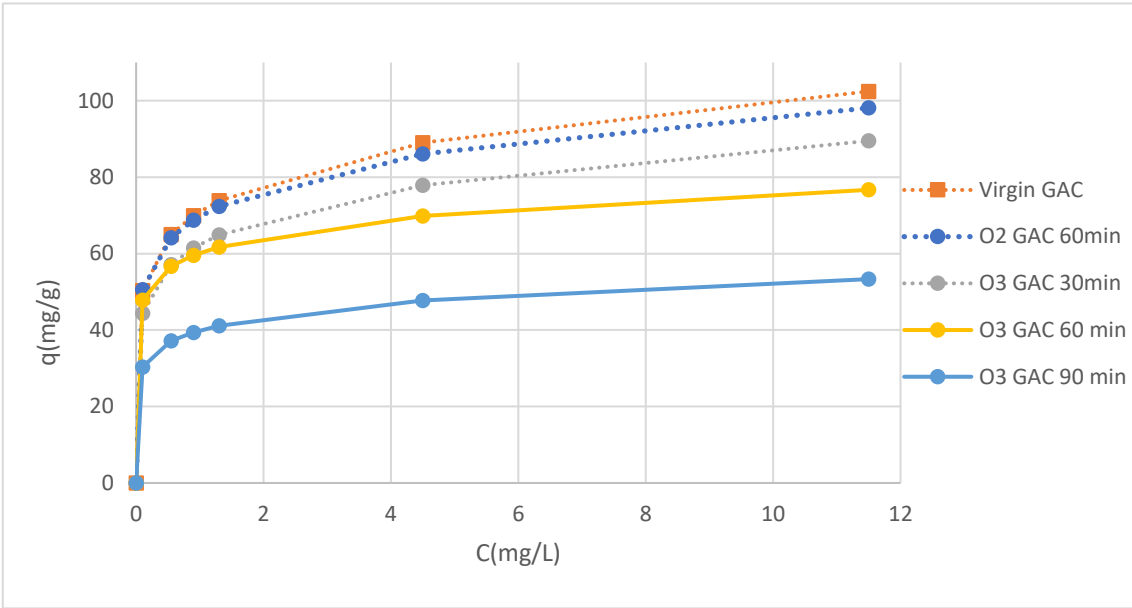


Figure 36: Q vs C graph for activated carbon exposure to ozone/oxygen

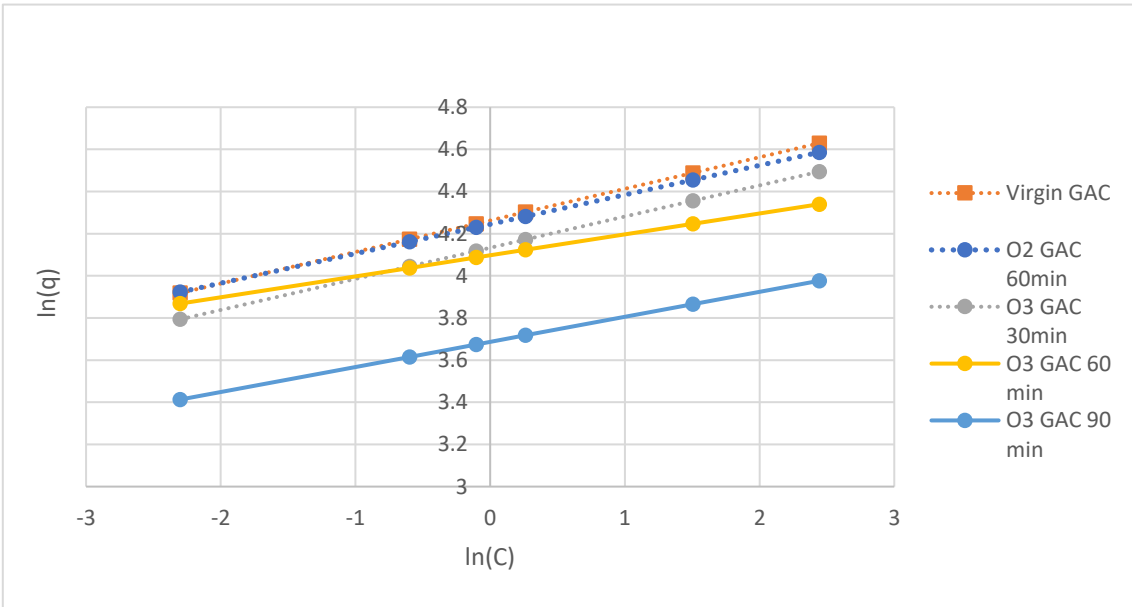


Figure 37: Freundlich isotherm for activated carbon exposed to ozone/oxygen

Table 19: Adsorption of methylene blue on activated carbon exposed to ozone/oxygen

Activated carbon	MBN (mmole/g)
Virgin GAC	0.242±0.013
GAC oxygenated for 60 minutes	0.233±0.010
GAC ozonated for 30 minutes	0.216±0.014
GAC ozonated for 60 minutes	0.196±0.0004
GAC ozonated for 90 minutes	0.163±0.0017

The effect of varying ozone exposure times on GAC adsorption capacity was determined by comparing the Freundlich isotherm and methylene blue numbers. The methylene blue numbers were determined using the least-squares fitting regression to determine the q_{max} Langmuir value. As shown in Table 19, similar to the iodine results, the methylene blue number decreases as the ozone exposure increases, thus the adsorption capacity is reducing. Figure 37 clearly shows that as the activated carbon is exposed to more ozone, the Y-intercept in the isotherm decreases. The peak height of the q vs C curve decreases with increased ozone exposure as shown in Figure 36, this is due to a decrease in adsorption capacity with an increase in ozone exposure. Figure 36 clearly shows that the adsorption isotherm is Type I. Type I isotherms are most commonly recorded during chemisorption or physisorption in highly microporous materials, therefore, this is expected.

The adsorption capacity of the activated carbon after 90-minute ozonation time produced a 32.7 % decrease in original adsorption capacity (0.242 to 0.163 mmole/g). These results are similar to as seen in the literature. However, other variables in addition to ozone exposure time such as flowrate, mixing and ozone concentration affect the degree of ozonation. As seen in Valdes et al. (2002), when using a flowrate of 76 mg /min of ozone, the methylene

blue adsorbed onto the virgin activated carbon was 0.309 mmole/g. This was gradually reduced with an increase in ozone exposure. After the activated carbon was exposed to ozone for 120 mins, the methylene blue absorbed was 0.242 mmole/g. Also, as seen in the FTIR graphs, the amount of oxygen chemically adsorbed onto the activated carbon surface increased with ozone exposure. The increase in oxygen groups is shown by the increase in bands that represent carboxylic moieties. The oxygen extracts electrons from the π band on the activated carbon, which reduces the interactions between the activated carbon and the methylene blue molecules. The reason for this phenomenon is due to the reduced strength of the dispersion forces between the π bond of the graphite planes of the activated carbon and the π electron system for the aromatic ring of the methylene blue molecules, these dispersion forces are responsible for adsorption to take place (Valdes et al., 2002).

4.2.4 The pH point of zero charge

Ozone exposure can modify the surface chemistry properties of the activated carbon, due to the oxidation reactions between ozone and the carbon surface (Valdes, Sanchez-Polo, & Zaror, 2003). Thus, the effect of ozonation on the pH_{pzc} of GAC was studied.

Table 20: pH_{pzc} results for activated carbon exposed to ozone/oxygen

Activated carbon	pH_{pzc}
Virgin GAC	9.92
GAC oxygenated for 60 minutes	9.93
GAC ozonated for 30 minutes	9.65
GAC ozonated for 60 minutes	9.69
GAC ozonated for 90 minutes	9.52

Table 20 shows only a slight change in the pH_{pzc} of the virgin activated carbon sample from 9.92 to 9.52 after 90 mins ozonation. This change, although only slight, could indicate that the 90 min ozonation made the GAC surface slightly more acidic. The more acidic groups on the activated carbon surface leads to a more negatively charged surface. The increases in acidic groups with increased ozone exposure agree with the literature (Valdes et al., 2003). The pH_{pzc} is more acidic when ozonated is due to oxygenation reactions forming acid groups, whilst basic groups are reduced. In literature, there is a more significant change across the pH_{pzc} data for ozonated, and virgin activated carbon; this could be due to the concentration of ozone applied (Valdes et al., 2003). However, according to the results obtained in the present study (Table 20), it can be concluded that ozonation had no significant effect to change the pH_{pzc} of the GAC.

4.2.5 Fourier transform infrared spectroscopy measurement (FTIR)

The Fourier transform infrared spectroscopy measurement is used to determine the change in surface chemistry characteristics of the virgin activated carbon as shown in Section 4.1.4, compared with activated carbon treated with ozone for varying lengths of time. The spectra were measured from $750 - 4000 \text{ cm}^{-1}$. The band wavelength and their respective functional groups are stated in Table 21.

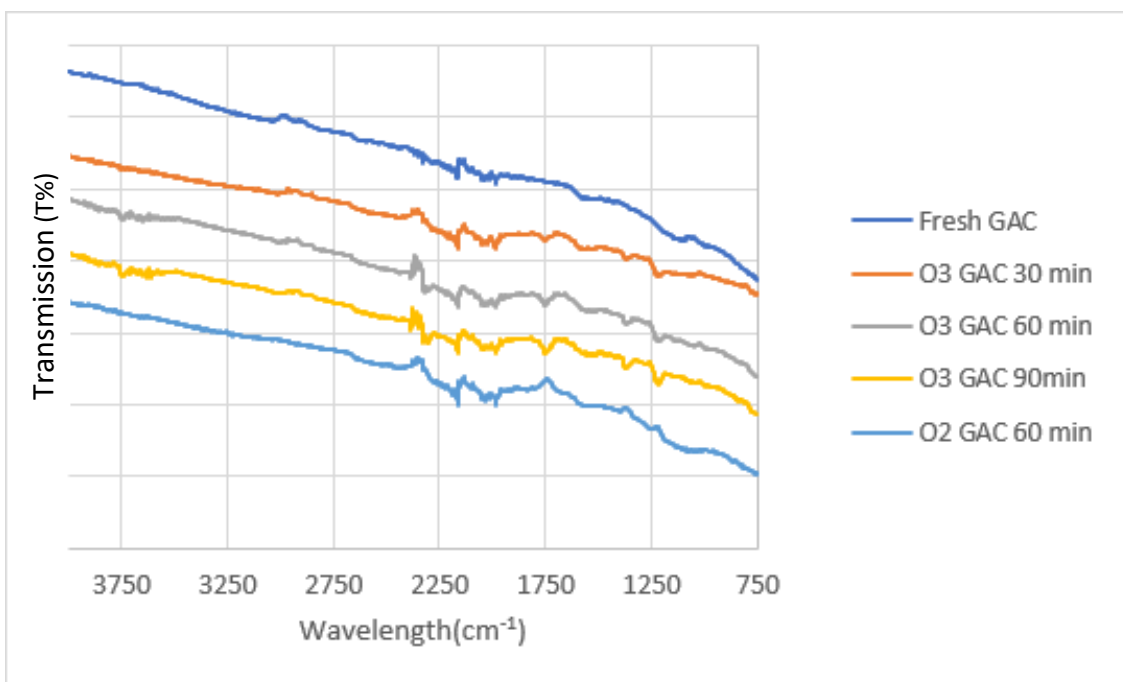


Figure 38: FTIR analysis of activated carbon exposed to ozone/oxygen

Table 21: Identification of the peaks observed in FTIR analysis of activated carbon exposed to ozone/oxygen

Wavelengths cm^{-1}	Indicated Species	Virgin GAC	Ozonated GAC 30 min	Ozonated GAC 60 min	Ozonated GAC 90 min	Oxygenated GAC 60 min
1100-1220	C-O	✓	✓	✓	✓	
1360	O-H		✓	✓	✓	
1750	C=O		✓	✓	✓	
1980 - 2050	C=C=C	✓	✓	✓	✓	✓
2160	C=C=O	✓	✓	✓	✓	✓
2300-2400	O=C=O	✓	✓	✓	✓	✓
3043	C-H	✓				
3640 - 3750	O-H		✓	✓	✓	

The peaks observed from the wavelength 3737 cm^{-1} to 3648 cm^{-1} indicate stretching of the O-H bond. This is expected during ozonation of activated carbon, thus is consistent with literature (Lota et al., 2016). The peaks observed from the wavelength 2383 cm^{-1} to 2301 cm^{-1} represents the O=C=O bond (carbon dioxide). The peak observed at 2162 cm^{-1} represents stretching of the C=C=O bond found in ketene groups. The peaks observed from the wavelengths 2044 cm^{-1} to 1980 cm^{-1} represents the C=C=C band of an allene group. The peak observed at 1751 cm^{-1} represents stretching at C=O. The peak observed at 1366 represents

the bending of the O-H bond found in carboxylic acids and alcohols. The peak observed at 1217 cm^{-1} represents the stretching modes of the C-O bonds; these covalent bonds are present in esters and acids.

As seen in Table 21 and Figure 38, the peaks that are in both the virgin and the ozonated activated carbon are: the peaks at $1100\text{-}1200\text{ cm}^{-1}$ that indicate C-O bond, the peaks at $1980\text{-}2050\text{ cm}^{-1}$ that indicates the C=C=C bond, the peak at 2160 cm^{-1} that indicates the C=C=O bond and the peaks at $2300\text{-}2400\text{ cm}^{-1}$ that indicate the O=C=O bond. The ozonated GAC has lots of peaks that are not present on the virgin GAC surface. Thus, these peaks are formed by the ozonation of the activated carbon. The peaks observed at 1360 cm^{-1} and at $3640\text{-}3750\text{ cm}^{-1}$ for ozonated samples represent the O-H bond found in carboxylic acids, which are formed due to the oxidation of the virgin activated carbon. The peak observed at 1750 cm^{-1} represents the C=O bond which also was formed due to the oxidation of the virgin activated carbon.

As seen in the table, peak 3043 cm^{-1} which represents the C-H bond was observed in the virgin GAC but was not observed on the surface of the ozonated GAC samples. This proves that ozonation of the activated carbon decreases the C-H bonds due to these bonds being oxidised to form carboxylic groups and or other highly oxidised species. The observed peaks in the range of $2300\text{ - }2400\text{ cm}^{-1}$ which represent the O=C=O bonds (carbon dioxide) and the peak at 2162 cm^{-1} , which represent C=C=O bonds found in ketene groups, have significantly increased in intensity from virgin to 90min ozonated GAC. Carbon dioxide and C=C=O are highly oxidised compounds, thus, their increase is due to ozone oxidation reactions on the surface of GAC. Moreover, the peaks observed in the range of $1100\text{ - }1220\text{ cm}^{-1}$, which

represent the C-O bond found in alcohols, have significantly increased in intensity from virgin to 90min ozonated GAC, also due to ozone oxidation reactions.

As seen in Table 21 and Figure 38, the observed peaks at around 3700 cm^{-1} are present in the 30min, 60 min, and 90 min ozonated GAC samples; this peak represents the O-H bond, it is also clear that the intensity of this peak in the 90 min samples is much greater than the 60 min and 30 min ozonated GAC sample (intensity of the peak 90 min > 60 min > 30 min). The increase in the intensity of this peak proves that with higher ozone exposure, the intensity of the O-H bond increases. Thus, the activated carbon becomes more oxidised with an increase in ozone exposure time. This increase is in line with literature (Lota et al., 2016). The observed peaks in the range of $2300 - 2400\text{ cm}^{-1}$ represent the O=C=O bonds (carbon dioxide). It is clear that the intensity of this peak in the 90 min samples is much greater than the 60 min and 30 min ozonated GAC sample (intensity of the peak 90 min > 60 min > 30 min). The increase in peak intensity also agrees with the earlier conclusion. The peaks at 1751 cm^{-1} which represents the C=O bond, and the peak at 1366 cm^{-1} which represents O-H are present in the 30min, 60 min, and 90 min ozonated GAC samples, it is clear that the intensity of this peak in the 90 min samples is much greater than the 60 min and 30 min ozonated GAC sample (intensity of the peak 90 min > 60 min > 30 min). So, the increase in the ozone exposure time increases the number of oxidised species on the activated carbon surface.

4.3 Spent GAC characterisation

Six different activated carbon samples were received from Dwr Cymru (Welsh Water) that had varying bed ages and the regeneration dates (2013 to 2020). Therefore, each carbons

adsorption capacity had the potential to vary significantly. Iodine number tests were conducted on all six of the activated carbon samples to determine the adsorption capacity of each respectively.

Table 22: Iodine numbers and regeneration dates for the six spent GAC samples

Activated Carbon	q(mmole/g)	Regeneration Date
GAC-A	2.90±0.052	Nov 2020
GAC-B	1.26±0.023	Jan 2015
GAC-C	1.77±0.031	Mar 2013
GAC-D	1.53±0.028	Oct 2013
GAC-E	2.05±0.037	Dec 2018
GAC-F	2.38±0.043	June 2020

As seen in Table 22, the adsorption capacity of each carbon varies from 2.90 to 1.26 mmole/g. It is clear from Table 22 that carbons that were last regenerated more than five years ago have low iodine numbers, thus need regenerating again. On the other hand, although the age of the GAC can determine that the activated carbons adsorption capacity is low, it is not a reasonable estimate of the exact adsorption capacity of the activated carbon. GAC-B shows this, it has an iodine number of 1.26 mmole/g and was last regenerated in January 2015, but GAC- C has an iodine number of 1.77 mmole/g but was last regenerated in March 2013. The adsorption of GAC is ineffectively determined using the time in use, this coincides with literature (Ritson & Graham, 2019).

The Fourier transform infrared spectroscopy measurement is used to determine the surface chemistry characteristics of the spent activated carbon samples.

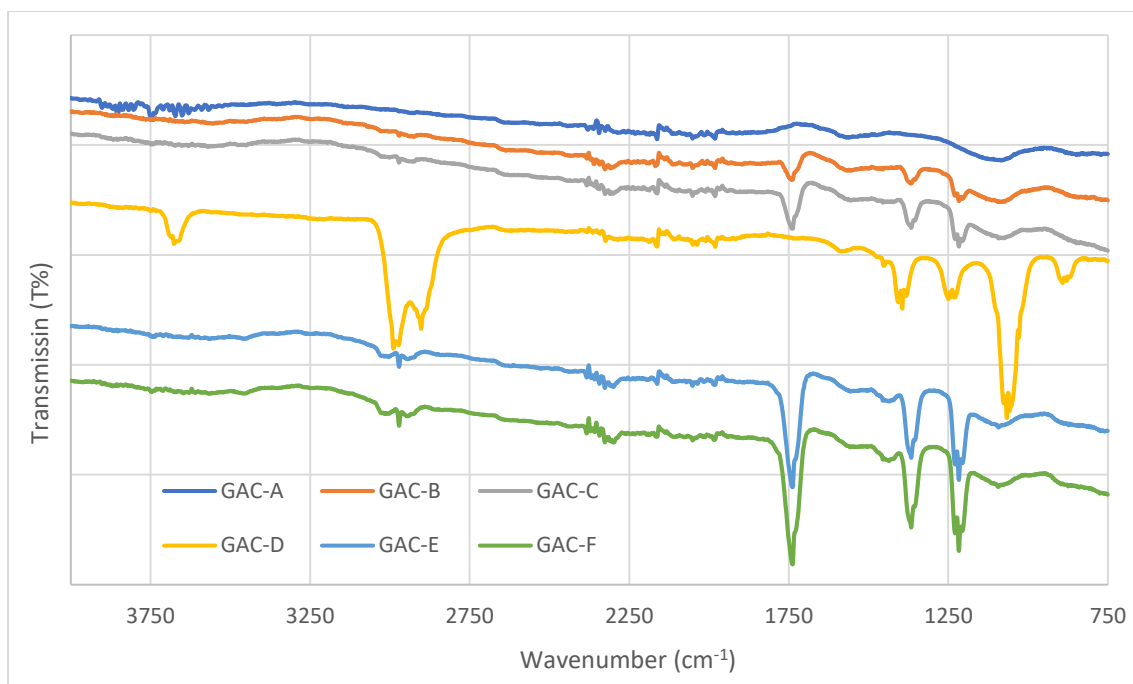


Figure 39: FTIR analysis of the spent activated carbons

Table 23: Identification of the peaks observed in FTIR analysis of spent activated carbon

Wavelength (cm ⁻¹)	Possible indicated species
3760-3680	O-H
3000-2900	N-H
2400-2300	O=C=O
2050 - 1980	C=C=C
1740	C=O
1400-1360	C-H or O-H
1240-1220	C-N or C-O
1070	C-O or S=O
900	C=C

The peaks observed between 3680 cm⁻¹ to 3760 cm⁻¹ represent the stretching of the O-H bond in an alcohol group. The peaks observed from 2900 cm⁻¹ to 3000 cm⁻¹ represent the stretching of the N-H found in an amine group. The peaks observed between 2300 cm⁻¹ to 2400 m⁻¹ represents the O=C=O stretching bond. The peaks observed between 1980 cm⁻¹ to 2050 cm⁻¹ represent the stretching of C=C=C bond of an allene group. The peak observed at 1740 cm⁻¹

represents the stretching of C=O bond. The peaks observed at 1360 cm^{-1} to 1400 cm^{-1} could represent the bending of O-H or C-H bonds. The peaks observed at 1220 cm^{-1} to 1240 cm^{-1} could represent the stretching of the C-N or C-O bonds. The peaks observed at 1070 cm^{-1} could represent the stretching of C-O or S=O bonds. The peak observed at 900 cm^{-1} represents the bending of C=C bond. The peaks observed at 900 cm^{-1} , 1240 cm^{-1} , 1400 cm^{-1} , 1740 cm^{-1} , 2400 cm^{-1} , 3000 cm^{-1} and 3760 cm^{-1} are not present in the virgin activated carbon thus bonds observed from these peaks are formed from contaminants that are adsorbed on the activated carbons surface for example the amine salt group at peak 3000 – 2900 cm^{-1} .

The spent GAC-D was ozonated for 30 and 60 minutes using the same method as stated in section 3.3. Ozonation of spent GAC is used to regenerate the activated carbons, thus increase the adsorption capacity by removing contaminants from the active sites, consequently increasing the iodine number. The iodine numbers before and after ozonation were determined.

Table 24: Iodine number of GAC-D with varying exposure to ozone

Activated carbon	q(mmole/g)
GAC-D	1.53±0.028
30 min ozonated GAC-D	1.91±0.034
60 min ozonated GAC-D	1.71±0.031

As shown in Table 24, the initial 30 min ozonation exposure of the spent activated carbon increased the iodine number from 1.53 mmole/g to 1.91 mmole/g. Thus, this is a 24.95 % increase in the iodine number. The increase in the iodine number proves that ozonation of the activated carbon removes the contaminants on the surface of the activated carbon through the oxidation of the species. Therefore, the activated carbon (GAC-D) was partially regenerated and its adsorption capacity has increased. However, a further increase in ozonation time to 60 minutes reduced the IN of the GAC to 1.71 mmole/g, possibly due to

modification of the carbon surface chemical properties and adsorptive textual characteristics (Valdes et al., 2002). As the chemical properties are modified, the adsorption capacity can be reduced due to oxygen groups blocking active sites on the surface of the activated carbon (Valdes et al., 2002). It is crucial to determine the optimal regeneration time required for the highest removal of contaminants with the minimal damage to activated carbon structure. The iodine number results along with the FTIR data suggests that a lower ozonation time potentially would increase the iodine number thus the adsorption capacity of the GAC-D.

GAC-D was ozonated for 30 and 60 min in order to determine the change in the properties of spent activated carbon with varying ozone exposure. FTIR was used to determine the change in the surface chemistry across the three samples and evaluate the effect of varying ozone exposure on removing contaminants on the surface of the activated carbon.

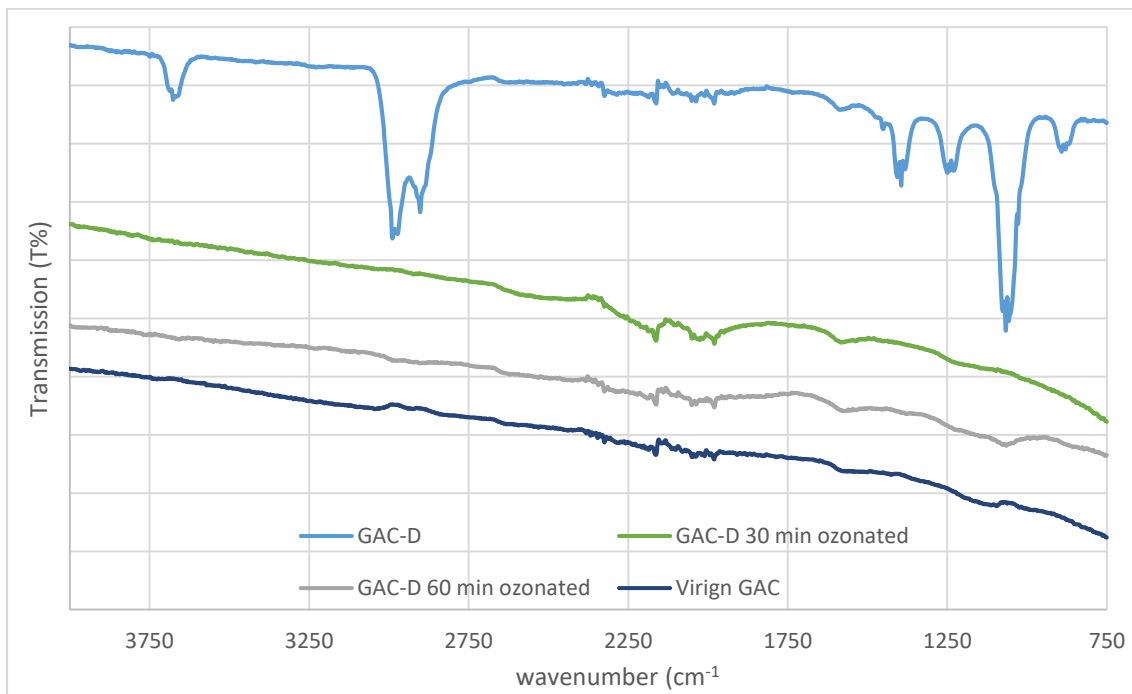


Figure 40: FTIR analysis of ozonated spent activated carbon

As seen in Figure 40, spent GAC shows the appearance of several strong peaks than virgin GAC. Upon application of ozone, these peaks have been fully removed, which indicates that ozonation have removed the adsorbed species from the spent GAC due to oxidation. Since the FTIR of ozonated GAC looks very similar to virgin GAC, it can be stated that regeneration of the GAC took place successfully with respect to the surface chemistry. However, further optimisation of the process and evaluation of the fate of the removed species in solution are required.

4.4 Geosmin and MIB adsorption

The geosmin and MIB adsorption experiment was used to determine how effective activated carbon is at removing geosmin and MIB from water through adsorption. Varying masses of activated carbon were added to water samples dosed with G-MIB. As the mass of the activated carbon is increased, the removal of geosmin and MIB should decrease, due to the increase in adsorption.

Fluorescence spectrometry was used to determine the change in the amount of geosmin and MIB after the activated carbon adsorption. The fluorescence intensity value (a.u.) is determined for each sample. The greater the fluorescence intensity, the more geosmin and MIB present in the sample. To produce a calibration curve emission and excitation wavelengths were selected from the initial experiment, then the calibration curve was produced, as seen in Figure 41.

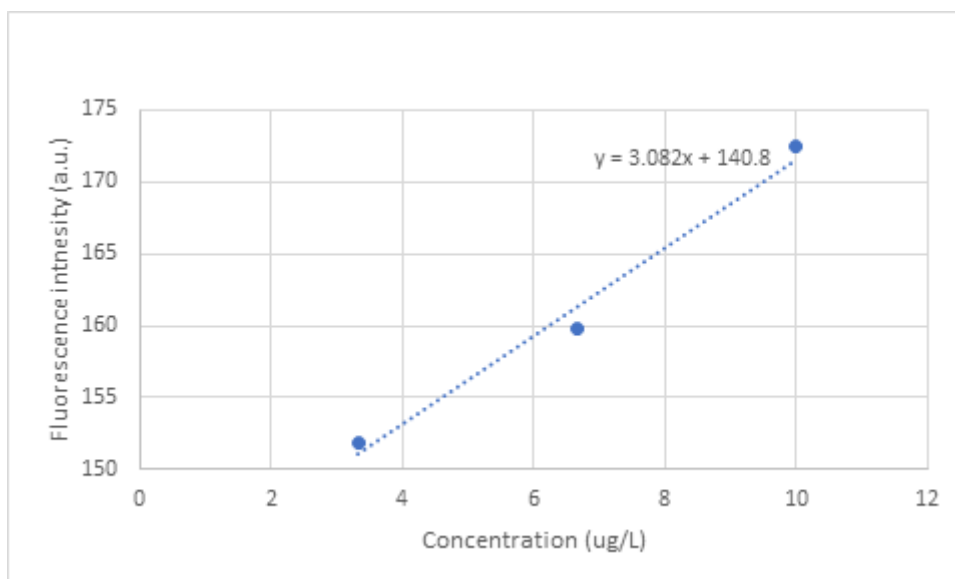


Figure 41:G-MIB Fluorescence intensity vs concentration calibration curve

The calibration curve was produced using the fluorescence intensity values determined from each sample solution, the sample solutions were a mixture of 10 µg/L G-MIB solution and distilled water starting at 0 mL of water and 3mL of G-MIB, changing in 1mL increments. The calibration curve shows that as the concentration in the G-MIB solution decreases, the fluorescence intensity also decreases linearly.

The adsorption of G-MIB experiment was conducted using 0-30 mg masses of activated carbon in 500 mL volume. The fluorescence intensity results are converted into concentration values using the calibration curve. The results are presented in Table 25.

Table 25: G-MIB adsorption data

Mass (mg)	Fluorescence intensity (a.u.)	Concentration(µg/L)
0.00	172.43	10.26
10.00	172.56	10.30
20.00	164.14	7.57
30.00	162.21	6.95

As seen in Table 25, the fluorescence intensity value for the 10 mg sample does not fit the pattern, as the fluorescence intensity value is higher for 10mg than 0 mg of activated carbon, thus, this value is excluded from the results because of the large error that would result from measuring such a very low mass. Figure 42 shows that the GAC uptake of GMIB increases linearly with the aqueous concentration. This is particularly true because of the low concentration (i.e. dilute system) used in the experiments.

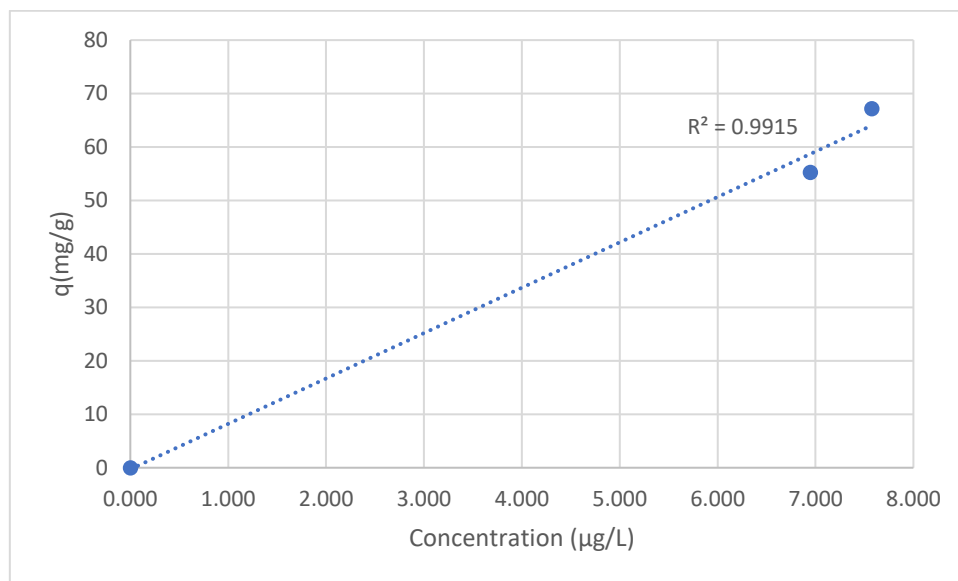


Figure 42: GMIB uptake by GAC

The results are as expected, with an increase in the activated carbon present in the G-MIB solution as greater adsorption of the geosmin and MIB contaminants should take place. The 30mg sample of activated carbon reduced the concentration of G-MIB by 32% from 10.26 to 6.95 µg/L.

The geosmin and MIB adsorption experiment was used to determine how effective activated carbon is at removing geosmin and MIB from water through adsorption. Varying masses of activated carbon were added to water samples dosed with G-MIB. A more detailed study on

the adsorption of G-MIB should be studied to evaluate the effect of ozone-regenerated GAC on G-MIB adsorption. Also, analysis of G-MIB should be done by GC-MS, which is a more accurate method than fluorescence.

This chapter presented and discussed the experimental results obtained in this study. The data showed that ozonation of virgin activated carbon reduces its adsorption capacity due to oxidation of the surface of the material. However, application of ozone on spent GAC revealed that ozone removed adsorbed contaminants on its surface after being used in the water treatment process and lead to increased adsorption capacity for iodine. It can thus be concluded that ozonation has potential to regenerate GAC in-situ without the need for GAC removal and transport for external regeneration.

5.0 Conclusions and recommendations for future work

5.1 Summary

The objective of this research project was to evaluate the effect of ozone on the regeneration of GAC, specifically looking at the impact of ozonation time on key characteristics of the GAC. The project also aimed at evaluating the effect of ozonation on a real spent GAC and the adsorption of G-MIB on GAC.

Activated carbon is highly microporous and thus was developed to remove contaminants, for example, geosmin and MIB. Over time the activated carbon becomes spent and thus needs regeneration. Thermal regeneration is currently used, but this process is not *in-situ*, has a high carbon footprint, and produces carbon burn off. Ozone regeneration is used to reactivate the carbon and remove the geosmin and MIB adsorbed onto the surface due to it not causing burn off and can be performed *in-situ*, but it can affect the activated carbons surface chemistry if high doses are used.

The project achieved successful results that can be taken forward to further evaluate the ozone technology as a potential *in-situ* regeneration method for GAC.

5.2 Conclusions

- Increasing the ozone treatment time increases the dissolved ozone concentration within the water.
- Increasing the concentration of ozone used to treat activated carbon decreases the activated carbons adsorption capacity. The adsorption capacity is reduced due to the increased amount of carboxylic and highly oxidised species present in the activated carbon, thus there are fewer active sites available for adsorption. The adsorption

capacity of the activated carbon after 90-minute ozonation time produced a 35.18 % decrease in original adsorption capacity for iodine number and a reduction of 32.72 % in methylene blue adsorption capacity.

- The effect of ozonation at lower exposure times was more beneficial since 30-minute ozonation yielded lower reductions in iodine and methylene blue numbers. The iodine and methylene blue numbers of the 30 minute ozonated samples yielded a decrease of 11.1% and 10.94%, respectively when compared with the virgin carbon adsorption capacity.
- Increasing the concentration of ozone used to treat activated carbon increases the amount of carboxylic and highly oxidised species present in the activated carbon.
- Increasing the concentration of ozone used to treat activated carbon decreases the pH point of zero charge slightly, thus increases the acidity of the activated carbons surface chemistry.
- Ozone can successfully regenerate activated carbon, ozone regeneration of spent activated carbon, 30-minute ozonation treatment produced a 24.95 % increase in the adsorption capacity of iodine spent activated carbon.
- Ozone regeneration of spent activated carbon removes all adsorbed contaminants that are present on the spent activated carbon surface using a 30-minute ozonate treatment thus the optimal regeneration of activated carbon is less than 30 minutes.
- Increasing the mass of activated carbon used to treat the G-MIB solution increases the removal of G-MIB from the sample, 30mg of activated carbon reduces the concentration of G-MIB by 32%.

5.3 Recommendations for future work

- The optimal ozone regeneration requirements should be obtained for the regeneration of iodine spent activated carbon, the optimal ozonation time at the specified conditions is less than 30 minutes.
- Isotherms for G-MIB adsorption experiment with conclusive results should be produced, this should be done by using better analytical equipment for the analysis of geosmin & MIB, for example, the GC/MS or HPLC should be used for more accurate and reliable results.
- Lower G-MIB concentrations should be used as the OTC of geosmin and MIB ranges from around 7- 20 ng/L.
- Greater variation of ozone concentrations should be used when regenerating the activated carbon to evaluate over and under regeneration more profoundly.
- Detailed economic analysis of *in-situ* ozone regeneration in comparison to thermal/steam regeneration should be evaluated.
- Activated carbon should be saturated with geosmin and MIB, the adsorption capacity should be determined and then regenerated using ozone, the adsorption capacity after regeneration should be found to determine the removal of geosmin and MIB.
- Other characterisation methods should be used to determine a more varied analysis of the change in activated carbon after ozonation.
- The change in the methylene blue number after ozonating spent activated carbon should be evaluated.
- Different variations of activated carbon should be used (PAC).

- The rate of regeneration of the activated carbon when using ozone should be determined and compared with thermal/steam regeneration used in industry currently.

This chapter summaries the conclusions and recommendations for future work, the main points addressed in this chapter are that ozone can be used to regenerate spent activated carbon but optimisation of the ozonation process is essential to obtaining a higher adsorption capacity of the ozonated carbon when it is put back into service.

6.0 References

- Adam, O. E.-A. A. (2016). Removal of Resorcinol from Aqueous Solution by Activated Carbon: Isotherms, Thermodynamics and Kinetics. *American Chemical Science Journal*, 16(1), 1-13. doi: 10.9734/ACSJ/2016/27637
- Afonso, M. R. A., & Silveira, V. (2005). Characterization of equilibrium conditions of adsorbed silica-gel/water bed according to Dubinin-Astakhov and Freundlich. *Engenharia Térmica (Thermal Engineering)*, 4(1), 3-7. doi: 10.5380/reterm.v4i1.3540
- Alhamami, M., Doan, H., & Cheng, C. H. (2014). A Review on Breathing Behaviors of Metal-Organic-Frameworks (MOFs) for Gas Adsorption. *Materials*, 7(4), 3198-3250. doi: 10.3390/ma7043198
- Allen, S. J., & Whitten, L. (1998). The Production and Characterisation of Activated Carbon: A Review. *Asia-Pacific Journal of chemical engineering*, 6(5), 231-261. doi: 10.1002/apj.5500060501
- Alvarez, P. M., Beltran, F. J., Gomez-Serrano, V., Jaramillo, J., & Rodriguez, E. M. (2004). Comparison between thermal and ozone regenerations of spent activated carbon exhausted with phenol. *Water Research*, 38(8), 2155-2165. doi: 10.1016/j.watres.2004.01.030
- Ambroz, F., & Macdonald, T. J. (2018). Evaluation of the BET theory for the characterization of meso and microporous MOFs. *Small Methods*, 2(11) doi: 10.1002/smtd.201800173
- Andreadakis, A., & Mamais, D. (2010). Removal of taste and odour from potable water by ozone and Powdered Activated Carbon (PAC). *International Journal of Environment and Waste Management*, 5(3), 392 - 409. doi: 10.1504/IJEW.2010.032016
- Ania, C. O., Cabal, B., Parra, J. B., & Pis, J. (2007). Importance of the hydrophobic character of activated carbons on the removal of naphthalene from the aqueous phase. *Adsorption Science & Technology*, 25(3-4), 155-167. doi: 10.1260/026361707782398164
- Antal, M. J., & Gronli, M. (2003). The art, science, and technology of charcoal production. *Industrial & Engineering Chemistry Research*, 42(8), 1619-1640. doi: 10.1021/ie0207919
- Aworn, A., Thiravetyan, P., & Nakbanpote, W. (2008). Preparation and characteristics of agricultural waste activated carbon by physical activation having micro- and mesopores. *Journal of Analytical and Applied Pyrolysis*, 82(2), 279-285. doi: 10.1016/j.jaap.2008.04.007
- Aygun, A., Yenisoay-Karakas, S., & Duman, I. (2003). Production of granular activated carbon from fruit stones and nutshells and evaluation of their physical, chemical and adsorption properties. *Microporous and Mesoporous Materials*, 66(2-3), 189-195. doi: 10.1016/j.micromeso.2003.08.028
- Babel, S., & Kurniawan, T. A. (2004). Cr(VI) removal from synthetic wastewater using coconut shell charcoal and commercial activated carbon modified with oxidizing agents and/or chitosan. *Chemosphere*, 54(7), 951-967. doi: 10.1016/j.chemosphere.2003.10.001
- Bader, H., & Hoigne, J. (1981). Determination of ozone in water by the indigo method *Water Research*, 15(4), 449-456. doi: 10.1016/0043-1354(81)90054-3
- Bansal, R., & Goyal, M. (2005). *Activated carbon adsorption* (1st ed.). Boca Raton: Taylor & Francis.
- Bedner, M., & Saito, K. (2020). Development of a liquid chromatography atmospheric pressure chemical ionization mass spectrometry method for determining off-flavor compounds and its application toward marine recirculating aquaculture system monitoring and evaluation of aeration as a depuration approach. *Journal of Chromatography A*, 1609 doi: 10.1016/j.chroma.2019.460499
- Bentley, R., & Meganathan, R. (1981). Geosmin and methylisoborneol biosynthesis in streptomycetes - evidence for an isoprenoid pathway and its absence in non-differentiating isolates. *Febs Letters*, 125(2), 220-222. doi: 10.1016/0014-5793(81)80723-5
- Berenguer, R., Marco-Lozar, J. P., Quijada, C., Cazorla-Amoros, D., & Morallon, E. (2010). Comparison among Chemical, Thermal, and Electrochemical Regeneration of Phenol-Saturated Activated Carbon. *Energy & Fuels*, 24(6), 3366-3372. doi: 10.1021/ef901510c
- Bernal, V., Giraldo, L., & Moreno-Pirajan, J. C. (2018). Physicochemical Properties of Activated Carbon: Their Effect on the Adsorption of Pharmaceutical Compounds and Adsorbate-Adsorbent Interactions. *C-Journal of Carbon Research*, 4(4) doi: 10.3390/c4040062
- Biniak, S., Trykowski, G., Pakula, M., Swiatkowski, A., Malinowska, Z., & Popiel, S. (2010). Effects of Ozone Dissolved in Water on the Physicochemical Properties of Activated Carbons Applied in Drinking Water Treatment. *Adsorption Science & Technology*, 28(6), 521-531. doi: 10.1260/0263-6174.28.6.521
- Boehm, H. P. (1994). Some aspects of the surface-chemistry of carbon-blacks and other carbons. *Carbon*, 32(5), 759-769. doi: 10.1016/0008-6223(94)90031-0

- Bristow, R. L., Young, I. S., Pemberton, A., Williams, J., & Maher, S. (2019). An extensive review of the extraction techniques and detection methods for the taste and odour compound geosmin (trans-1, 10-dimethyl-trans-9-decalol) in water. *Trac-Trends in Analytical Chemistry*, 110, 233-248. doi: 10.1016/j.trac.2018.10.032
- Brunauer, S., Deming, L. S., Deming, W. E., & Teller, E. (1940). On a theory of Van der Waals adsorption of gases. *Journal of the American Chemical Society*, 62(7), 1723-1732. doi: 10.1021/ja01864a025
- Bubanale, S. (2017). History, Method of Production, Structure and Applications of Activated Carbon. *International Journal of Engineering Research & Technology*, 6(6) doi: 10.17577/IJERTV6IS060277
- Buczek, B. (2016). Preparation of Active Carbon by Additional Activation with Potassium Hydroxide and Characterization of Their Properties. *Advances in Materials Science and Engineering* doi: 10.1155/2016/5819208
- Callewaert, J. (2014). *Activated carbon pores*. from <https://www.desotec.com/en/carbonology/carbonology-cases/activated-carbon-pores>
- Chen, G., Dussert, B. W., & Suffet, I. H. (1997). Evaluation of granular activated carbons for removal of methylisoborneol to below odor threshold concentration in drinking water. *Water Research*, 31(5), 1155-1163. doi: 10.1016/s0043-1354(96)00362-4
- Cheremisinoff, P. N., & Ellerbusch, F. (1978). *Carbon adsorption handbook*. Michigan: Ann Arbor Science Publishers.
- Coble, P. G. (2014). Aquatic organic matter fluorescence (pp. 3-34). New York: Cambridge University Press.
- Collivignarelli, C., & S.Sorlini. (2004). AOP's with ozone and UV radiation in drinking water: contaminants removal and effects on disinfection byproducts formation. *Water Science and Technology*, 49(4), 6-51. doi: 10.2166/wst.2004.0218
- Cook, D., Newcombe, G., & Sztajn bok, P. (2001). The application of powdered activated carbon for MIB and geosmin removal: Predicting PAC doses in four raw waters. *Water Research*, 35(5), 1325-1333. doi: 10.1016/s0043-1354(00)00363-8
- Crittenden, J. C. (2012). *MWH's water treatment*. Hoboken, N.J: Wiley.
- Cuhadaroglu, D., & Uygun, O. A. (2008). Production and characterization of activated carbon from a bituminous coal by chemical activation. *African Journal of Biotechnology*, 7(20), 3703-3710. doi: 10.5897/AJB08.588
- Çeçen, F., & Aktas, O. (2012). *Activated carbon for water and wastewater treatment*. Weinheim: Wiley-VCH.
- Dean, J. R. (2000). *Extraction methods for environmental analysis*. John Wiley & Sons Inc.
- Duran-Valle, C. J., Gomez-Corzo, M., Pastor-Villegas, J., & Gomez-Serrano, V. (2005). Study of cherry stones as raw material in preparation of carbonaceous adsorbents. *Journal of Analytical and Applied Pyrolysis*, 73(1), 59-67. doi: 10.1016/j.jaap.2004.10.004
- El-Hendawy, A. N. A., Alexander, A. J., Andrews, R. J., & Forrest, G. (2008). Effects of activation schemes on porous, surface and thermal properties of activated carbons prepared from cotton stalks. *Journal of Analytical and Applied Pyrolysis*, 82(2), 272-278. doi: 10.1016/j.jaap.2008.04.006
- Elhadi, S. L. N., Huck, P. M., & Slawson, R. M. (2006). Factors affecting the removal of geosmin and MIB in drinking water biofilters. *Journal American Water Works Association*, 98(8), 108-119. doi: 10.1002/j.1551-8833.2006.tb07738.x
- Elias-Maxil, J. A., Rigas, F., de Velasquez, M. T. O., & Ramirez-Zamora, R. M. (2011). Optimization of Fenton's reagent coupled to Dissolved Air Flotation to remove cyanobacterial odorous metabolites and suspended solids from raw surface water. *Water Science and Technology*, 64(8), 1668-1674. doi: 10.2166/wst.2011.528
- Emmett, P. H., & Brunauer, S. (1937). The use of low temperature van der Waals adsorption isotherms in determining the surface area of iron synthetic ammonia catalysts. *Journal of the American Chemical Society*, 59(8), 1553-1564. doi: 10.1021/ja01287a041
- EPA. (2001). *The history of drinking water treatment*. Washington, D.C.: U.S. Environmental Protection Agency, Office of Water.
- Ergenekon, D. P. (2010). Adsorption lecture notes, ENVE542, Air Pollution Control Technologies.
- Everett, D. H., & Koopal, L. K. (1971). Manual of symbols and terminology for physicochemical quantities and units - adsorption and spreads monolayers *Pure and Applied Chemistry*, 51(1), 1-41. doi: 10.1351/pac197951010001
- Evers, R. (2014). *Development of a Liquid Chromatography Ion Trap Mass Spectrometer Method for Clinical Drugs of Abuse Testing with Automated On-Line Extraction Using Turbulent Flow Chromatography* (Doctorate of Biomedical Science). University of Portsmouth, Portsmouth.

- Farinella, N. V., Matos, G. D., & Arruda, M. A. Z. (2007). Grape bagasse as a potential biosorbent of metals in effluent treatments. *Bioresource Technology*, 98(10), 1940-1946. doi: 10.1016/j.biortech.2006.07.043
- Flores, R. M. (2014). *Coal and coalbed gas* (1st ed.): Elsevier.
- Gamal, M. E., Mousa, H. A., & El-Naas, M. H. (2018). Bio-regeneration of activated carbon: A comprehensive review. *Separation and purification technology*, 197, 345-359. doi: 10.1016/j.seppur.2018.01.015
- Gerber, N. N., & Lechevalier, H. A. (1965). Geosmin, an Earthy-Smelling Substance Isolated from Actinomycetes. *Applied Microbiology*, 13(6), 935-938. doi: 10.1128/am.13.6.935-938.1965
- Giglio, S., Chou, W. K. W., Ikeda, H., Cane, D. E., & Monis, P. T. (2011). Biosynthesis of 2-methylisoborneol in cyanobacteria. *Environmental Science & Technology*, 45(3), 992-992. doi: 10.1021/es102992p
- Glassman, I., Yetter, R. A., & Glumac, N. G. (2014). *Combustion*: Elsevier Academic Press.
- Gottschalk, C. (2010). *Ozonation of Water and Waste Water* Weinheim: Wiley-VCH.
- Greenbank, M., & Knepper, J. (2002). *GAC/PAC: Use of powdered activated carbon for portable water treatment in small systems*. from <https://wcponline.com/2002/11/21/gacpac-use-powdered-activated-carbon-potable-water-treatment-small-systems/>
- Greenbank, M., & Spotts, S. (1995). Effects of Starting Material on Activated Carbon Characteristics and Performance. *Industrial Water Treatment*
- Guo, Y. Q., & Du, E. D. (2012). The Effects of Thermal Regeneration Conditions and Inorganic Compounds on the Characteristics of Activated Carbon Used in Power Plant. *2012 International Conference on Future Electrical Power and Energy System, Pt A*, 17, 444-449. doi: 10.1016/j.egypro.2012.02.118
- Hall, E. L., & Dietrich, A. M. (2000). A Brief History of Drinking Water. *Opflow*, 26(6), 46-49. doi: 10.1002/j.1551-8701.2000.tb02243.x
- Hao, G. P., Li, W. C., Wang, S. A., Wang, G. H., Qi, L., & Lu, A. H. (2011). Lysine-assisted rapid synthesis of crack-free hierarchical carbon monoliths with a hexagonal array of mesopores. *Carbon*, 49(12), 3762-3772. doi: 10.1016/j.carbon.2011.05.010
- Hijnen, W. A. M., Suylen, G. M. H., Bahlman, J. A., Brouwer-Hanzens, A., & Medema, G. J. (2010). GAC adsorption filters as barriers for viruses, bacteria and protozoan (oo)cysts in water treatment. *Water Research*, 44(4), 1224-1234. doi: 10.1016/j.watres.2009.10.011
- Ho, Y. S. (2004). Citation review of Lagergren kinetic rate equation on adsorption reactions. *Scientometrics*, 59(1), 171-177. doi: 10.1023/B:SCIE.0000013305.99473.cf
- Islam, M. S., Aug, B. C., Gharehkhani, S., & Affi, A. B. M. (2015). Adsorption capability of activated carbon synthesized from coconut shell. *Carbon Letters*, 20(1), 1-9. doi: 10.5714/CL.2016.20.001
- Johnson, P. J., Setsuda, D. J., & Williams, R. S. (1999). Activated carbon for automotive applications. *Carbon materials for advanced technologies*, 235-268. doi: 10.1016/B978-008042683-9/50010-8
- Jung, S. W., Baek, K. H., & Yu, M. J. (2004). Treatment of taste and odor material by oxidation and adsorption. *Water Science and Technology*, 49(9), 289-295.
- Juttner, F., & Watson, S. B. (2007). Biochemical and ecological control of geosmin and 2-methylisoborneol in source waters. *Applied and Environmental Microbiology*, 73(14), 4395-4406. doi: 10.1128/AEM.02250-06
- Karthikeyan, S., Balasubramanian, R., & Yer, C. S. P. (2007). Evaluation of the marine algae *Ulva fasciata* and *Sargassum* sp for the biosorption of Cu(II) from aqueous solutions. *Bioresource Technology*, 98(2), 452-455. doi: 10.1016/j.biortech.2006.01.010
- Kasha, M. (1950). Characterization of electronic transitions in complex molecules. *Discussions of the Faraday Society*, 9, 14-19. doi: 10.1039/DF9500900014
- Kim, K. T., & Park, Y. G. (2021). Geosmin and 2-MIB Removal by Full-Scale Drinking Water Treatment Processes in the Republic of Korea. *Water*, 13(5) doi: 10.3390/w13050628
- Koch, B., Gramith, J. T., Dale, M. S., & Ferguson, D. W. (1992). Control of 2-Methylisoborneol and geosmin by ozone and peroxone: A pilot study. *Water Sci Technol*, 25(2), 291-298. doi: 10.2166/WST.1992.0064
- Kolapkar, S. (2018). *Pyrolysis of Fiber-Plastic Waste Blends* (Masters of science in Mechanical Engineering). Michigan technological university, Michigan.
- Komárek, J. (2009). Recent changes in cyanobacteria taxonomy based on a combination of molecular background with phenotype and ecological consequences (genus and species concept). *Hydrobiologia*, 639(1), 245-259. doi: 10.1007/s10750-009-0031-3
- Kutschera, K., Bornick, H., & Worch, E. (2009). Photoinitiated oxidation of geosmin and 2-methylisoborneol by irradiation with 254 nm and 185 nm UV light. *Water Research*, 43(8), 2224-2232. doi: 10.1016/j.watres.2009.02.015

- Lawton, L. A., Robertson, R. F., Bruce, F. G., & Robertson, P. K. (2003). The destruction of 2-Methylisoborneol and Geosmin using titanium dioxide photocatalysis. *Applied Catalysis B Environmental*, 44(1) doi: 10.1016/S0926-3373(03)00005-5
- Lei, S., Miyamoto, J., Kanoh, H., Nakahigashi, Y., & Kaneko, K. (2006). Enhancement of the methylene blue adsorption rate for ultramicroporous carbon fiber by addition of mesopores. *Carbon*, 44(10), 1884-1890. doi: 10.1016/j.carbon.2006.02.028
- Leon, M., Silva, J., Carrasco, S., & Barrientos, N. (2020). Design, Cost Estimation and Sensitivity Analysis for a Production Process of Activated Carbon from Waste Nutshells by Physical Activation. *Processes*, 8(8) doi: 10.3390/pr8080945
- Li, D., & Liu, S. (2019). *Water Quality Monitoring and Management* (1st ed.). London: Elsevier.
- Liang, C. Z., Wang, D. S., Chen, J. Q., Zhu, L., & Yang, M. (2007). Kinetics analysis on the ozonation of MIB and geosmin. *Ozone-Science & Engineering*, 29(3), 185-189. doi: 10.1080/01919510701294197
- Liou, T. H. (2010). Development of mesoporous structure and high adsorption capacity of biomass-based activated carbon by phosphoric acid and zinc chloride activation. *Chemical Engineering Journal*, 158(2), 129-142. doi: 10.1016/j.cej.2009.12.016
- Lota, G., Krawczyk, P., Lota, K., Sierczynska, A., Kolanowski, L., Baraniak, M., & Buchwald, T. (2016). The application of activated carbon modified by ozone treatment for energy storage. *Journal of Solid State Electrochemistry*, 20(10), 2857-2864. doi: 10.1007/s10008-016-3293-5
- Mahmoudi, K., Hamdi, N., & Srasra, E. (2015). Study of Adsorption of Methylene Blue onto Activated Carbon from Lignite. *Surface Engineering and Applied Electrochemistry*, 51(5), 427-433. doi: 10.3103/s1068375515050105
- Manocha, S. M. (2003). Porous carbons. *Sadhana*, 28(1), 335-348. doi: 10.1007/bf02717142
- Marcilla, A., Gomez-Siurana, A., & Valdes, F. J. (2009). A New Dubinin-Radushkevich-Modified BET Combined Equation To Correlate with a Single Procedure the Full Relative Pressure Range of 77 K N-2 Isotherms of Solids with Different Textural Properties. *Industrial & Engineering Chemistry Research*, 48(24), 10820-10826. doi: 10.1021/ie900912x
- Marsh, H. (2006). *Activated carbon* (1st ed.). Amsterdam: Elsevier.
- Meriem Belhachemi, F. A. (2011). Comparative adsorption isotherms and modeling of methylene blue onto activated carbons. *Applied Water Science*, 1(3), 111-117. doi: 10.1007/s13201-011-0014-1
- Mianowski, A., Owczarek, M., & Marecka, A. (2007). Surface area of activated carbon determined by the iodine adsorption number. *Energy Sources Part a-Recovery Utilization and Environmental Effects*, 29(9), 839-850. doi: 10.1080/00908310500430901
- Milman, B. L. (2015). General principles of identification by mass spectrometry. *Trac-Trends in Analytical Chemistry*, 69, 24-33. doi: 10.1016/j.trac.2014.12.009
- Moreno-Castilla, C., & Rivera-Utrilla, J. (2001). Carbon materials as adsorbents for the removal of pollutants from the aqueous phase. *Mrs Bulletin*, 26(11), 890-894. doi: 10.1557/mrs2001.230
- Ndiongue, S., Anderson, W. B., Tadwalkar, A., Rudnickas, J., Lin, M., & Huck, P. M. (2006). Using pilot-scale investigations to estimate the remaining geosmin and MIB removal capacity of full-scale GAC-capped drinking water filters. *Water Quality Research Journal of Canada*, 41(3), 296-306. doi: 10.2166/wqrj.2006.033
- Nerenberg, R., Rittmann, B. E., & Soucie, W. J. (2000). Ozone/biofiltration for removing MIB and geosmin. *Journal American Water Works Association*, 92(12), 85-+. doi: 10.1002/j.1551-8833.2000.tb09073.x
- Nowicki, P., Pletczak, R., & Wachowska, H. (2008). Siberian anthracite as a precursor material for microporous activated carbons. *Fuel*, 87(10-11), 2037-2040. doi: 10.1016/j.fuel.2007.10.008
- Nunes, C. A., & Guerreiro, M. C. (2011). Estimation of surface area and pore volume of activated carbons by methylene blue and iodine numbers. *Quimica Nova*, 34(3), 472-U309. doi: 10.1590/s0100-40422011000300020
- Okibe, F. G., Gimba, C. E., Ajibola, V. O., & Ndukwe, I. G. (2013). Preparation and surface characteristics of activated carbon from *Brachystegia eurycoma* and *Prosopis africana* seed hulls. *International Journal of ChemTech Research*, 5(4), 1991-2002.
- Omur-Ozbek, P., Little, J. C., & Dietrich, A. M. (2007). Ability of humans to smell geosmin, 2-MIB and nonadial in indoor air when using contaminated drinking water. *Water Science and Technology*, 55(5), 249-256. doi: 10.2166/wst.2007.186
- Ormad, M. P., Miguel, N., Claver, A., Matesanz, J. M., & Ovelleiro, J. L. (2008). Pesticides removal in the process of drinking water production. *Chemosphere*, 71(1), 97-106. doi: 10.1016/j.chemosphere.2007.10.006

- Piccin, J., Pinto, L. A., & Cadaval, T. R. (2017). Adsorption isotherms in Liquid Phase: Experimental, Modeling and interpretations *Adsorption Isotherms in Liquid Phase: Experimental, modeling and interpretations* (pp. 19-55): Springer.
- Potgieter, J. H. (1991). Adsorption of methylene blue on activated carbon. *Chemistry and Ecology*, 24(4), 285-295. doi: 10.1080/02757540802238341
- Qi, F., Chen, Z. L., Xu, B. B., & Xu, Z. Z. (2008). Degradation of 2-methylisoborneol in drinking water by bauxite catalyzed ozonation. *Journal of Water Supply Research and Technology-Aqua*, 57(6), 427-434. doi: 10.2166/aqua.2008.198
- Ritson, J. P., & Graham, N. J. D. (2019). Water extractable organic matter (WEOM) as an indicator of granular activated carbon (GAC) bed life and water quality outcomes in drinking water treatment. *Environmental Science-Water Research & Technology*, 5(9), 1593-1598. doi: 10.1039/c9ew00303g
- Rivas, F. J., Beltran, F. J., Gimeno, O., & Frades, J. (2004). Wet air and extractive ozone regeneration of 4-chloro-2-methylphenoxyacetic acid saturated activated carbons. *Industrial & Engineering Chemistry Research*, 43(15), 4159-4165. doi: 10.1021/ie030756h
- Rodriguez-Reinoso, F. (1998). The role of carbon materials in heterogeneous catalysis. *Carbon*, 36(3), 159-175. doi: 10.1016/s0008-6223(97)00173-5
- Rodriguez-Reinoso, F., Molinasabio, M., & Munecas, M. A. (1992). Effect of Microporosity and Oxygen Surface Groups of Activated Carbon in the Adsorption of Molecules of Different Polarity *Journal of Physical Chemistry*, 96(6), 2707-2713. doi: 10.1021/j100185a056
- Rodriguez-Reinoso, F., & Silvestre-Albero, J. (2016). Effect of porosity and chemical structure on adsorption. *Journal of Radioanalytical and Nuclear Chemistry*, 308(2) doi: 10.1007/s10967-015-4408-7
- Rosenfeldt, E. J., Melcher, B., & Linden, K. G. (2005). UV and UV/H₂O₂ treatment of methylisoborneol (MIB) and geosmin in water. *Journal of Water Supply: Research and Technology*, 54(7), 423-434. doi: 10.2166/aqua.2005.0040
- Safe Drinking Water Committee. (1980). Drinking Water and Health. Washington: National Academies Press.
- Salvador, F., Martin-Sanchez, N., Sanchez-Hernandez, R., & Sanchez-Montero, M. J. (2015). Regeneration of carbonaceous adsorbents. Part II: Chemical, Microbiological and Vacuum Regeneration. *Microporous and Mesoporous Materials*, 202, 277-296. doi: 10.1016/j.micromeso.2014.08.019
- Sarici-Ozdemir, C. (2014). Removal of methylene blue by activated carbon prepared from waste in a fixed-bed column. *Particulate Science and Technology*, 32(3), 311-318. doi: 10.1080/02726351.2013.851132
- Scharf, R. G., Johnston, R. W., Semmens, M. J., & Hozalski, R. M. (2010). Comparison of batch sorption tests, pilot studies, and modeling for estimating GAC bed life. *Water Research*, 44(3), 769-780. doi: 10.1016/j.watres.2009.10.018
- Schönbein, C. F. (1854). Über verschiedene Zustände des Sauerstoffs (On various states of oxygen). *Ann Chem Pharm*, 89(3), 257-300. doi: 10.1002/jlac.18540890302
- Shah, I. K., Pre, P., & Alappat, B. J. (2013). Steam regeneration of adsorbents: An experimental and technical review. *Chem Sci Trans*, 2(4), 1078-1088. doi: 10.7598/cst2013.545
- Shahwan, T. (2015). Lagergren equation: Can maximum loading of sorption replace equilibrium loading? *Chemical Engineering Research & Design*, 96, 172-176. doi: 10.1016/j.cherd.2015.03.001
- Sharma, R. C. (1998). The determination of 2-Methylisoborneol and geosmin in water using fluorescence spectroscopy. *The Analyst*, 123(10), 2155-2160. doi: 10.1039/A803621G
- Siemens, W. (1857). Ueber die elektrostatische Induction und die Verzögerung des Stroms in Flaschendrahten. *Poggendorff's Ann Phys. Chem.*, 102, 66 - 122. doi: 10.1002/andp.18571780905
- Sing, K. S. W., Everett, D. H., Haul, R. A. W., Moscou, L., Pierotti, R. A., Rouquerol, J., & Siemieniewska, T. (1985). Reporting physisorption data for gas solid systems with special reference to the determination of surface-area and porosity (recommendations 1984). *Pure and Applied Chemistry*, 57(4), 603-619. doi: 10.1351/pac198557040603
- Skubiszewska-Zieba, J. (2010). VPO catalysts synthesized on substrates with modified activated carbons. *Applied Surface Science*, 256(17), 5520-5527. doi: 10.1016/j.apsusc.2009.12.129
- Snoeyink, V. L., & Weber, W. J. (1967). The surface chemistry of active carbon; a discussion of structure and surface functional groups. *Environ. Sci. Technol*, 1(3), 228-234. doi: 10.1021/es60003a003
- Sonntag, C. v., & Gunten, U. v. (2012). Chemistry of ozone in water and wastewater treatment. London: IWA Publishing.
- Srinivasan, R., & Sorial, G. A. (2011). Treatment of taste and odor causing compounds 2-methyl isoborneol and geosmin in drinking water: A critical review. *Journal of Environmental Sciences*, 23(1), 1-13. doi: 10.1016/s1001-0742(10)60367-1

- Strezov, V., Patterson, M., Zymła, V., Fisher, K., Evans, T. J., & Nelson, P. F. (2007). Fundamental aspects of biomass carbonisation. *Journal of Analytical and Applied Pyrolysis*, 79(1-2), 91-100. doi: 10.1016/j.jaap.2006.10.014
- Suffet, I. H. (1980). An evaluation of activated carbon for drinking water treatment. *Journal AWWA*, 72(1), 41-50. doi: 10.1002/j.1551-8833.1980.tb04461.x
- Valdes, H., Sanchez-Polo, M., Rivera-Utrilla, J., & Zaror, C. A. (2002). Effect of ozone treatment on surface properties of activated carbon. *Langmuir*, 18(6), 2111-2116. doi: 10.1021/la010920a
- Valdes, H., Sanchez-Polo, M., & Zaror, C. A. (2003). Effect of ozonation on the activated carbon surface chemical properties and on 2-mercaptobenzothiazole adsorption. *Latin American Applied Research*, 33(3), 219-223.
- Valeur, B. (2002). Molecular fluorescence. Weinheim, Germany: Wiley-VCH.
- Valix, M., Cheung, W. H., & Zhang, K. (2006). Role of heteroatoms in activated carbon for removal of hexavalent chromium from wastewaters. *Journal of Hazardous Materials*, 135(1-3), 395-405. doi: 10.1016/j.jhazmat.2005.11.077
- Vanvliet, B. M. (1991). The regeneration of activated carbon. *Journal of the South African Institute of Mining and Metallurgy*, 91(5), 159-167.
- Watson, S. B., Brownlee, B., Satchwill, T., & Hargesheimer, E. E. (2000). Quantitative analysis of trace levels of geosmin and MIB in source and drinking water using headspace SPME. *Water Research*, 34(10), 2818-2828. doi: 10.1016/S0043-1354(00)00027-0
- Wigmans, T. (1989). Industrial-Aspects of Production and Use of Activated Carbons. *Carbon*, 27(1), 13-22. doi: 10.1016/0008-6223(89)90152-8
- Worch, E. (2012). Adsorption technology in water treatment. Berlin: De Gruyter.
- Wu, A. G., Duan, T. T., Tang, D., Zheng, Z. G., Zhu, J. X., Wang, R. S., . . . Zhu, Q. (2014). Review the Application of Chromatography in the Analysis of Nitric Oxide-derived Nitrite and Nitrate Ions in Biological Fluids. *Current Analytical Chemistry*, 10(4), 609-621. doi: 10.2174/157341101004140701123515
- Yang, T., & Lua, A. C. (2006). Textural and chemical properties of zinc chloride activated carbons prepared from pistachio-nut shells. *Materials Chemistry and Physics*, 100(2-3), 438-444. doi: 10.1016/j.matchemphys.2006.01.039
- Zhu, Z. L., Li, A. M., Yan, L., Liu, F. Q., & Zhang, Q. X. (2007). Preparation and characterization of highly mesoporous spherical activated carbons from divinylbenzene-derived polymer by ZnCl₂ activation. *Journal of Colloid and Interface Science*, 316(2), 628-634. doi: 10.1016/j.jcis.2007.09.016

7.0 Appendices

7.1 Iodine number experiment

Three replications were conducted for the virgin GAC sample and an average of the three was taken.

Table 26: Virgin iodine number replications

Replication	Iodine number (mg/g)
1	907.35
2	902.20
3	932.92
Average	914.16±16.45

As seen in Table 26, the average iodine number for the virgin GAC was 3.60 mmole/g and the error is 0.065 mmole/g. Three replications were conducted for each of the iodine number experiments, the average iodine number and errors were determined for each sample.

X/M vs C graphs were produced for each GAC sample, these graphs were used to determine the iodine numbers for each sample, as shown in Figure 28 in section 4.1.1. The first replication X/M vs C graphs are shown in Figure 43.

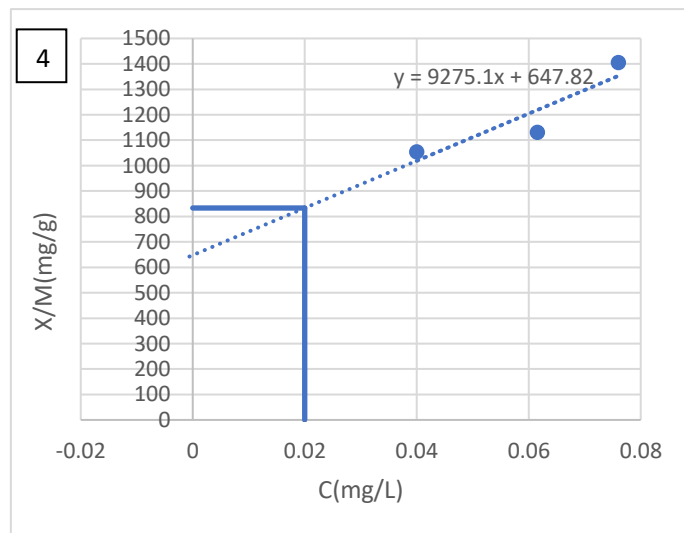
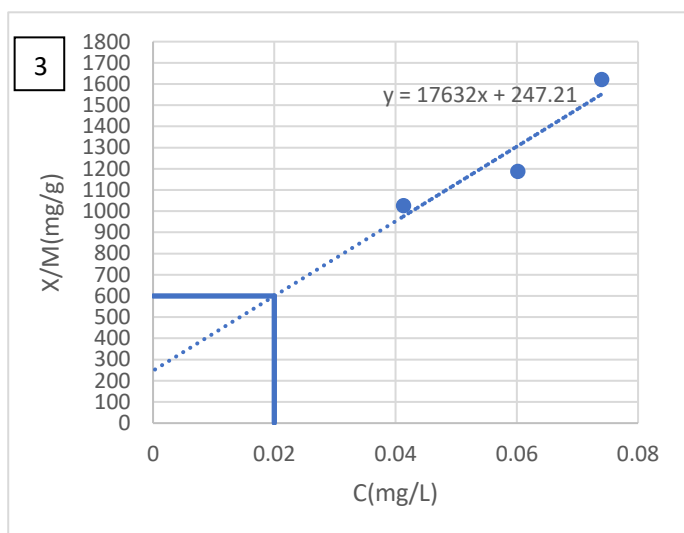
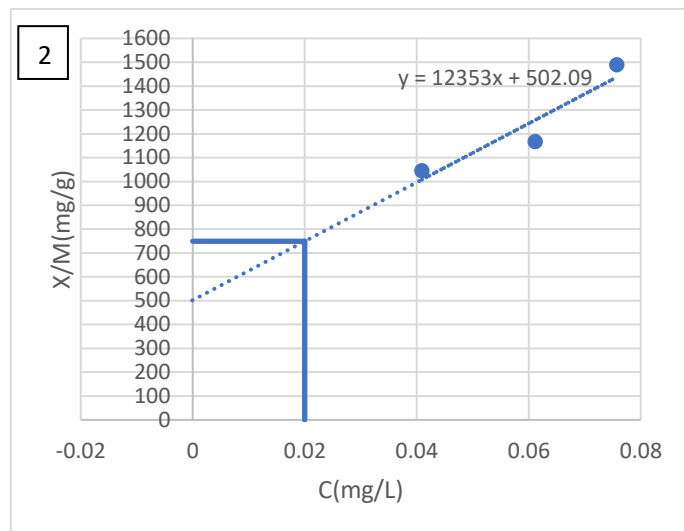
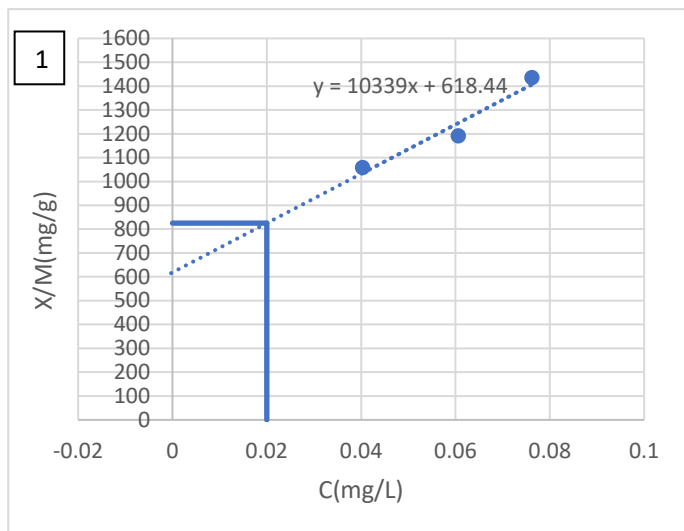


Figure 43: Iodine number X/M vs C graphs: 1) 30 min ozonated GAC 2) 60 min ozonated GAC 3) 90min ozonated GAC 4) 60 min oxygenated GAC

7.2 Methylene blue

The calibration curve was produced by diluting the methylene blue solution with incremental increases in the volume of water applied. Table 27 shows that the concentration curve was produced using 0.5 mL incremental changes in the methylene blue solution and water volume. The volumes changed from 3 mL of the methylene blue solution and 0 mL of water to 0 mL of the methylene blue solution and 3 mL of water.

Table 27: Calibration curve values for methylene blue

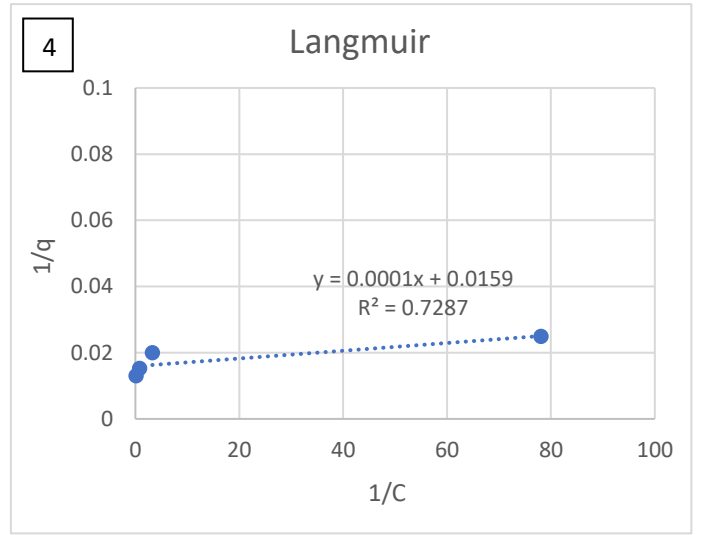
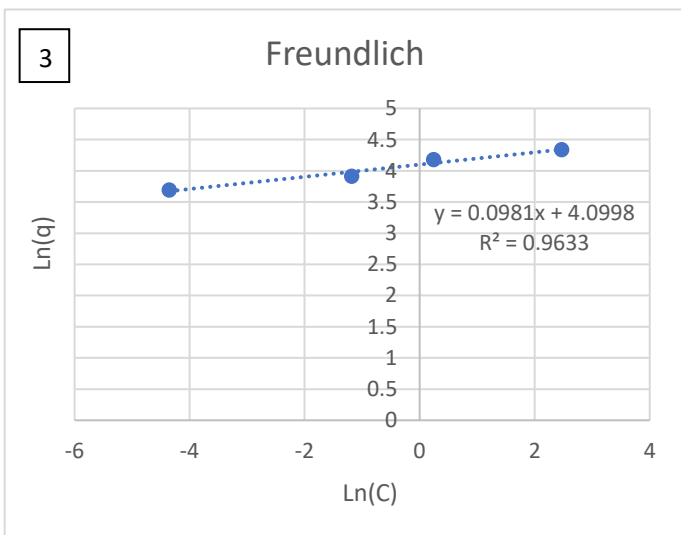
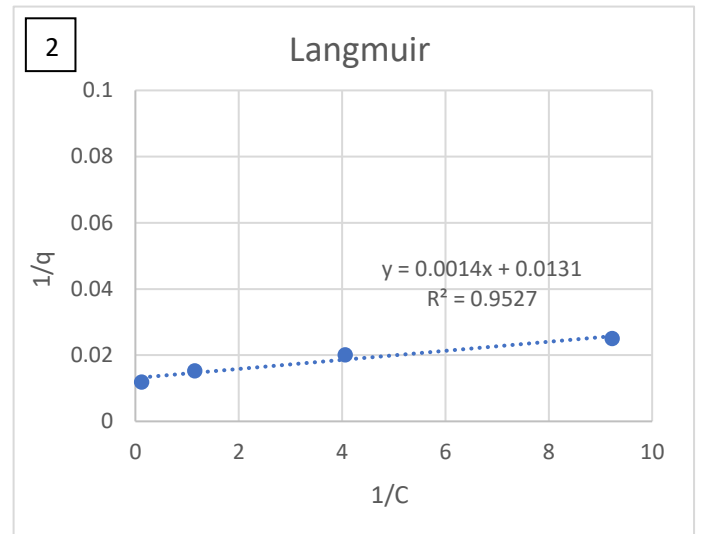
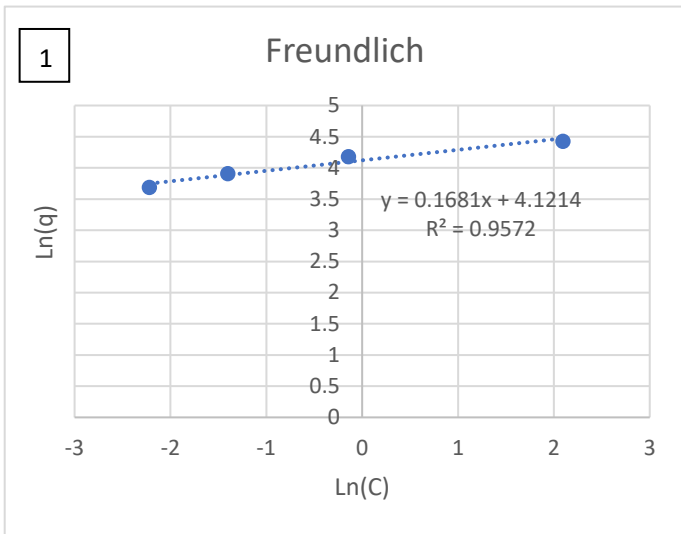
$V_{\text{Water}}(\text{mL})$	$V_{\text{MB}}(\text{mL})$	$V_{\text{Total}}(\text{mL})$	Concentration (mg/L)	Absorbance @ 625nm
0.0	3.0	3.0	15.0	1.307
0.5	2.5	3.0	12.5	1.193
1.0	2.0	3.0	10.0	1.026
1.5	1.5	3.0	7.5	0.814
2.0	1.0	3.0	5.0	0.581
2.5	0.5	3.0	2.5	0.281
3.0	0.0	3.0	0.0	0.000

The mass of the carbon sample and the adsorbance of the methylene blue solution for each sample is collected during the methylene blue experiment, the concentration and the amount of methylene blue adsorbed per mass of activated carbon. Table 28 shows the data obtained during the first replication of the virgin GAC sample.

Table 28: Methylene blue number experiment for virgin GAC raw data

Mass(g)	Absorbance(Au)	C_f (mg/L)	$Q(\text{mg/g})$	$1/C_f$	$1/q$	Inc	$\text{Ln}q$
0.0101	1.456	14.345	141.209	0.070	0.007	2.663	4.950
0.0202	0.636	6.266	86.602	0.160	0.012	1.835	4.461
0.0299	0.040	0.394	66.362	2.538	0.015	-0.931	4.195
0.0400	0.020	0.197	49.803	5.075	0.020	-1.624	3.908
0.0501	0.007	0.069	39.865	14.500	0.025	-2.674	3.686

As seen in Table 28 the reciprocal of concentration and q are found, the Ln of C and q are also determined. These values are used to plot the Langmuir and Freundlich isotherms. Three replications for each GAC sample were conducted and an average methylene blue number was obtained. The first replication for the Langmuir and Freundlich isotherms are seen in Figure 44.



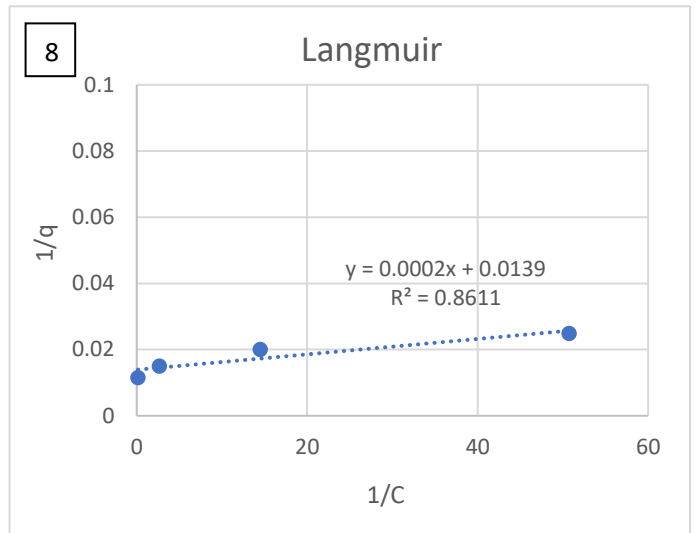
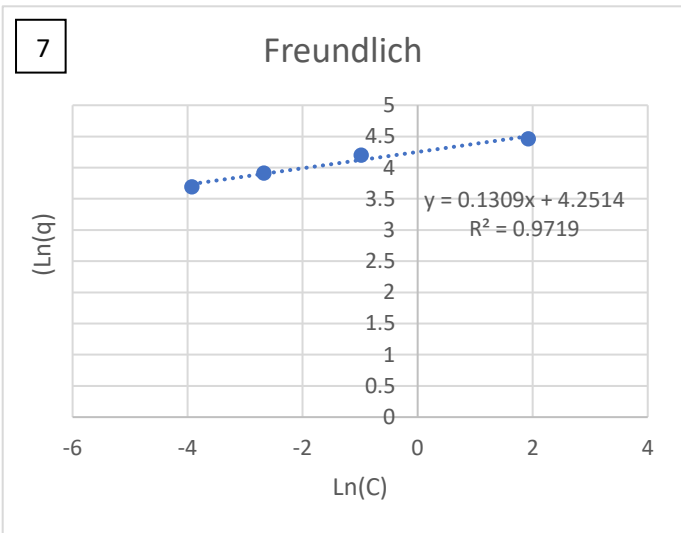
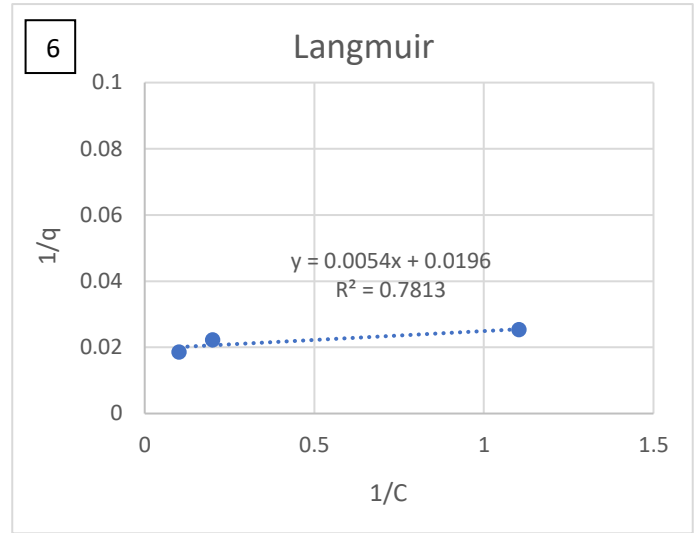
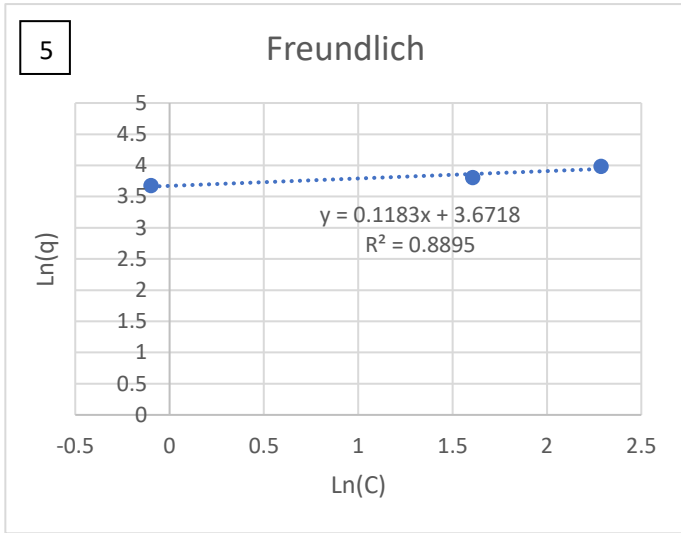


Figure 44: Langmuir and Freundlich isotherms for ozonated activated carbon samples: 1) Freundlich isotherm for 30 minute ozonated GAC sample 2)) Langmuir isotherm for 30 minute ozonated GAC sample 3)) Freundlich isotherm for 60 minute ozonated GAC sample 4) Langmuir isotherm for 60 minute ozonated GAC sample 5) Freundlich isotherm for 90 minute ozonated GAC sample 6)) Langmuir isotherm for 90 minute ozonated GAC sample 7)) Freundlich isotherm for 30 minute oxygenated GAC sample 8) Langmuir isotherm for 30 minute oxygenated GAC sample

7.3 pH point of zero charge

The pH point of zero charge is when the pH at which the surface charge of the material is zero.

The pH was used to measure the acidity of the various carbon samples. Table 29 shows how the raw data was collected.

Table 29: pH_{pzc} raw data for virgin GAC

pH initial	Mass(g)	pH initial reading	pH final reading
2	0.1501	2.01	2.08
4	0.1503	3.99	9.46
6	0.1506	6.03	9.81
8	0.1498	7.95	9.83
10	0.1495	10.02	9.96
12	0.1497	12.01	11.98

7.4 Fourier transform infrared spectroscopy measurement (FTIR)

The adsorbance and the transmission were measured using the FTIR of the virgin activated GAC sample, both the adsorbance and transmission can characterise the activated carbon samples, transmission is more commonly used, both give very similar results as seen in Figures 45 & 46.

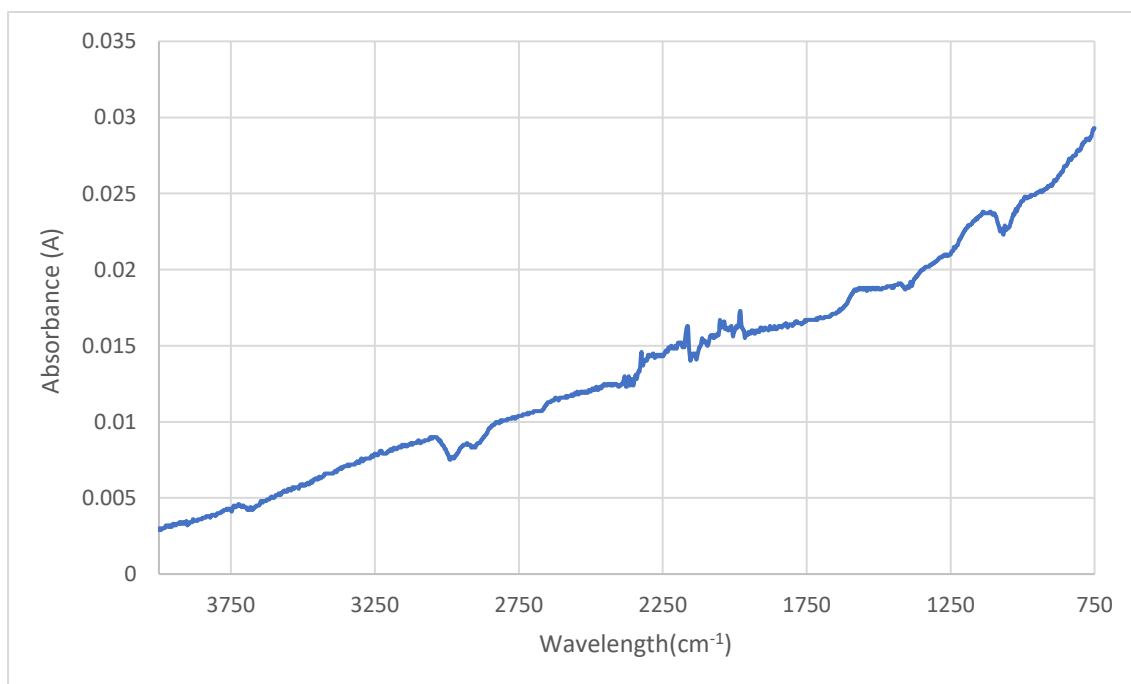


Figure 45: FTIR data of virgin activated carbon measuring the adsorbance

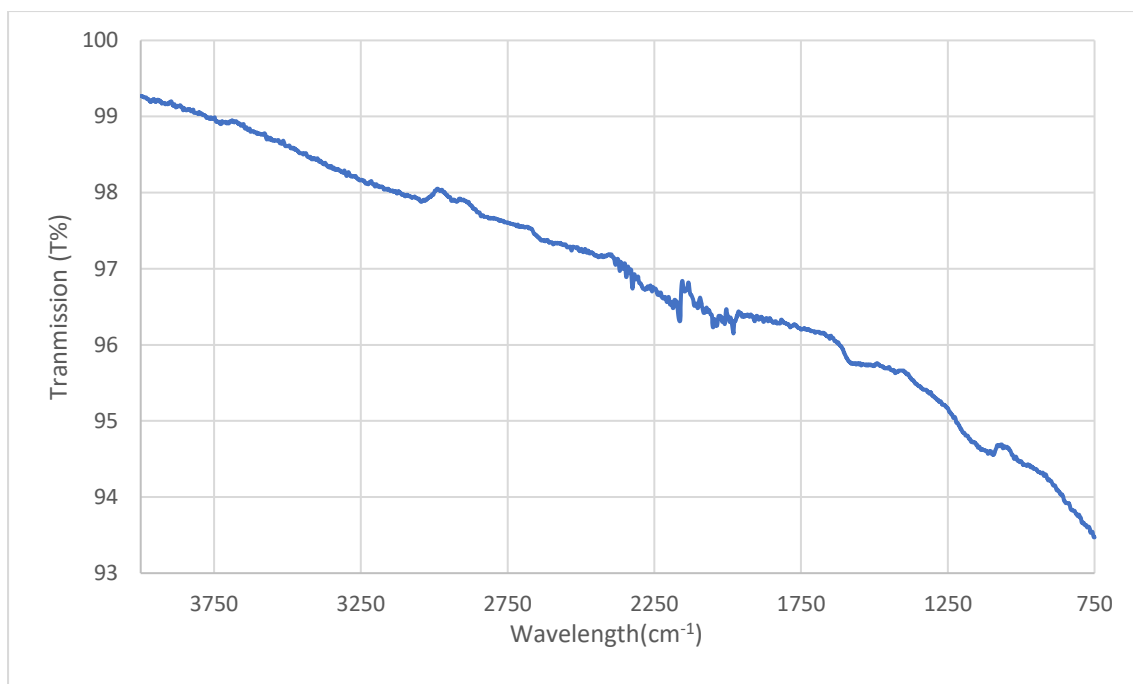


Figure 46: FTIR data of the virgin activated carbon measuring the transmission

As seen the Figures 45 & 46, similar peaks are obtained thus, it was decided that only the transmission was necessary to characterise the surface chemistry of the activated carbon samples. Figure 47 shows the Perkin-Elmer Spectrum Two FTIR that was used for these experiments.

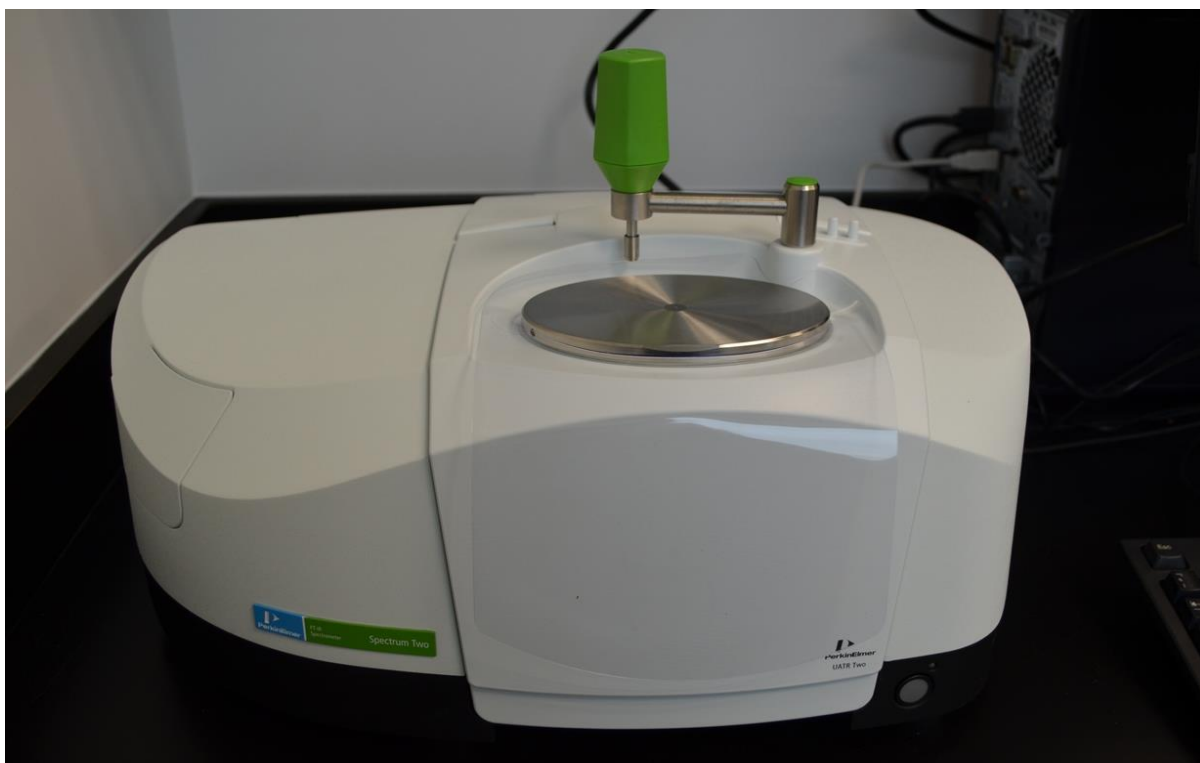


Figure 47: Image of the Perkin-Elmer Spectrum Two FTIR

7.5 Ozonation of activated carbon

The ozonation experiments were conducted using the ozone rig created, which consisted of an oxygen canister, ozone generator, ozone analyser, flowmeters, diffuser and the ozone reactor, the ozone rig used is shown in Section 3.3 and the ozone reactor is shown in Figure 48.

Table 30: Indigo experimental results

Ozone exposure length (min)	Ozone concentration (mg/L)
30	0.081±0.0119
60	0.562±0.0363
90	1.921±0.0747



Figure 48: Image of the ozone reactor

7.6 Geosmin and MIB adsorption experiment

Figure 49 shows the incubation shaker that was used for the mixing of the G-MIB samples.

Figure 50 shows the Fluorescence spectrometry system used for the analysis of the geosmin and MIB samples.



Figure 49: Image of Fluorescence spectrometry



Figure 50: Image of Incu-Shake MAXI